Politecnico di Torino

Master's degree program Civil Engineering

Vibration Analysis and Comfort Verification of a Steel Pedestrian Bridge Using FEM and Mitigation Strategies

Candidate:
Mahdi Bahramirahmani

Supervisor:
Prof. Gabriele Bertagnoli

Co-supervisor:
Ing. Matteo Lusso
Prof. Mario Ferrara

Academic year 2025-2026

I declare that the contents and structure of this dissertation are original and do not in any way infringe the rights of third parties, including those relating to the protection of personal data.

…….....

Mahdi Bahramirahmani

Torino, 02,14, 2026

“Everything should be made as simple as possible,

but not simpler.”
Albert Einstein

Acknowledgements.

Mahdi Bahramirahmani, I would like to thank Prof. Gabriele Bertagnoli, who supervised this thesis, for being available and for providing me with precious methodological and scientific guidance.

I would also like to thank Eng. Matteo Lusso, who provided me with technical guidance and with whom I had many stimulating discussions to enrich this work.

A special thank you to LTG srl, which provided me with essential resources, data, and expertise for the realization of this work, creating a stimulating bridge between academia and business.

I am also grateful to my colleagues and fellow students, with whom I had many stimulating discussions, sharing challenges and experiences.

And, last but not least, I would like to thank my family and my closest friends for their constant encouragement during all these university years.

Summary.

This thesis is focused on how a steel bridge for pedestrians moves and whether those who are walking across it will feel comfortable due to the vibrations created by their movements, with particular emphasis on the horizontal (side-to-side) vibrations. The evaluation is based on the use of the Sétra–AFGC guidelines developed for screening the resonance risk of structures due to pedestrian-induced activity and then verifying the satisfactory comfort level by comparing calculated accelerations with accepted limits, when necessary.

There is a three-dimensional finite element model of the bridge (in MIDAS Gen) generating the main structural members (beam/truss) and associated elastic links to represent the boundary conditions. As the bridge structure is designated to be a Class II structure, it means that dynamic checks must be done on it. The initial step in evaluating the bridge for vibrations and resonance requirements was the performance of a modal (eigenvalue) analysis to determine the natural frequencies of the structure and to identify the potential resonance from pedestrian walking harmonics. The mode shapes demonstrated that the structure had low-frequency horizontal mode shapes, and based upon the Sétra sensitivity range, the low-frequency horizontal resonance levels could cause extreme vibrations and required additional comfort verification, specifically in the horizontal directions.

After the modal analysis was completed, time-history analyses were conducted on the bridge using Sétra-type simplified harmonic loading functions applied at representative control points defined in the bridge deck. For the horizontal accelerations, the conservative comfort limit of a_{lim} = 0.10 m/s² was established. However, for the bridge's reference configuration, the serviceability requirements could not be met.

Abstract.

This thesis offers a thorough assessment of the dynamic performance and vibration comfort of a steel pedestrian footbridge under pedestrian-induced loading, building on the Sétra–AFGC framework. Because of its low mass and natural frequencies that can coincide with walking harmonics, the bridge is categorized as a Class II structure, necessitating thorough serviceability checks that go beyond simple static design. MIDAS Gen is used to create a high-fidelity 3D finite element model that captures both local and global dynamics, such as the elasticity of supporting bearings, realistic boundary conditions, and deck-support interaction.

There are two phases to the analysis. Within the critical frequency bands for human-induced excitation, prominent horizontal modes in both lateral and longitudinal directions are revealed by a modal analysis, which first determines the natural frequencies and mode shapes. Simplified harmonic time-history loads representing single pedestrians and crowd effects are applied in a second stage of analysis because these modes fall within the sensitivity range specified by Sétra. A conservative comfort limit of 0.10 m/s² for horizontal vibrations is compared to peak deck accelerations at important control points. According to the results, the bridge in its reference configuration surpasses this threshold: lateral accelerations are around 0.11 m/s², and longitudinal accelerations reach about 0.53 m/s². This clearly indicates a resonance issue and non-compliance with comfort criteria.

To mitigate this excessive response, various mitigation measures are proposed and evaluated. These measures are widening the gap between central supports, increasing the cross-section of central columns to enhance their stiffness, providing bracing to unbraced ends, and replacing Teflon bearings with rubber bearings. The analysis shows that increasing the central column's stiffness has a major impact on increasing its frequencies and reducing its accelerations. Combining all mitigation measures, therefore, provides the best solution to reducing resonance effects and making the bridge comfortable for pedestrians.

The results show the significance of considering dynamic serviceability in early stages of design and provide guidelines for retrofitting existing light-weight bridges.

Table of contents

Table of figures

List of tables

1 INTRODUCTION

This report describes the design choices, input data, and verifications of the structural COMONENTS forming the deck of the pedestrian and cycling footbridge planned in the Meisino Park, located in the province of Turin (TO).

Parco del Meisino is a major riverside green area in north-eastern Turin, set on the right bank of the Po River in a semicircular landscape shaped by the river corridor and the first foothills of the Superga hill system. It forms part of the wider **Meisino–Isolone di Bertolla protected area**, established to safeguard wetlands and riparian habitats around the **confluence of the Po and the Stura di Lanzo**, an ecologically sensitive zone within the Po protected-areas network.

Beyond its recreational value (walking and cycling routes along the Po), the site is notable for its biodiversity: the mosaic of riverbanks, wet meadows, reedbeds and alluvial woods supports rich birdlife, and the broader reserve has long been recognized for the presence of important waterbird communities and habitat types typical of lowland river systems.

Historically, parts of the area closest to the river included the **Galoppatoio/ former military facilities** (linked to a 19th-century military training and shooting area), later incorporated into the river park system developed by the City of Turin starting in the early 2000s; over time, abandoned sections have re-vegetated and now function as valuable refuge zones for avifauna within the urban fabric

In recent years, the municipality has also promoted regeneration initiatives aimed at combining environmental education with low-impact outdoor activities—an approach that reflects the strategic role of Meisino as both an urban “ecological infrastructure” and a public space connecting neighborhoods to the Po River landscape.
The structure in question is part of a broader park renovation project and aims to connect two areas that are currently perceived by visitors as separate elements, since there is no direct connection that allows users to cross Corso Don Luigi Sturzo.

Figure 1-1 Area of park subjected to the interventions

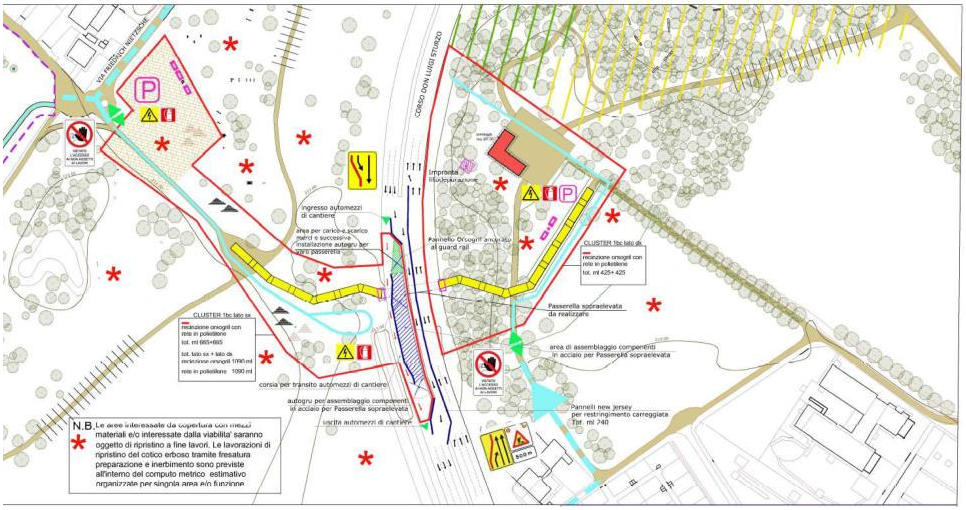

Figure 1-2 Area of park subjected to the interventions

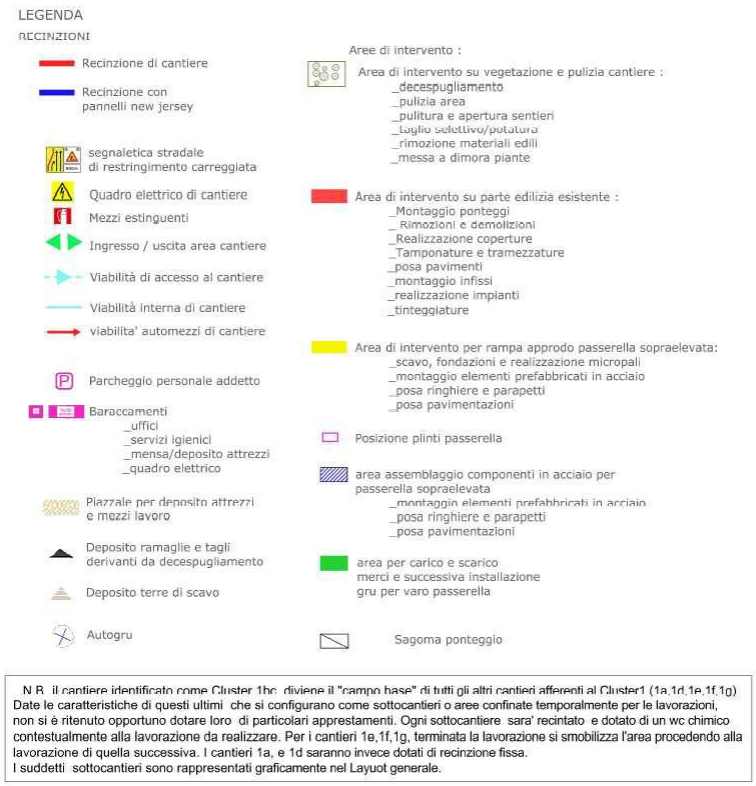

Figure 1-3 Construction site layout plan and legend

2 DESCRIPTION OF STRUCTURE

The structure is made of steelwork with a deck width of 3.7 meters and extends over a total length of 204 meters. It consists of two ramps, 72 m and 100 m long respectively, and a central span with a clear length of 32 meters.

The structure will be built using **Cor-Ten steel type S355 J2 WP**. All structural profiles are made from welded plates using suitable Cor-Ten steel electrodes and are connected by means of gussets and corrosion-protected bolts.

The deck is supported by portal frames made of hollow tubular profiles. The column bases will be anchored to the ground using **screw micro piles**, without the use of concrete footings, and flush with the ground surface.

By adopting horizontal slots, the footbridge is divided into **five independent blocks**, each longitudinally braced along its axis. **Transverse stability** is ensured by the portal frames supporting the deck.

Each block consists of ramps with a maximum length of **10.00 meters**, interrupted at landings where the **longitudinal bracing** of the structure is located. Between one landing and the next, the ramps rest continuously on **intermediate portal frames**.

The **deck girders** are horizontally braced by a system of crossbeams and diagonal members forming a rigid plane, on which **omega-shaped profiles** are placed to support the walking surface.

For isolated portal frames, two **Titan 52/26 screw micro piles** with a length of 8.00 m are provided, while for braced frame groups, **four similar micro piles** are provided for each column.

The **central deck**, corresponding to the 32-meter span, is supported by a **truss structure** made of fixed tubular profiles. For the columns supporting the central deck only, **four Titan 52/26 screw piles**, each 8.00 m long and transversely connected by **reinforced concrete footings**, will be installed.

The ramps, with landings located every **maximum 10 meters**, have slopes ranging from **10%** in the initial sections to **8%** in the final ones. A **handrail** parallel to the ramp is provided, with **vertical posts every 150 cm**, together with a **Geobrugg-type rockfall protection and anti-fall mesh**, made of high-strength steel wire.

Since the footbridge will be accessible **only to pedestrians and cyclists**, the **transit of emergency vehicles** on the structure is excluded.

Below are some images of the **calculation models** of the different parts of the footbridge.

We are considering part of bridge that is **part 3**.

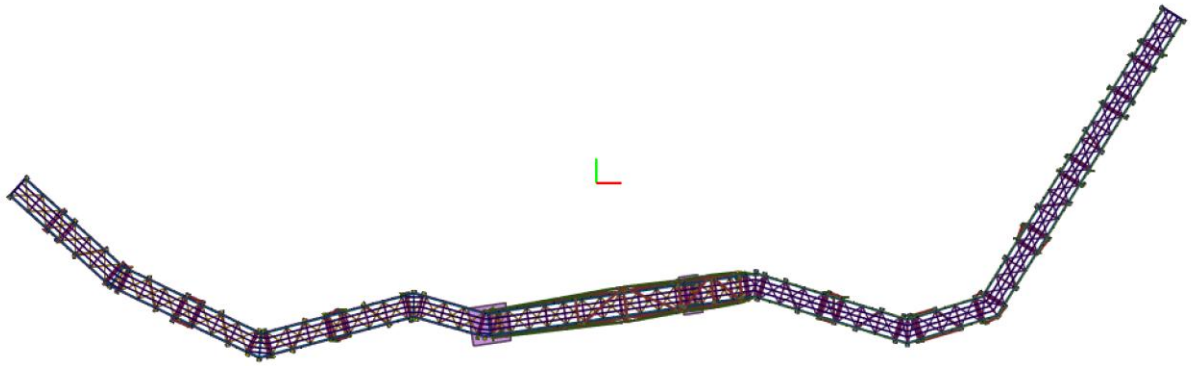

Figure 2-1 2D model

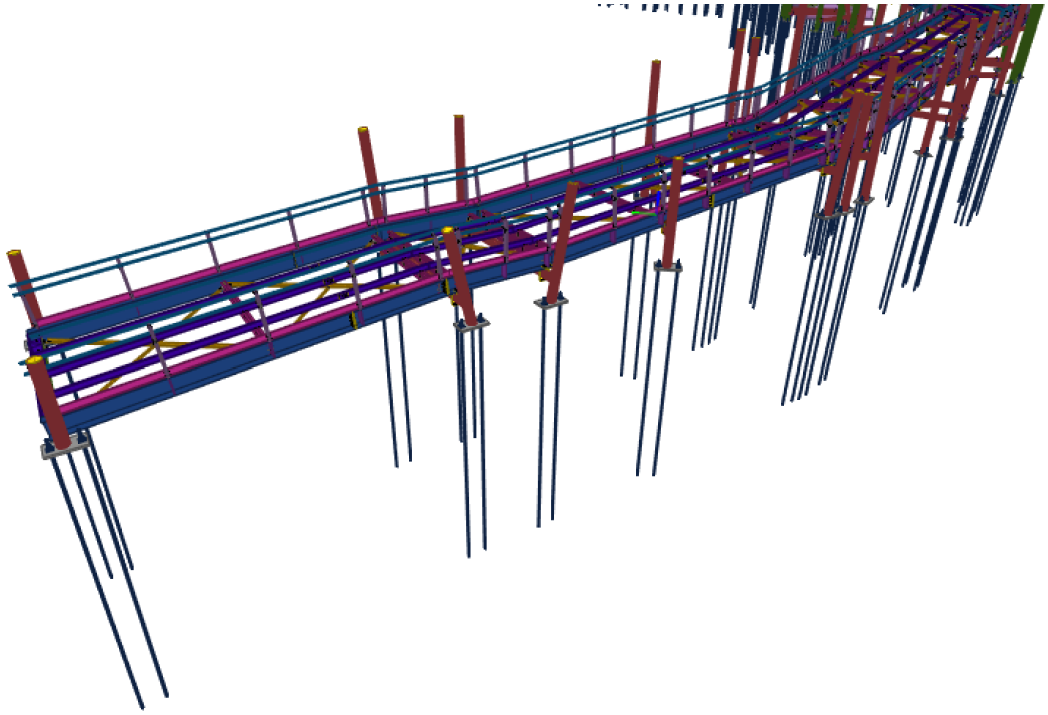

Figure 2-2 3D model

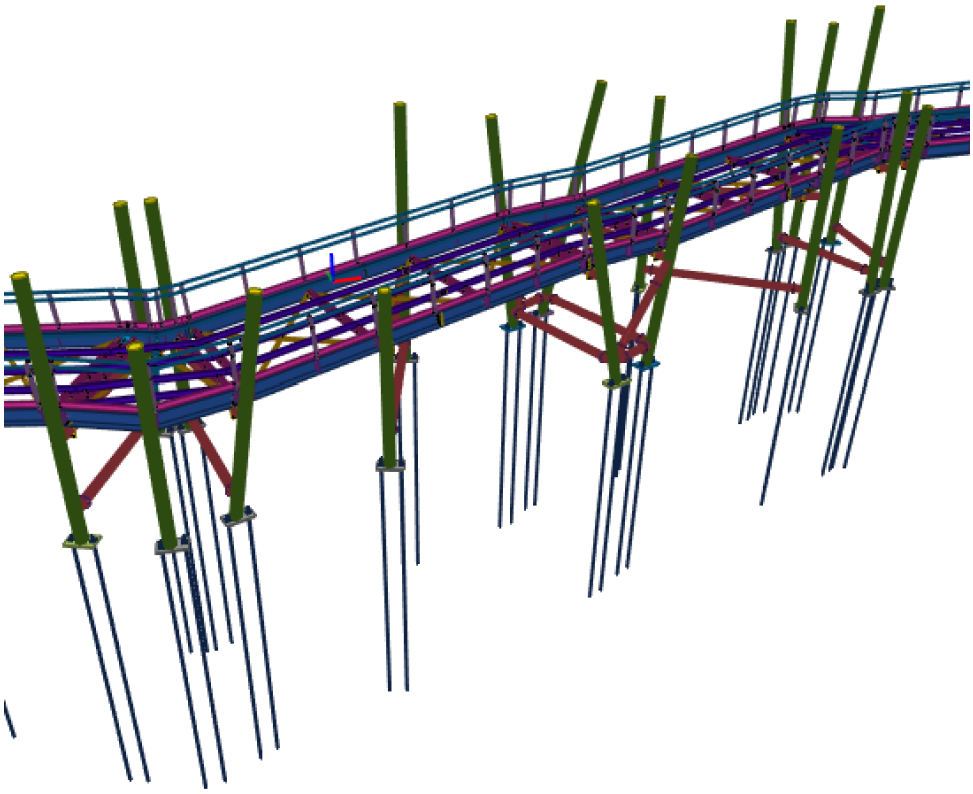

Figure 2-3 3D model

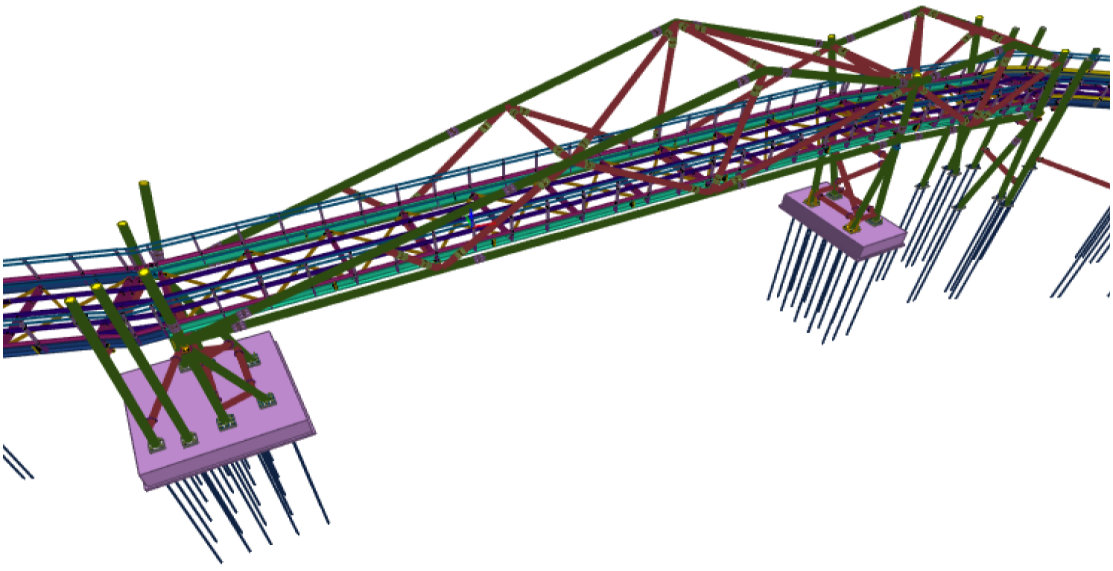

Figure 2-4 3D model

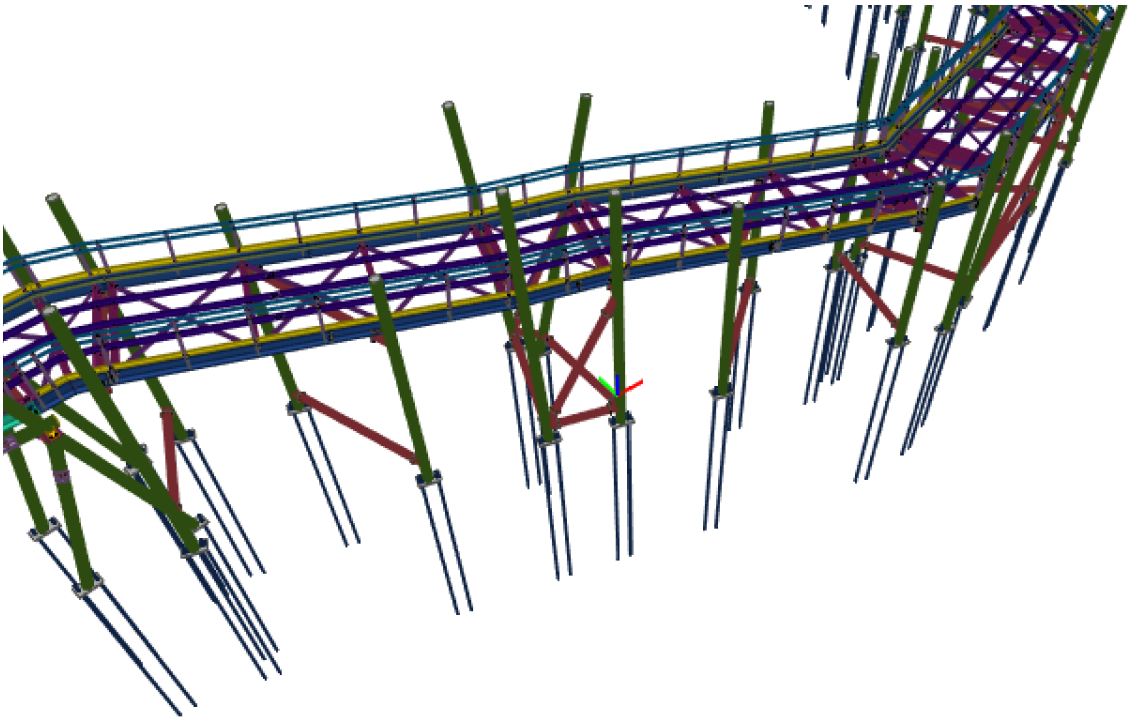

Figure 2-5 3D model

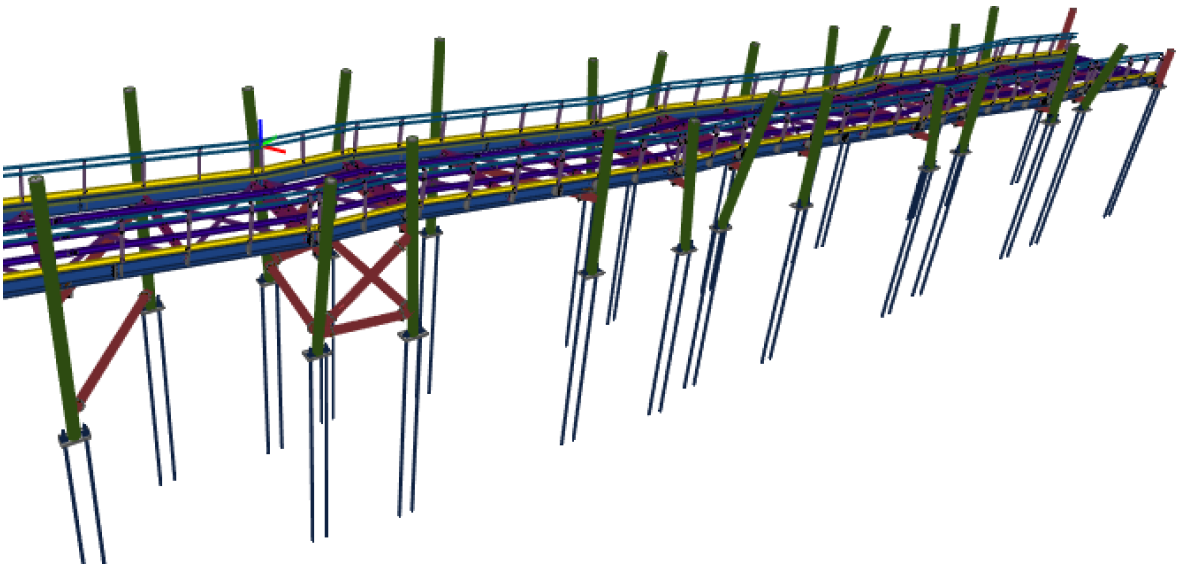

Figure 2-6 3D model

2.1 DESCRIPTION OF FEM MODEL

The finite element model of the footbridge was developed using **Midas Gen** to represent the structural behavior of the steel pedestrian and cycling bridge. The model reproduces a **three-dimensional truss-type structure** with a **deck width of 3.7 meters**, central span supported by a system of **portal frames** and **tubular trusses** that ensure overall stiffness and stability.

The main structural members are modeled with **tubular and omega-shaped steel profiles**, while the **deck system** consists of secondary beams and stiffeners supporting the walking surface. The materials are defined as **Cor-Ten steel type S355 J2 WP**, modeled with **linear elastic behavior**. A variety of section types were used to represent the structural components, including tubular members (CHS), channels (C), omega sections, and flat plates.

The **static load cases** include the self-weight of the structure, the weight of the deck panels and parapets, permanent loads, and a **pedestrian live load of 70 kg/m²**. In addition, **dynamic analyses** were performed, including both **response spectrum** and **time-history analyses**. The response spectrum analysis was conducted using site-specific seismic parameters according to **NTC 2018** and **Eurocode 8**, while the time-history analysis included several excitation cases based on sinusoidal and seismic input functions.

The finite element model effectively reproduces the **stiffness, mass distribution, and overall geometry** of the real structure, allowing for accurate evaluation of **internal forces, displacements, and dynamic response**. The truss configuration ensures efficient load transfer within the structure, while the combination of longitudinal and transverse bracing provides global stability under both static and seismic loading conditions.

In this bridge, the supports are equipped with **Teflon (PTFE) sliding bearings**. These bearings are designed to **allow horizontal displacement of the deck** while providing adequate vertical load-carrying capacity. Teflon is commonly used in sliding bearings due to its **very low friction coefficient** and **excellent chemical stability**. However, it is important to note that **Teflon has limited mechanical strength**, particularly in compression and shear.

Under service and dynamic load conditions, the PTFE layer behaves elastically only within a restricted stress range. Once the applied stresses exceed the allowable capacity of the Teflon layer, its stiffness decreases significantly and it can no longer resist additional horizontal forces. At this stage, the bearing transitions from elastic deformation to **pure sliding mode**, allowing the bridge deck to move freely in the horizontal direction.

This controlled sliding mechanism is intentional:

- Vertically, the bearing provides **high stiffness** and safely carries the permanent and variable loads from the deck.
- Horizontally, once the resistance limit of the Teflon surface is exceeded, the bearing **loses its ability to develop further shear force**, and the deck **continues to move with very low friction**.

Such behavior is critical for protecting the structure from excessive stress concentrations, thermal expansion forces, pedestrian-induced vibrations, and accidental overloads. It ensures that the bridge deck can deform or displace without overstressing the substructure or the bearing components.

2.2 MATERIAL MODELLING

The materials that make up the structure are assumed to exhibit linear-elastic behavior; the properties of these elements are reported in the summary tables in the following sections on input data. For the St. Andrew's cross bracing members with high slenderness, the model was simplified by representing only a single element and omitting stability checks, in order to ensure that stiffness and strength are provided only by the tension diagonal.

2.3 STEEL PROFILE MODELLING

The sections were included in the FEM model with their exact geometry. Linear beam elements, truss elements, and shell elements are used.

2.4 IDEALIZATION OF ACTION

In accordance with the above-mentioned standards, the following actions were considered in the calculations:

- ✓ structural self-weight
- ✓ permanent loads carried by the main structure
- ✓ variable loads (crowd live load)
- ✓ wind
- ✓ thermal deformations
- ✓ seismic action

Each action is applied to the structure through:

- ✓ the element self-weight, automatically calculated by the software by applying the unit weight.
- ✓ nodal masses or uniformly distributed masses on beam and shell elements (Load Patch: loaded areas) to simulate permanent and variable loads.
- ✓ point, line, and surface loads.
- ✓ imposed support settlements at nodes.

2.5 TYPE OF ACTION

A linear-elastic analysis was performed. In addition, a linear dynamic seismic analysis (modal analysis) was carried out to verify the seismic load cases. Global behavior is considered verified if the individual members are verified. The analysis was performed in accordance with the above-mentioned standards and the principles of structural engineering (structural mechanics).

2.6 CRITERIA FOR VERIFICATION

2.6.1 Resistance verification

The resistance checks follow the provisions for ultimate limit state design set out in Chapter 6 of UNI EN 1993-1-1. The verification criterion requires the design effect of actions, S_{Ed}, to be less than or equal to the design resistance, S_{Rd}: S_{Ed}/S_{Rd}<1

In particular, in the case of combined axial and bending effects, the conservative approximation in which the utilization ratios are summed linearly is adopted, as in § 6.2.1(7):

$$\frac{N_{\{Ed\}}}{N_{\{Rd\}}}+\frac{M_{\{1,Ed\}}}{M_{\{1,Rd\}}}+\frac{M_{\{2,Ed\}}}{M_{\{2,Rd\}}}\leq 1$$

The partial safety factors used are divided into resistance checks and stability (buckling) checks. The values of $\gamma_{M0}$and $\gamma_{M1}$are reported below:

$$\gamma_{M0}= 1.05$$

$$\gamma_{M1} = 1.05$$

The ultimate limit that can be reached for Class 1 and 2 sections is the fully plasticized section, whereas for Class 3 sections only elastic verification is permitted. The limit state is therefore associated with exceeding the yield strength in the most highly stressed fiber of the section. The ultimate axial resistance, which is the same for both elastic and plastic analysis, is calculated using the following relationship:

$$N_{\{Rd\}} = N_{\{Rd,pl\}} = \frac{A\, f_y}{\gamma_{M0}}$$

For the ultimate bending resistance, the section modulus $W$is taken as the plastic modulus (W_{pl}) for Class 1 and 2 sections, and as the elastic modulus $W_{el,\min}$ for Class 3 sections.

According to the provisions of § 6.2.8, the presence of shear forces exceeding 50% of the design shear resistance is accounted for by introducing a reduction factor in the material yield strength:

$$f\_\{y,v\} = 1 - \rho$$

$$\rho = \left(\frac{2V_{\{Ed\}}}{V_{\{pl,Rd\}}} - 1\right)^2$$

Eventually

$$M_{\{1Rd\}} = M_{\{V,Rd\}} = \frac{W \cdot (1 - \rho\,) f_y}{\gamma_{M0}}$$

Shear resistance checks (§ 6.2.6) are distinguished between Class 1 and 2 sections, for which the maximum ratio between the applied and resisting actions is calculated, and Class 3 sections, for which the safety factor is calculated as a stress ratio:

$$\frac{V_{\{Ed\}}}{V_{\{Rd\}}} <= 1 \text{ calss 1 and 2}$$

$$\frac{ted}{\frac{f_y}{(\sqrt[3]{3}\gamma_{M0})}} <= 1$$

where $V_{Rd} = V_{pl,Rd}$. In the presence of combined torsional effects, the reduction factors prescribed in § 6.2.7(9) are applied. Torsion checks (§ 6.2.7) are carried out by calculating the shear stresses at significant points of the cross-section according to the rules of Structural Engineering (Structural Mechanics).

In particular, for open sections (Saint-Venant torsion):

$$tT = \frac{T \cdot s}{J_t}$$

For closed sections (Bredt):

$$t\,T = \frac{T}{2\backslash Omega \cdot s}$$

In determining the stress T_{Ed}, the stresses due to torsion are added to those due to shear forces.

$$\frac{\left(t_{\{V1,Ed\}}\right) + \left(t_{\{V2,Ed\}}\right) + \left(t_{\{T,Ed\}}\right)}{\frac{f_y}{\sqrt[3]{3}\gamma_{M0}}} <= 1$$

2.6.2 STABILITY VERIFICATION

Stability checks for compressed steel members are carried out in accordance with the provisions of § 6.3 of UNI EN 1993-1-1. The standard requires accounting for flexural buckling about axes 1 and 2 and for lateral-torsional buckling (LT) by means of reduction factors χ.

A compressed member is verified if the following inequalities are satisfied:

$$\frac{N_{\{Ed\}}}{\chi_{1N_{\{b,Rd\}}}} + \frac{k_{\{yy\}(M_{\{1,Ed\}})}}{\chi_{\{LT\}M_{\{1,b,Rd\}}}} + \frac{k_{\{yz\}(M_{\{2,Ed\}})}}{M_{\{2,b,Rd\}}} <= 1$$

$$\frac{N_{\{Ed\}}}{\chi_{2N_{\{b,Rd\}}}} + \frac{k_{\{zy\}(M_{\{1,Ed\}})}}{\chi_{\{LT\}M_{\{1,b,Rd\}}}} + \frac{k_{\{zz\}(M_{\{2,Ed\}})}}{M_{\{2,b,Rd\}}} <= 1$$

Where:

$N_{1,ED}$, $M_{1,Ed}$, and $M_{2,Ed}$ are the maximum internal forces/actions in the member; $N_{b,Rd}$, $M_{b,1,Rd}$, and $M_{b,2,Rd}$ are the design resistances, calculated using the partial factor γ_{M1}; χ are the reduction factors for flexural and torsional instability (buckling).

k_{yy}, k_{yz}, k_{zy}, and k_{zz} are the interaction factors. Ludi calculates these factors using both methods (A and B) proposed by the standard in the annexes.

For the purpose of verifying a compressed member, the following slenderness parameters are defined:

$\lambda_1 = \ell_{0,1}/i_1$ $\lambda_2 = \ell_{0,2}/i_2$ $\lambda_\theta = \ell_{0,\theta}/i_{min}$

where $\lambda_0$is the member's effective buckling length and $i$is the radius of gyration of the cross-section.

To define the individual reduction factors χ, it is necessary to calculate the equivalent slenderness (as a function of the critical load) and the coefficient (as a function of the critical load and the material imperfection factor α).

$$\lambda = sqrt\left(\frac{A \cdot f_y}{N_{\{cr\}}}\right)$$

In the formulas used, the imperfection factors $\alpha$and $\alpha_{LT}$are tabulated in Tables 6.1 and 6.3 depending on the steel grade and the section type in Eurocode; the critical loads are calculated using the well-known relationship:

$$N_{\{cr\}} = \frac{\pi^{2(EA)}}{\lambda^2}$$

For the calculation of M_{cr}, the Eurocode does not specify a calculation method; it only requires that it incorporates the actual moment distribution and the end restraints applied at the member ends. In this report, the critical moment is calculated following the guidance of the British standard BS 5950:2000, *Structural use of steelwork in building*, Lateral torsional buckling.

$$M_{\{cr\}} = \frac{P_b \cdot W}{m_{\{LT\}}}$$

where $p_b$is the buckling stress, $W$is the elastic or plastic section modulus depending on the section class, and $m_{LT}$is the equivalence factor between a beam subjected to a constant bending moment and one with an arbitrary moment distribution.

$$m_{\{LT\}} = 0.2 + \frac{0.15M_2 + 0.5M_3 + 0.15M_4}{M_{\{max\}}} >= 0.44$$

Here, M_2, M_3, and $M_4$are the bending moments calculated respectively at ¼ λ, ½ λ, and ¾ λ.

The buckling stress $p_b$is tabulated (BS 5950 Tables 16 and 17) as a function of the material, the fabrication type (rolled or welded), and the member's equivalent slenderness λ_{LT}.

$$\lambda_{LT} = u v \lambda \sqrt{\beta_W}$$

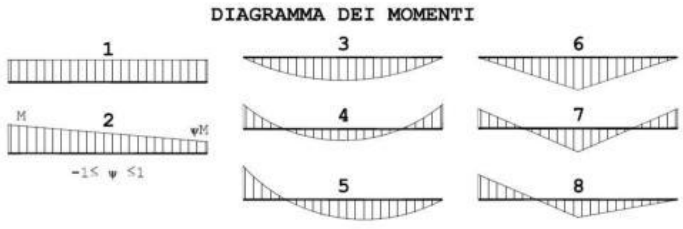

2.6.3 VERIFICATION OF NODES

All structures were analyzed using linear-elastic analysis to determine the static internal forces. Global behavior is considered verified if the individual members are verified. The analysis was performed in accordance with the above-mentioned standards, applying the principle of superposition of effects in the linear range and the principles of structural engineering (structural mechanics).

2.6.3.1 RESISTANCE VERIFICATION OF WELDS

The stress in the throat section of the fillet weld is determined in accordance with EN 1993-1-8, Clause 4.5.3:

$$\sigma_{w,Ed} = \sqrt{\sigma_{\perp}^2 + 3\left(\tau_{\perp}^2 + \tau_{\parallel}^2\right)}$$

$$\sigma_{w,Rd} = \frac{f_u}{\beta_w \gamma_{M2}}$$

$$0.9\,\sigma_{w,Rd} = \frac{f_u}{\gamma_{M2}}$$

$$U_t = \min\left(\frac{\sigma_{w,Ed}}{\sigma_{w,Rd}};\ \frac{\sigma_{\perp}}{0.9\,\sigma_{w,Rd}}\right)$$

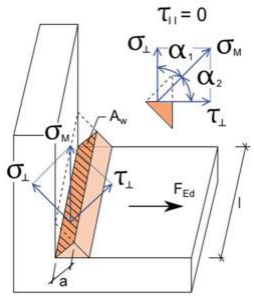

Figure 2-7 Weld scheme

2.6.3.2 Resistance verification of bolts

Tensile resistance:

$$F_{\{t,Rd\}} = \frac{0.9 f_{\{ub\}A_S}}{\gamma_{M0}}$$

Plate punching resistance (EN 1993-1-8):

$$B_{\{p,Rd\}} = 0.6 * \pi * d_m * t_p * f_u * gamma_{\{M2\}}$$

Shear resistance:

$$F_{v,Rd} = \alpha_v \cdot f_{ub} \cdot A / \gamma_{M_2}$$

Bearing resistance (EN 1993-1-8):

$$Fb,Rd = k_1 \cdot a_b \cdot f_u \cdot d \cdot t / \gamma_{M_2}$$

Tensile utilization ratio [%]:

$$U_{tt} = F_{t,Ed} / Min\,(F_t, R_d, B_p, R_d)$$

Shear utilization ratio [%]:

$$U_{ts} = V / Min\,(F_v, R_v, F_b, R_d)$$

Shear–tension interaction [%]:

$$U_{tts} = (V/F_{v,Rd}) + (F_{t,Ed} / 1.4\,F_t, R_d)$$

where:

- ✓ A – gross cross-sectional area of the bolt, or the tensile stress area of the bolt if the threads are included in the shear plane.
- ✓ As - bolt tensile stress area;
- ✓ $F_{\{t,Rd\}}$ – ultimate tensile strength of the bolt material;
- ✓ d_m- bolt head diameter;
- ✓ d -bolt diameter;
- ✓ t_p– plate thickness;
- ✓ f_u – ultimate tensile strength of the steel;
- ✓ $\alpha_v = 0.6$for bolt property classes (4.6, 5.6, 8.8);
  $\alpha_v = 0.5$for bolt property classes (4.8, 5.8, 6.8, 10.9);
- ✓ $k_1 \leq 2.5$– from Table 3.4;
- ✓ $\alpha_b \leq 1.0$– from Table 3.4;
- ✓ $F_{t,Ed}$– design bolt tension;
- ✓ V – bolt shear resistance.

2.7 STRUCTURAL IDEALIZATION AND BOUNDARY CONDITION

The structure was idealized by neglecting the contribution of members whose stiffness and strength are negligible compared to the main structural components. A three-dimensional model of all elements forming the primary structure was therefore developed.

The boundary conditions are provided through six elastic stiffness constants.

The FEM model therefore consists of the following elements:

- ✓ nodes;
- ✓ beam: linear elements;
- ✓ truss: linear elements resisting only axial tension and compression;
- ✓ load patch: planar load-distribution elements.

Because we are interested in vibration of only block 4 that is in the following image external boundaries and internal boundaries (beam and release), elastic links as follows :

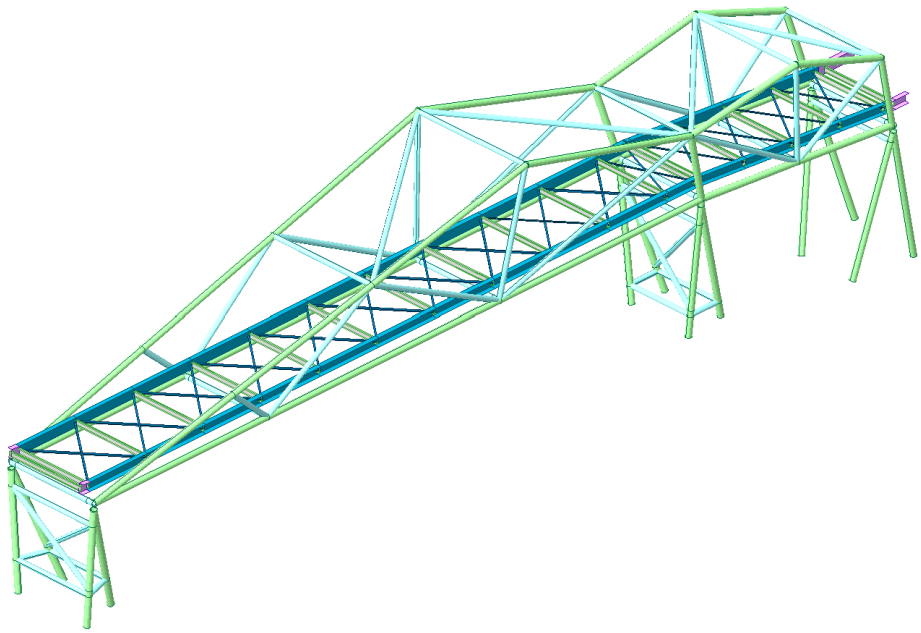

Figure 2-8 FEM model

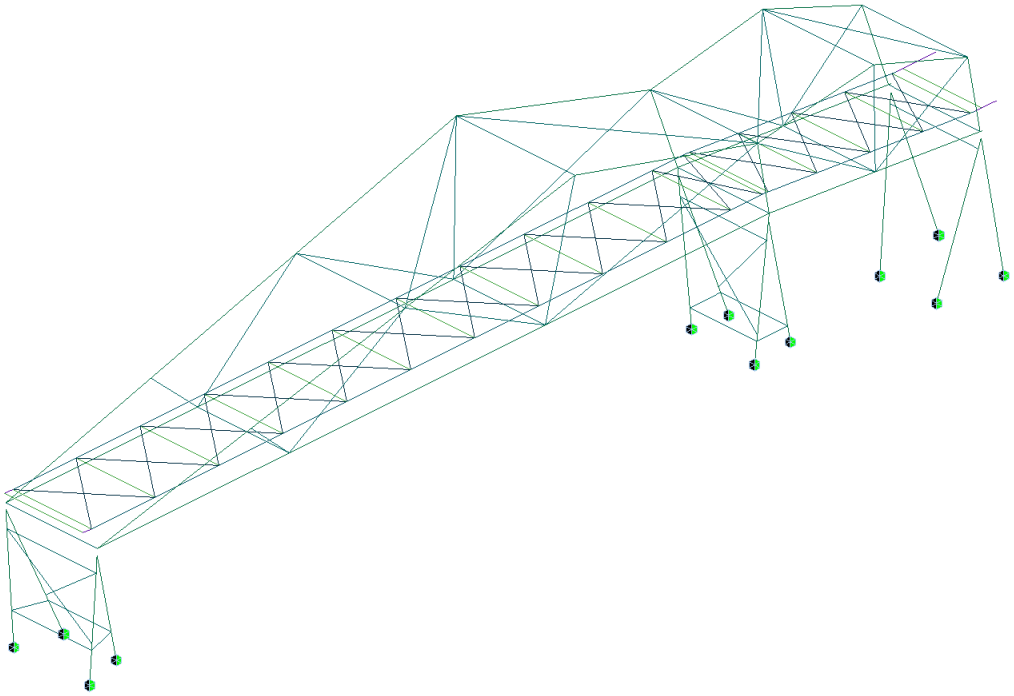

Figure 2-9 External boundaries

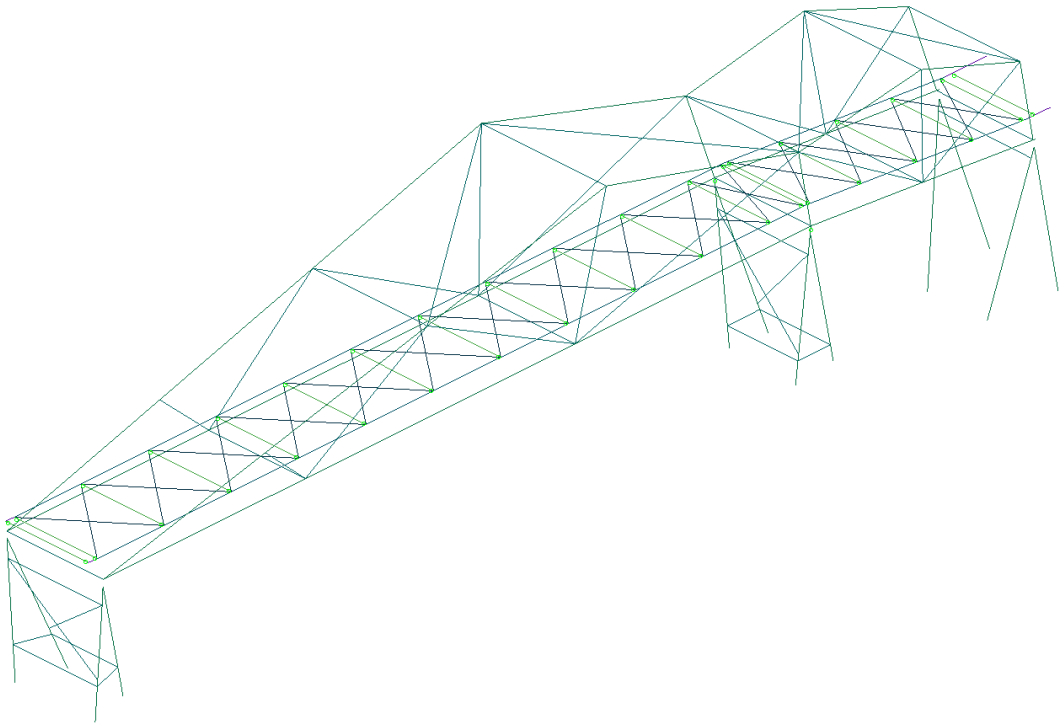

Figure 2-10 Internal boundaries

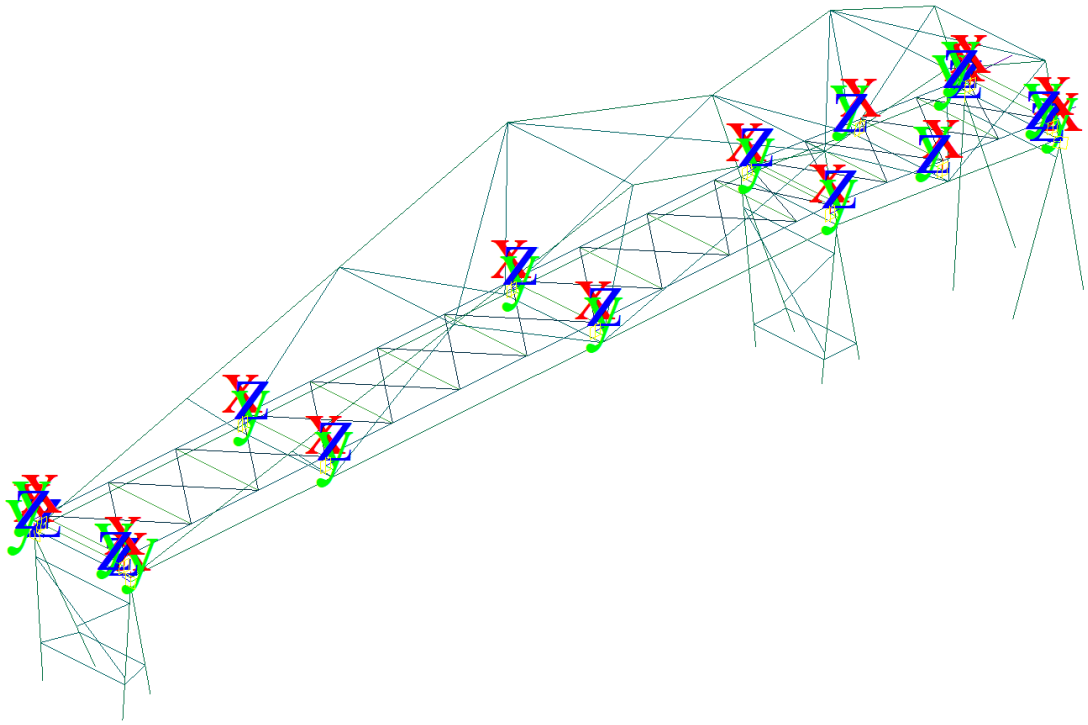

Figure 2-11 Elastic links

2.8 REGULATION AND REFERENCE DOCUMENTS

The structural analysis of the structure under consideration will be carried out using the usual methods of Structural Engineering (Structural Mechanics) and in accordance with the regulations and laws currently in force in Europe.

• **CNR-DT207/2008** – Guidelines for the evaluation of wind actions and their effects on structures
• **UNI EN 1990:2006 – Eurocode 0**: Basis of structural design
• **UNI EN 1991-1-1:2004 – Eurocode 1**: Actions on structures – Part 1-1: General actions – Densities, self-weight, imposed loads for buildings
• **UNI EN 1991-1-4:2010 – Eurocode 1**: Actions on structures – Part 1-4: General actions – Wind actions
• **UNI EN 1992-1-1:2015 – Eurocode 2**: Design of concrete structures – Part 1-1: General rules and rules for buildings
• **UNI EN 1993-1-1:2014 – Eurocode 3**: Design of steel structures – Part 1-1: General rules and rules for buildings
• **UNI EN 1993-1-8:2005 – Eurocode 3**: Design of steel structures – Part 1-8: Design of joints
• **UNI EN 1993-1-9:2005 – Eurocode 3**: Design of steel structures – Part 1-9: Fatigue
• **UNI EN 1998-1:2013 – Eurocode 8**: Design of structures for earthquake resistance – Part 1: General rules, seismic actions and rules for buildings
• **Eurocode National Annexes**
• **Ministerial Decree of January 17, 2018** – Technical Standards for Construction
• **Explanatory Circular of January 21, 2019 No. 7/C.S.LL.PP** – Instructions for the application of the updated Technical Standards for Construction referred to in the Ministerial Decree of January 17, 2018

•**The Sétra** footbridge design.

2.9 CALCULATION SOFTWARE

2.9.1 Structural steel analysis

The finite element modeling was carried out using the structural analysis software **Midas Gen**, developed by **MIDAS IT Co., Ltd.** (South Korea) and widely used for the analysis and design of building and bridge structures.

Midas Gen enables both **linear and nonlinear static and dynamic analyses** of three-dimensional structures with nodes having **six degrees of freedom**, employing an advanced **finite element method (F.E.M.) solver**. The software allows the modeling of **beam, truss, plate, and shell elements**, as well as the definition of **support, boundary conditions, and load combinations** in compliance with **Eurocodes and other international standards**.

Loads can be applied as **nodal forces, distributed loads, surface loads, or self-weight**, and the program provides powerful tools for **structural verification, design, and optimization** of **steel, concrete, and composite structures**.

2.9.2 Joints of steel structure

The verification of the joints was carried out using the program **Idea StatiCa 23.1**, which is capable of evaluating the strength of standard steel connections in compliance with **Eurocode 3**.

Idea StatiCa®
Calculate yesterday's estimates

2.10 UNITS

The units of measurement used, unless otherwise specified, are understood as follows:

The units of measurement used, unless otherwise explicitly specified, are to be understood as follows:

Length:	**m**
Time:	**s**
Mass:	**kg**
Force:	**kN**
Stress:	**MPa**
Moments:	**kN·m**
Area:	**m²**
Elastic/plastic section modulus:	**m³**
Moment of inertia:	**m⁴**
Cross-sections:	**m²**

2.11 MECHANICAL PROPERTY OF MATERIAL

The following mechanical properties are used in the calculations for the **metal structure** related to the **footbridge**.

2.11.1 Structural steel

Structural steel S355 J2WP – CORTEN type

- ✓ Ultimate strength: **f_u = 5100 kg/cm²**
- ✓ Yield strength: **f_y = 3550 kg/cm²**
- ✓ Modulus of elasticity (mean value): **E_{sm}=2,100,000kg/cm²**

Bolts grade 8.8

- ✓ Ultimate strength: **f_{ub} = 8000 kg/cm²**
- ✓ Yield strength: **f_{yb} = 6400 kg/cm²**

The following steel will be used:
Structural steel S460NH

- ✓ Ultimate strength: **f_u = 5600 kg/cm²**
- ✓ Yield strength: **f_y = 4600 kg/cm²**
- ✓ Modulus of elasticity (mean value): **E_{sm} = 2,100,000 kg/cm²**

✓ **Reinforced Concrete**
✓ **Foundation structures – Concrete class C25/30**

- ✓ Characteristic cubic compressive strength: **R_{ck} = 300 kg/cm²**
- ✓ Characteristic cylindrical compressive strength: **f_{ck} = 250 kg/cm²**
- ✓ Design cylindrical compressive strength: **f_{cd} = 142 N/mm²**
- ✓ Secant modulus of elasticity: **E = 312,000 kg/cm²**
- ✓ Reduction coefficient for long-term strength: **α_{cc} = 0.85**
- ✓ Partial safety factor for concrete: **γ_c = 1.50**
- ✓ Exposure class: **XC2**, cover thickness: **5 cm**

A cement grout (to be injected) will also be provided, with a cubic compressive strength of 45 MPa at 28 days and pumped at a maximum pressure of 20 bar. Its characteristics are as follows:

✓ **Cement grout – Concrete class C35/45**

- ✓ Characteristic cubic compressive strength: **R_{ck} = 450 kg/cm²**
- ✓ Characteristic cylindrical compressive strength: **f_{ck} = 350 kg/cm²**
- ✓ Design cylindrical compressive strength: **f_{cd} = 198 N/mm²**
- ✓ Secant modulus of elasticity: **E = 312,000 kg/cm²**

✓ **Steel B 450 C**

- ✓ Characteristic tensile strength: **f_{tk} = 5400 kg/cm²**
- ✓ Characteristic yield strength: **f_{yk} = 450 kg/cm²**

- ✓ Design yield strength: **f_{yd} = 391 kg/cm²**
- ✓ Mean modulus of elasticity: **E_{sm} = 210,000 kg/cm²**
- ✓ Partial safety factor for steel: **γ_s = 1.05**

2.11.2 Exposure class and concrete cover

- ✓ The characteristics and performance of concrete can be significantly influenced by the **environmental conditions** of the location where the structure will be built.
  Depending on these conditions, the following parameters are prescribed: **strength class**, **water/cement ratio (w/c)**, and **concrete cover**.
- ✓ The **UNI EN 206-1 standard** defines the following **exposure classes**:

Table 4.4N: Values of minimum cover, $c_{min,dur}$, requirements with regard to durability for reinforcement steel in accordance with EN 10080.

Environmental Requirement for $c_{min,dur}$ (mm)							
Structural Class	Exposure Class according to Table 4.1						
	X0	XC1	XC2 / XC3	XC4	XD1 / XS1	XD2 / XS2	XD3 / XS3
S1	10	10	10	15	20	25	30
S2	10	10	15	20	25	30	35
S3	10	10	20	25	30	35	40
S4	10	15	25	30	35	40	45
S5	15	20	30	35	40	45	50
S6	20	25	35	40	45	50	55

Table 2-1 Environmental requirements $C_{min,dur}$

For the calculation of the concrete cover, **Eurocode 2 (EC2)** proposes the following formula:

$$c_{nom} = c_{min} + \Delta c_{dev}$$

The c_{min} value must be equal to the greatest of the following:

$$c_{min} = \text{MAX}\ (c_{min,b}\ ;\ c_{min,dur}\ ;\ 10\ \text{mm})$$

where:

- ✓ $c_{min,b}$ = minimum concrete cover required for **reinforcement bond**, equal to the **nominal diameter of the bars**;
- ✓ $c_{min,dur}$ = minimum concrete cover related to **environmental conditions (durability)** and the **exposure class** of the structure.

  For a structure with a nominal service life of 50 years, the recommended structural class is class S4.
  The minimum concrete cover required is 25 mm for foundation structures. To this, the recommended additional value Δc_{dev} of 10 mm must be added for a cast-in-place structure.

Based on good practice for underground structures, a total cover of 50 mm is adopted for the foundation elements.

Structural class	Design life (years)	Typology
S3	50	Ordinary buildings and structures
S4	100	Major civil engineering works (e.g., bridges, tunnels)
S5	200	Monumental or special long-life structures

Table 2-2 Design life

Table 4.3N: Recommended structural classification

Structural Class							
Criterion	**Exposure Class according to Table 4.1**						
	X0	XC1	XC2 / XC3	XC4	XD1	XD2 / XS1	XD3 / XS2 / XS3
Design Working Life of 100 years	increase class by 2	increase class by 2	increase class by 2	increase class by 2	increase class by 2	increase class by 2	increase class by 2
Strength Class [1) 2)]	≥ C30/37 reduce class by 1	≥ C30/37 reduce class by 1	≥ C35/45 reduce class by 1	≥ C40/50 reduce class by 1	≥ C40/50 reduce class by 1	≥ C40/50 reduce class by 1	≥ C45/55 reduce class by 1
Member with slab geometry (position of reinforcement not affected by construction process)	reduce class by 1	reduce class by 1	reduce class by 1	reduce class by 1	reduce class by 1	reduce class by 1	reduce class by 1
Special Quality Control of the concrete production ensured	reduce class by 1	reduce class by 1	reduce class by 1	reduce class by 1	reduce class by 1	reduce class by 1	reduce class by 1

Table 2-3 Structural class

2.11.3 execution class

Regarding the definition of the Execution Class (EXC2) for the structure in question, the following Consequence Class is defined.

Consequence Class CC2: UNI EN 1990 – Annex B (Paragraph B.3.1)

Table B1 - Definition of consequences classes

Consequences Class	**Description**	**Examples of buildings and civil engineering works**
CC3	**High** consequence for loss of human life, *or* economic, social or environmental consequences **very great**	Grandstands, public buildings where consequences of failure are high (e.g. a concert hall)
CC2	**Medium** consequence for loss of human life, economic, social or environmental consequences **considerable**	Residential and office buildings, public buildings where consequences of failure are medium (e.g. an office building)
CC1	**Low** consequence for loss of human life, *and* economic, social or environmental consequences **small or negligible**	Agricultural buildings where people do not normally enter (e.g. storage buildings), greenhouses

Table 2-4 Consequence classification

Considering the Consequence Class CC2 and the type of loading (quasi-static or seismic), the following table allows the determination of the Execution Class EXC2: UNI EN 1993-1-1 – Annex C (Paragraph C.2.2)

Table C.1 — Choice of execution class (EXC)

Reliability Class (RC) or Consequences Class (CC)	Type of loading	
	Static, quasi-static or seismic DCL[a]	Fatigue[b] or seismic DCM or DCH[a]
RC3 or CC3	EXC3[c]	EXC3c
RC2 or CC2	EXC2	EXC3
RC1 or CC1	EXC1	EXC2

[a] Seismic ductility classes are defined in EN 1998-1: Low = DCL; Medium = DCM; High = DCH.
[b] See EN 1993-1-9.
[c] EXC4 may be specified for structures with extreme consequences of structural failure.

Table 2-5 Execution class

2.12 REFERENCE SYSTEM

2.12.1 Global reference system

X axis: Along the longitudinal direction

Y axis: Along the transverse direction

Z axis: Vertical direction (“+” from the ground toward the sky)

Multiple global reference systems have been generated, aligned with the longitudinal axis of the different parts of the footbridge and with the transverse plane of the portals, in order to assign the supports and constraints in the correct directions.

2.12.2 Local reference system

The local coordinate system is defined with respect to the element axes according to the following convention.

The beam element is defined by nodes N1 and N2 as shown below:

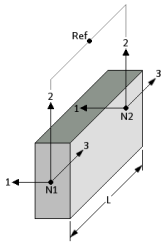

Principal coordinate system of a beam.

For a beam with a reference node, the principal axis system, shown above is defined as follows:

- 3 axis is directed from node N1 to node N2.
- 2 axis is normal to the 3 axis and lies in the plane formed by nodes N1, N2 and the reference node Ref. It is positive towards the side on which node Ref lies.
- 1 axis completes the right hand axis system.

Figure 2-12 Beam reference system

Reference system for column elements.

The default local axis system for these elements is shown below and is constructed from the nodes N1, N2, N3 for the triangle and N1, N2, N3, N4 for the quadrilateral element as follows:

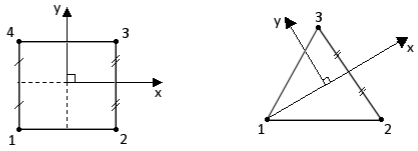

Local axis for 3 and 4 noded plate elements.

- Positive local x joins the mid-sides from side (N1,N4) to side (N2,N3) for the quadrilateral element, or goes from N1 to bisect side (N2,N3) for the triangle.
- Positive local y is normal to the local x axis directed away from side (N1,N2) and lies in the plane of the plate.

Figure 2-13 Local reference system of columns

3 GEOTECHNICAL CHARACTERIZATION AND FOUNDATION VERIFICATION

3.1 SCOPE OF GEOTECHNICAL STUDY

This chapter summarizes the **geotechnical investigations**, the **interpretation of the subsoil stratigraphy**, and the **geotechnical model** adopted for design. It also reports the **foundation solution** (micro piles + pile caps) and the **verification results** carried out for the project foundations, including bearing capacity, settlements, and lateral resistance. The content is based on the official "Relazione Geotecnica" developed from in-situ and laboratory tests.

3.2 INVESTIGATION AND AVAILABLE DATA

A dedicated investigation campaign was performed to characterize the soil within the "**volume significativo**" (the zone of soil significantly affected by the structure and foundations). The campaign included:

- ✓ **2 continuous core boreholes** (sondaggi a carotaggio continuo)
- ✓ **6 continuous dynamic super-heavy penetration tests (DPSH)**
- ✓ **Seismic/geophysical tests**: **2 MASW** (surface-wave method) and **2 HVSR** (H/V spectral ratio)
- ✓ **Laboratory testing** on **10 disturbed/remolded soil samples**, performed by an authorized laboratory (GD Test s.r.l., Torino).

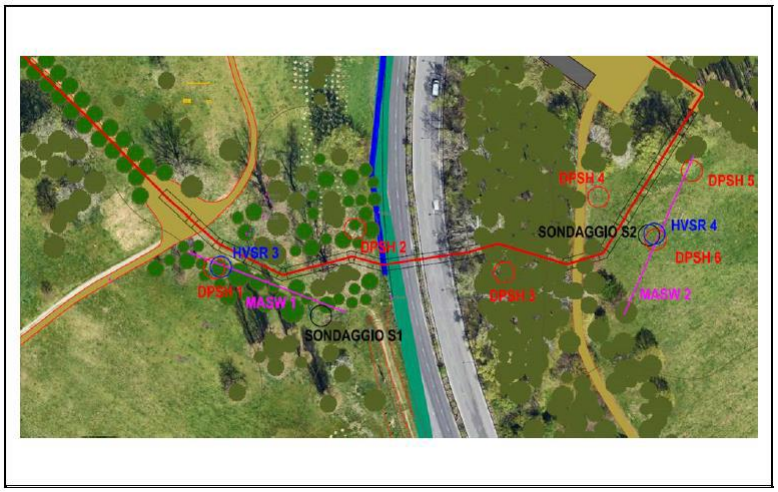

Figure 3-1 Construction blocks

These tests allow defining: the stratigraphy and thickness of layers, the soil density/consistency trends with depth (mainly from DPSH), and a seismic soil category for structural seismic action definition.

3.3 GEOLOGICAL AND GEOTECHNICAL SETTING AND STRATIGRAPHY

Based on boreholes and DPSH tests, the subsoil is interpreted as a sequence typical of **alluvial environments** (Po River context), with superficial anthropogenic materials followed by natural alluvial deposits.

Result of DPSH 1 for block 1

SPT2		
36 dati		
n°	Quota[cm]	N
1	0	0
2	-30	6
3	-60	8
4	-90	5
5	-120	4
6	-150	4
7	-180	4
8	-210	3
9	-240	4
10	-270	3
11	-300	5
12	-330	7
13	-360	6
14	-390	3
15	-420	2
16	-450	7
17	-480	9
18	-510	16
19	-540	23
20	-570	23
21	-600	17
22	-630	18
23	-660	29
24	-690	22
25	-720	22
26	-750	16
27	-780	11
28	-810	12
29	-840	22
30	-870	27
31	-900	27
32	-930	16
33	-960	9
34	-990	17
35	-1020	41
36	-1050	72

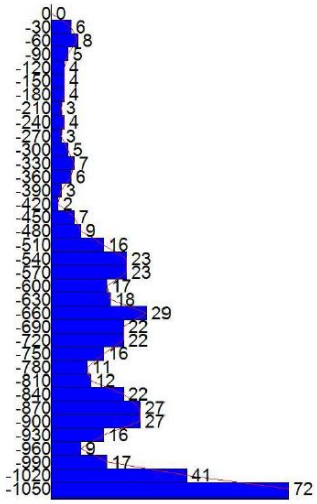

Figure 3-2 DPSH1 block 1

Result of DPSH 2 for block 3:

SPT2	
36 dati	
n°	Quota[cm] N
1	0 0
2	-30 6
3	-60 8
4	-90 5

5	-120	4
6	-150	4
7	-180	4
8	-210	3
9	-240	4
10	-270	3
11	-300	5
12	-330	7
13	-360	6
14	-390	3
15	-420	2
16	-450	7
17	-480	9
18	-510	16
19	-540	23
20	-570	23
21	-600	17
22	-630	18
23	-660	29
24	-690	22
25	-720	22
26	-750	16
27	-780	11
28	-810	12
29	-840	22
30	-870	27
31	-900	27
32	-930	16
33	-960	9
34	-990	17
35	-1020	41
36	-1050	72

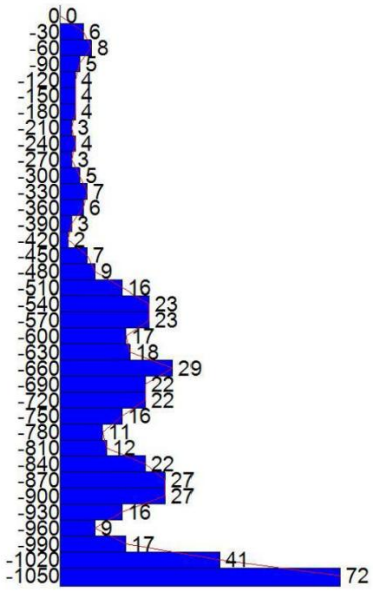

Figure 3-3 DPSH2 block 3

Result of DPSH 3 for block 3

SPT1		
34 dati		
n°	Quota[cm]	N
1	0	0
2	-30	11
3	-60	13
4	-90	19
5	-120	17
6	-150	5
7	-180	3
8	-210	1
9	-240	1
10	-270	3
11	-300	5
12	-330	19
13	-360	37
14	-390	42
15	-420	21
16	-450	15
17	-480	23
18	-510	35
19	-540	34
20	-570	21
21	-600	20
22	-630	23
23	-660	35
24	-690	64
25	-720	70
26	-750	70
27	-780	70
28	-810	70
29	-840	70
30	-870	70
31	-900	70
32	-930	70
33	-960	70
34	-990	70

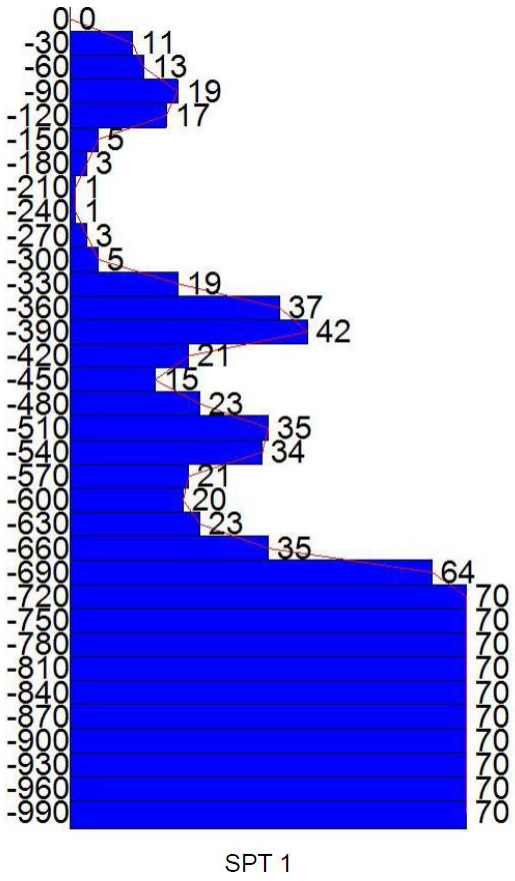

Figure 3-4 DPSH3 block 3

3.3.1 Superficial layer (topsoil + anthropic fill) - Complesso 1

Below a thin topsoil cover, the report identifies **fill/anthropic materials** made of **sandy–silty to sandy–gravelly soils**, containing fragments of bricks, stones, and anthropic debris (“matrix supported”). Their density varies from loose to medium dense.

The thickness of this fill layer is **variable**:

- minimum about **0.5 m** in some locations (e.g., CAR2, DPSH2, DPSH6),
- maximum about **1.5–2.0 m** in other points (e.g., CAR1, DPSH1),
- and it appears **almost absent** in DPSH-5.

3.3.2 Intermediate alluvial sands - Complesso 2A

Under the fill, the report describes **recent Holocene fluvial deposits**, mainly **fine to very fine sands**, often **silty**, sometimes weakly clayey and weakly gravelly, with **very loose to loose** density state. This unit is found below Complex 1 and extends down to depths that vary approximately from **~2.0 m** to **~4.5–5.0 m** from ground level, depending on the investigation point.

3.3.3 Deep alluvial / fluvio-glacial gravels - Complesso 2B

From the bottom of the sandy unit down to the maximum investigated depth (**15 m**), the report indicates **coarse alluvial/fluvio-glacial deposits** composed of **gravelly layers** (gravel–sand mixtures, sometimes with silt/clay fraction and cobbles). Cobbles can reach **10–15 cm** in size. The density is described as **medium dense to very dense**, and DPSH tests often show **refusal** due to large coarse clasts.

A relevant note for design: **no cemented hard conglomerate levels** were encountered.

3.4 INTERPRETATION OF DPSH PENETRATION RESULTS (SOIL DENSITY TREND)

The DPSH tests provide an N-value trend with depth that is consistent with the stratigraphic interpretation:

- In shallow layers (fill + loose sands), N-values are relatively low, reflecting a **loose state**.
- At greater depths, the N-values increase significantly, reflecting the **transition to dense gravels**, where refusal can occur.

The report explicitly identifies which DPSH tests are used as reference for the foundation blocks (e.g., **DPSH1 for Block 1**, **DPSH2 and DPSH3 for Block 3**), ensuring that each foundation verification uses the most relevant local soil profile.

3.5 GEOTECHNICAL MODEL AND DESIGN PARAMETERS

To perform design and verification, the soil is simplified into representative complexes with assigned parameters. The report provides the following design values.

3.5.1 Complex 1 — Fill + loose fine sands (very loose to lose)

- ✓ Natural unit weight: γ_n **= 1.8 t/m³**
- ✓ Friction angle: **φ = 25°**
- ✓ Effective cohesion: **c' ≈ 0 kPa** (conservative)
- ✓ Elastic modulus: E_s **= 2–4 MPa**

3.5.2 Complex 2B — Dense alluvial/fluvio-glacial gravels

- ✓ Natural unit weight: γ_n **= 1.95 t/m³**
- ✓ Friction angle: **φ = 36°**

- ✓ Effective cohesion: **c' ≈ 0 kPa** (conservative)
- ✓ Elastic modulus: **E_s = 5–15 MPa**

Complex 1 represents the weaker near-surface soils (fill + loose sands), while Complex 2B represents the competent deeper gravelly deposit with higher stiffness and shear strength, suitable for mobilizing micro pile resistance.

3.6 SEISMIC SITE CLASSIFICATION (INPUT FOR STRUCTURAL SEISMIC ACTION)

The report defines the seismic classification following national references and regional updates:

- ✓ The Municipality of **Torino** is classified as **Seismic Zone 3**.
- ✓ Based on MASW/HVSR investigations, the soil profile is classified as **Soil Category E** for seismic action definition (profile comparable to categories C or D but with bedrock/substrate depth ≤ 30 m).
- ✓ **Topographic Category T1** (flat ground or slopes with average inclination **i ≤ 15°**).

These classifications are the geotechnical inputs needed by the structural model to define design spectrum and amplification factors.

3.7 HYDROGEOLOGICAL CONDITIONS (GROUNDWATER)

The report identifies a **shallow groundwater table**:

- ✓ Average depth about **4.0–4.3 m** below ground in correspondence of piezometer **CAR1** (west of Via Don Sturzo),
- ✓ about **2.3–2.4 m** in correspondence of **DPSH4** (east of Via Don Sturzo).

Groundwater flow direction is approximately **SW → NE**, with a mean hydraulic gradient around **0.004**, consistent with the drainage influence of **Po River** and **Stura di Lanzo**.

The report also warns that during intense/prolonged rainfall, the piezometric surface can rise **close to ground level**, which is important for construction stages and durability considerations.

3.8 FOUNDATION SOLUTION ADOPTED

Considering the mechanical characteristics of the soil, the project adopts a deep foundation solution using micro piles:

- ✓ **Micro piles**: diameter **5.2 cm**, thickness **2.6 cm**, length **7.00–8.00 m**
- ✓ **Pile caps / plinths (plinti)** founded on micro piles

A key design assumption stated in the report: **the foundation bearing capacity is assumed to be absorbed by the micro piles** (i.e., the piles are the primary load-transfer mechanism rather than shallow soil bearing).

3.9 VERIFICATION CRITERIA AND DESIGN APPROACH (NTC 2018)

3.9.1 General requirement at ULS

For Ultimate Limit State, the following condition must be satisfied:

$$E_d \leq R_d$$

where E_d is the design action/effect and R_d is the design geotechnical resistance.

Partial factors and approach

The report applies **Approach 2** as per NTC 2018 (§2.6.1), using combination: **A1 + M1 + R3**.

- ✓ Actions amplified using A1 (STR) factors (NTC Table 6.2.I)
- ✓ Soil strengths reduced using M1 factors (NTC Table 6.2.II)
- ✓ Resistances divided by R3 factors (NTC Table 6.4.I)

Tabella 6.2.I - Coefficienti parziali per le azioni o per l'effetto delle azioni [cfr. D.M. 2018]

CARICHI	EFFETTO	Coefficiente parziale γ_F (o γ_E)	A1 (STR)	A2 (GEO)
Carichi permanenti G_1	Favorevole	γ_{G1}	1,00	1,00
	Sfavorevole		1,30	1,00
Carichi permanenti G_2[(1)]	Favorevole	γ_{G2}	0,80	0,80
	Sfavorevole		1,50	1,30
Azioni variabili Q	Favorevole	γ_{Qi}	0,00	0,00
	Sfavorevole		1,50	1,30

(1) Per i carichi permanenti G_2 si applica quanto indicato alla Tabella 2.6.I. Per la spinta delle terre si fa riferimento ai coefficienti γ_{G1}

Table 3-1 Coefficients of loads

Tabella 6.2.II - Coefficienti parziali per i parametri geotecnici del terreno [cfr. D.M. 2018]

PARAMETRO GEOTECNICO	Grandezza alla quale applicare il coefficiente parziale	Coefficiente parziale γ_M	M1	M2
Tangente dell'angolo di resistenza a taglio	$\tan\varphi_k$	$\gamma_{\varphi'}$	1,00	1,25
Coesione efficace	c'_k	$\gamma_{c'}$	1,00	1,25
Resistenza non drenata	c_{uk}	γ_{cu}	1,00	1,40
Peso dell'unità di volume	γ_γ	γ_γ	1,00	1,00

Table 3-2 Geotechnical coefficients

Tabella 6.4.I - Coefficienti parziali γ_R per le verifiche agli stati limite ultimi di fondazioni superficiali.

Verifica	Coefficiente Parziale (R3)
Carico limite	γ_R = 2,3
Scorrimento	γ_R = 1,1

Table 3-3 Verification of foundation coefficients

3.10 METHODS USED FOR MICRO PILE VERIFICATIONS

3.10.1 Axial capacity

Axial resistance is evaluated using the empirical method of **Bustamante & Doix (1985)**. The method is based on full-scale tests and evaluations:

- ✓ An average **grout bulb diameter** depending on soil stratigraphy and injection type,
- ✓ The **shaft friction** between grout bulbs and surrounding soil,
  leading to shaft resistance evaluation (the report introduces the expression $Q_{s,lim} = D_s\, L_s\, q$).

3.10.2 Settlement of pile groups (Poulos & Davis interaction factors)

Pile settlement is calculated using:

- ✓ Mobilization curve for the **single pile**, and
- ✓ Group interaction with the **interaction-factor method** by **Poulos & Davis (1980)**.

3.10.3 Lateral resistance

Lateral resistance is evaluated using **Broms (1964)**:

- ✓ For non-cohesive soils, ultimate resistance distribution is linked to passive pressure (Rankine), with $p_{lim} = 3K_p\sigma_v'$;
- ✓ For cohesive soils, a near-surface zero resistance zone is considered, followed by a constant resistance $p_{lim} = 9s_u$.

3.11 SUMMARY OF VERIFICATION RESULTS (BY FOUNDATION BLOCK)

In the numerical verification output, results are reported at several **mesh points (PM1, PM2, …)** for different **load cases (C1, C2, …)** and "**sestetti**" (groups of combinations used in the software). For thesis purposes, you only need to report the **worst (most severe) condition** and the table summaries.

3.11.1 Block 1 - 2 micro piles

Axial capacity (ULS): worst case at **PM2**, **C5**, **sestetto 12**.
The summary table gives: Rd = 13892 daN, Sd = 2435 daN → **fs = 5.70** (minimum).

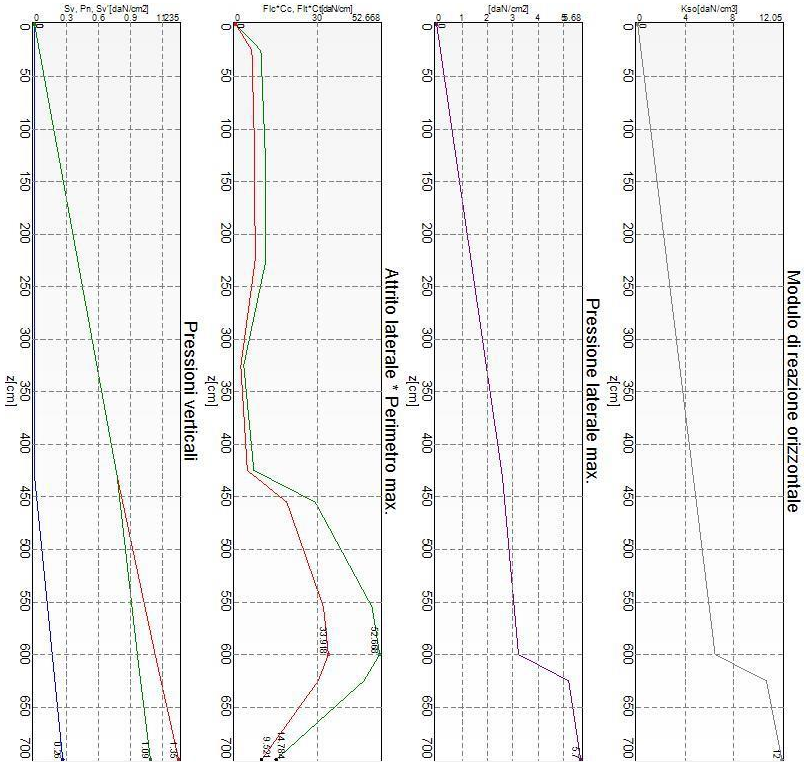

Figure 3-5 Axial resistance block 1-2 micro piles

Verifica: Capacità portante					
Punto	Caso	Ses.	R_d: Qt[daN]	S_d: Qt[daN]	fs[-]
PM1	C5	12	13892	2421	5.74
PM2	C5	12	13892	2435	5.70

Table 3-4 Bearing capacity block 1-2 micro piles

Settlement (rare combination): worst case at **PM2**, **C11**, **sestetto 12**.
Single pile settlement = −0.04 mm; group-induced = −0.01 mm → total settlement **≈ −0.05 mm.**

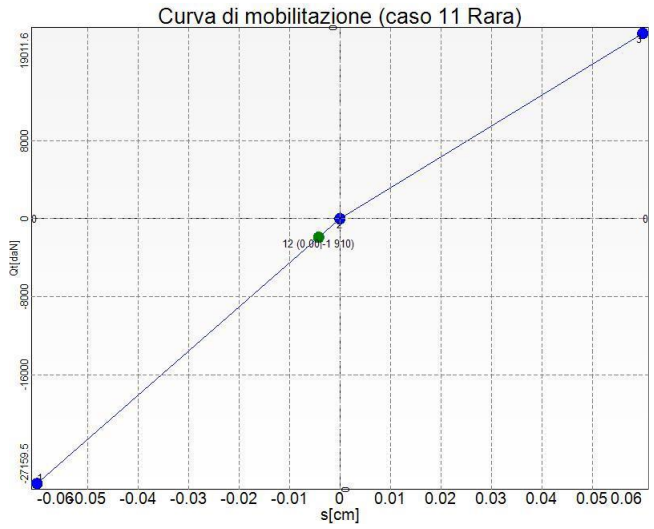

Figure 3-6 Settlement block 1-2

Lateral resistance (ULS): worst case at **PM2**, **C2**, **sestetto 1**.
Table indicates very high safety (**fs = 10.00**).

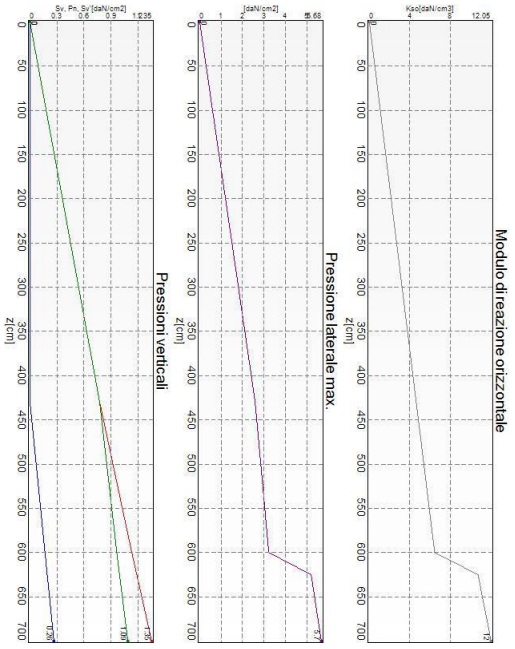

Figure 3-7 Lateral resistance ULS block 1-2 micro piles

Verifica: Resistenza trasversale					
Punto	Caso	Ses.	R_d: Rtr[daN]	S_d: Rtr[daN]	fs[-]
PM1	C1	2	23803	1443	10.00
PM2	C2	1	23803	1566	10.00

Table 3-5 verification of transversal resistance block 1-4 micro piles

Interpretation: This block shows very high safety margins in both axial and lateral ULS, with practically negligible settlements.

3.11.2 Block 1 - 4 micro piles

Axial capacity (ULS): worst case at **PM1**, **C1**, **sestetto 4**.
Minimum reported safety factor **fs = 5.09** (Rd = 8947 daN, Sd = 1758 daN).

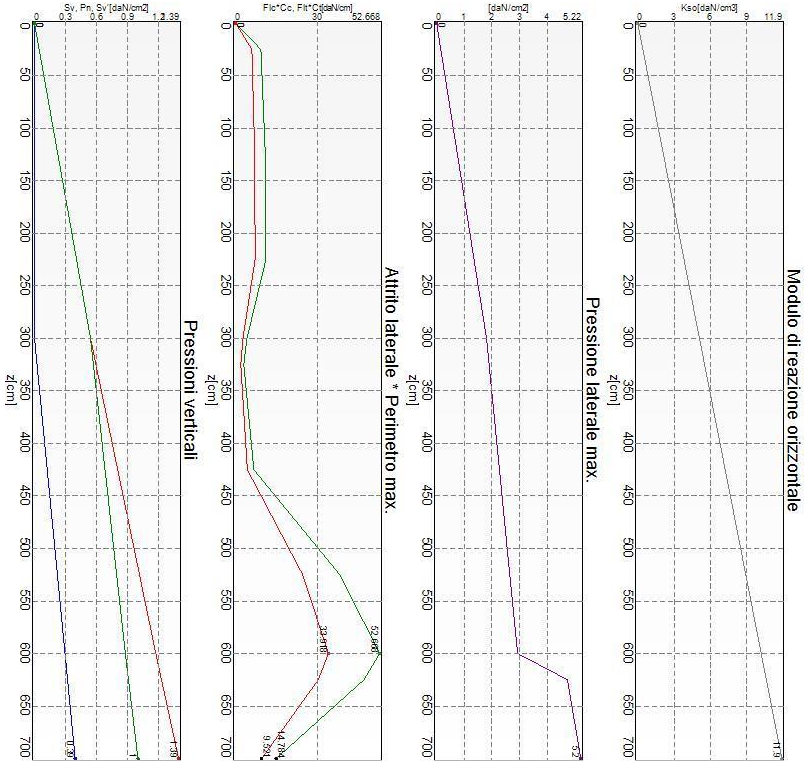

Figure 3-8 Axial resistance

Verifica: Capacità portante					
Punto	Caso	Ses.	R_d: Qt[daN]	S_d: Qt[daN]	fs[-]
PM1	C1	4	8947	1758	5.09
PM2	C1	4	8947	1486	6.02
PM3	C5	3	13892	1498	9.28
PM4	C1	4	8947	828	10.00

Table 3-6 Bearing capacity block 1-4 micro piles

Settlement (rare combination): worst case at **PM1**, **C8**, **sestetto 3**.
Single pile settlement = 0.04 mm; group-induced = 0.01 mm → total settlement **0.05 mm**.

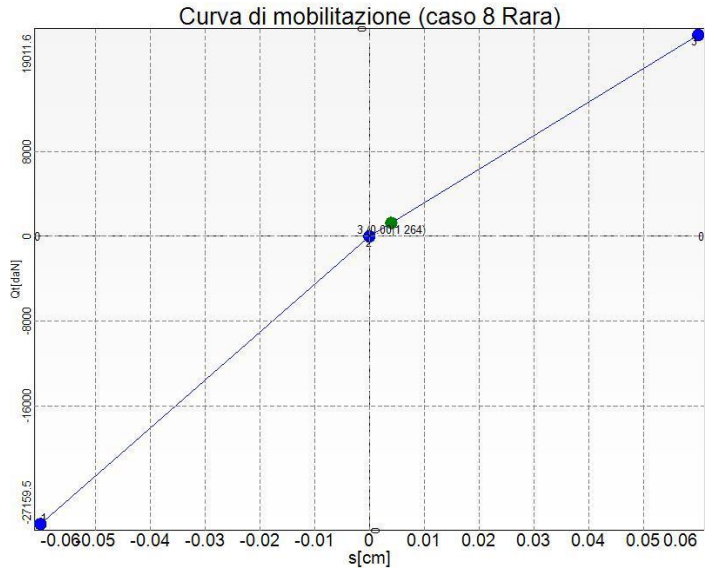

Figure 3-9 settlement block 1-4

Lateral resistance (ULS): worst case at **PM2**, **C6**, **sestetto 3**.
Minimum safety factor is **fs = 9.01**.

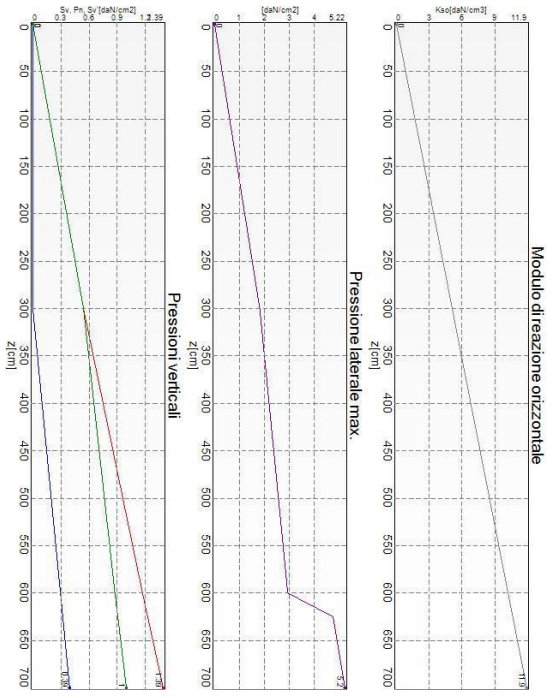

Figure 3-10 Lateral resistance block 1-4 micro piles

Verifica: Resistenza trasversale					
Punto	Caso	Ses.	R_d: Rtr[daN]	S_d: Rtr[daN]	fs[-]
PM1	C6	3	22066	2396	9.21
PM2	C6	3	22066	2449	9.01
PM3	C6	3	22066	2416	9.13
PM4	C6	3	22066	2361	9.34

Table 3-7 verification of transversal resistance block 1-4 micro piles

Interpretation: Increasing the number of micro piles maintains very high margins; settlement remains extremely small.

3.11.3 Block 3 - Plinto 1

This is the **most critical block in axial capacity** (lowest fs).

Axial capacity (ULS): worst case at **PM1**, **C5**, **sestetto 1**.
Rd = 10230 daN, Sd = 5788 daN → **fs = 1.77**

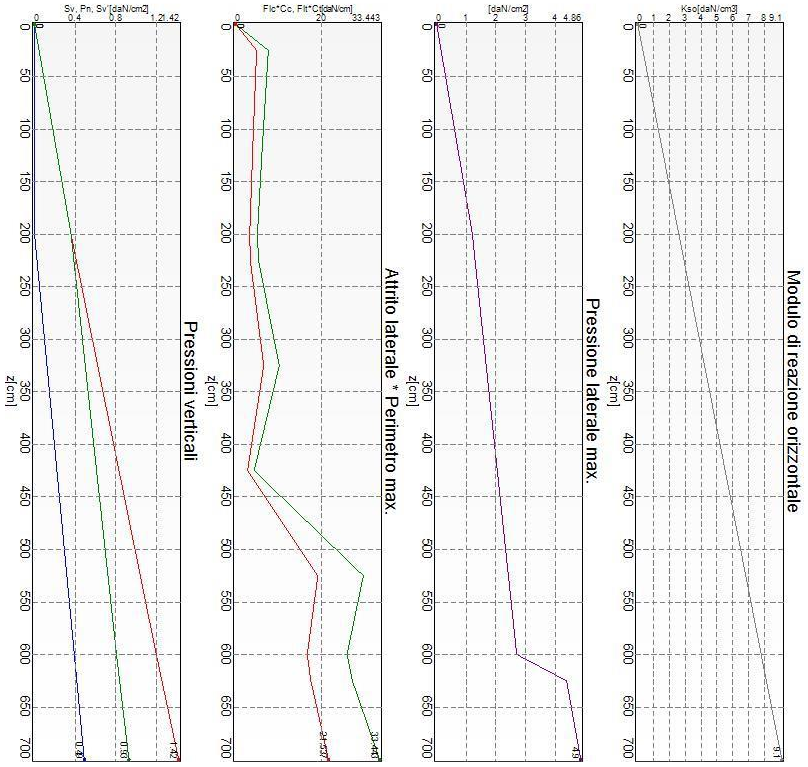

Figure 3-11 Axial resistance block 3-(Plinto 1)

Verifica: Capacità portante					
Punto	Caso	Ses.	R_d: Qt[daN]	S_d: Qt[daN]	fs[-]
PM1	C5	1	10230	5788	1.77
PM2	C5	1	10230	5776	1.77
PM3	C5	1	10230	5763	1.78

PM4	C5	1	10230	5751	1.78
PM5	C6	1	10230	5748	1.78
PM6	C5	1	10230	5787	1.77
PM7	C5	1	10230	5775	1.77
PM8	C5	1	10230	5763	1.78
PM9	C5	1	10230	5750	1.78
PM10	C6	1	10230	5754	1.78
PM11	C5	1	10230	5786	1.77
PM12	C5	1	10230	5774	1.77
PM13	C5	1	10230	5762	1.78
PM14	C5	1	10230	5750	1.78
PM15	C6	1	10230	5761	1.78
PM16	C5	1	10230	5786	1.77
PM18	C5	1	10230	5761	1.78
PM19	C6	1	10230	5754	1.78
PM20	C6	1	10230	5767	1.77
PM21	C5	1	10230	5785	1.77
PM22	C5	1	10230	5773	1.77
PM23	C5	1	10230	5761	1.78
PM24	C6	1	10230	5761	1.78
PM25	C6	1	10230	5774	1.77

Table 3-8 bearing capacity of block 3-(Plinto1)

Interpretation: Although it governs the axial design, the block still satisfies ULS (fs > 1.0), with a moderate margin compared to the other blocks.

3.11.4 Block 4 - Plinto 2

Axial capacity (life-safety limit state): worst case at **PM5**, **C12**, **sestetto 1**.
Minimum safety factor in the summary is **fs = 3.46**.

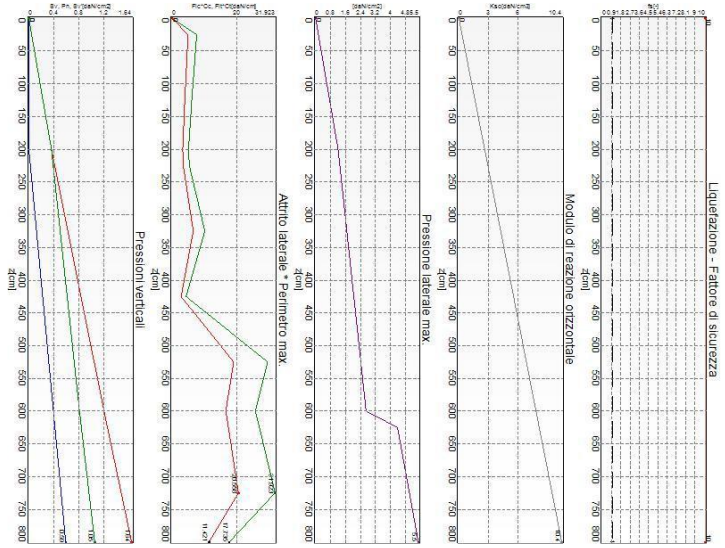

Figure 3-12 Axial capacity block 4-(Plinto 2)

Verifica: Capacità portante					
Punto	Caso	Ses.	R_d: Qt[daN]	S_d: Qt[daN]	fs[-]
PM1	C12	1	12726	3658	3.48
PM2	C12	1	12726	3662	3.48
PM3	C12	1	12726	3666	3.47
PM5	C12	1	12726	3673	3.46
PM6	C12	1	12726	3643	3.49
PM7	C12	1	12726	3647	3.49
PM8	C12	1	12726	3650	3.49
PM9	C12	1	12726	3654	3.48
PM10	C12	1	12726	3658	3.48
PM11	C12	1	12726	3628	3.51
PM13	C12	1	12726	3635	3.50
PM14	C12	1	12726	3639	3.50
PM15	C12	1	12726	3643	3.49

Table 3-9 Bearing capacity of block 4-(Plinto 2)

Settlement: worst case at **PM5**, **C10**, **sestetto 1**.

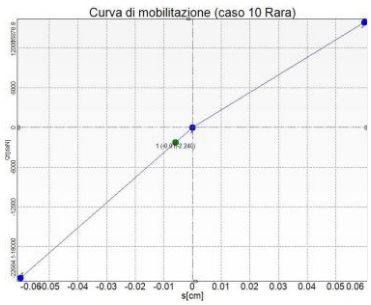

Figure 3-13 settlement block 4-(Plinto 2)

Verifica: Cedimento					
Punto	Caso	Ses.	R_d: Ced.[mm]	S_d: Ced.[mm]	fs[-]
PM1	C10	1	-50	0	10.00
PM2	C10	1	-50	0	10.00
PM3	C10	1	-50	0	10.00
PM5	C10	1	-50	0	10.00
PM6	C10	1	-50	0	10.00
PM7	C10	1	-50	0	10.00
PM8	C10	1	-50	0	10.00
PM9	C10	1	-50	0	10.00
PM10	C10	1	-50	0	10.00
PM11	C10	1	-50	0	10.00
PM13	C10	1	-50	0	10.00
PM14	C10	1	-50	0	10.00
PM15	C10	1	-50	0	10.00

Table 3-10 Verification of settlement block4-(Plinto 2)

Total settlement reported around **−0.06 mm**.

Interpretation: This block shows strong safety margins and negligible settlements.

Lateral resistance (ULS):

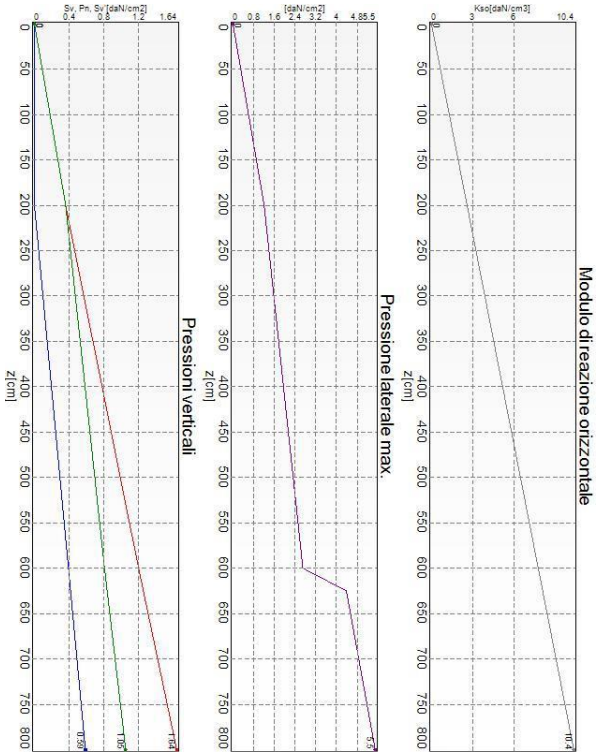

Figure 3-14 Lateral resistance block 4-(Plinto 2)

Verifica: Resistenza trasversale					
Punto	Caso	Ses.	R_d: Rtr[daN]	S_d: Rtr[daN]	fs[-]
PM1	C3	1	28106	1290	10.00
PM2	C3	1	28106	1293	10.00
PM3	C3	1	28106	1298	10.00
PM5	C3	1	28106	1309	10.00
PM6	C3	1	28106	1267	10.00
PM7	C3	1	28106	1271	10.00
PM8	C3	1	28106	1275	10.00
PM9	C3	1	28106	1280	10.00
PM10	C3	1	28106	1286	10.00
PM11	C3	1	28106	1244	10.00
PM13	C3	1	28106	1253	10.00
PM14	C3	1	28106	1258	10.00
PM15	C3	1	28106	1264	10.00

Table 3-11 Verification of lateral resistance block 4-(Plinto 2)

3.12 CHAPTER CONCLUSIONS

The investigation campaign identifies a soil profile with **variable superficial fill** over **loose sandy alluvial deposits**, underlain by a **dense gravelly alluvial/fluvio-glacial formation** (Complex 2B), which provides the main competent horizon for deep foundations.

Groundwater is shallow (≈2.3–4.3 m) and may rise significantly during heavy rainfall, which is relevant for construction and environmental conditions.

The foundation system adopts **micropiles (7–8 m)** with pile caps, and verifications performed with **NTC 2018 Approach 2 (A1+M1+R3)** confirm that all checked blocks satisfy ULS requirements, with particularly high margins in lateral resistance and very small, predicted settlements.

4 SEISMIC CHARACTERIZATION

With reference to the current regulations (NTC 2018), the design seismic actions are defined starting from the *"basic seismic hazard"* of the construction site. This represents the primary element of knowledge for determining seismic actions.

The seismic hazard is defined in terms of the maximum expected horizontal acceleration **ag** under free-field conditions on a reference rigid site with a flat topographic surface (category A, as defined in § 3.2.2 of the D.M. 2018), as well as in terms of the ordinates of the corresponding elastic acceleration response spectrum **Se(T)**, referring to predefined probabilities of exceedance **PVR**, as defined in § 3.2.1 of D.M. 2018, within the reference period **VR**, as defined in § 2.4 of D.M. 2018.

The spectral shapes are defined, for each probability of exceedance within the reference period **PVR**, based on the values of the following parameters for a horizontal rigid reference site:
ag: maximum horizontal acceleration at the site
Fo: maximum value of the amplification factor of the horizontal acceleration spectrum
Tc*: period marking the start of the constant velocity segment of the horizontal acceleration spectrum

In the following paragraphs, the evaluation of the seismic hazard parameters for the reference seismic zone in which the structure is located is presented. The **nominal life of a structural work (VN)** is understood as the number of years during which the structure, provided that ordinary maintenance is carried out, must be able to be used for its intended purpose.

In the presence of seismic actions, with reference to the consequences of an interruption of functionality or a possible collapse, constructions are divided into use classes defined as follows:

4.1 CLASS

- ✓ **Class I:** Constructions with only occasional presence of people, such as agricultural buildings.
- ✓ • **Class II:** Constructions intended for normal occupancy levels, without contents hazardous to the environment and without essential public or social functions. Industries with activities that are not dangerous for the environment. Bridges, infrastructure works, and road networks not classified as Use Class III or IV. Railway networks whose interruption would not cause emergency situations. Dams whose failure would not lead to significant consequences.
- ✓ **Class III:** Constructions intended for significant occupancy levels. Industries with activities that may be hazardous to the environment. Non-urban road networks not included in Use Class IV. Bridges and railway networks whose interruption would cause emergency situations. Dams with relevant consequences in the event of collapse.
- ✓ **Class IV:** Constructions with important public or strategic functions, including those related to civil protection management in case of natural disasters. Industries with activities particularly hazardous to the environment. Road networks of type A or B, as defined in Ministerial Decree 5 November 2001, No. 6792, "Functional and geometric standards for road construction," and of type C when forming routes connecting provincial capitals not otherwise served by type A or B roads. Bridges and railway networks of critical importance for maintaining communication routes,

especially after a seismic event. Dams connected to the operation of aqueducts and power generation plants.

For the present case, a **Use Class II** is considered, corresponding to a **use coefficient Cu = 1.0**.

Tab. 2.4.II – *Valori del coefficiente d'uso* C_U

CLASSE D'USO	I	II	III	IV
COEFFICIENTE C_U	0,7	1,0	1,5	2,0

Table 4-1 Coefficient C_u

4.2 REFERENCE AND RETURN PERIOD

The seismic actions on each construction are evaluated with respect to a reference period **VR**, which is obtained, for each type of construction, by multiplying its nominal life **VN** by the use coefficient **CU**:

VR = VN · CU = 50 · 1.0 = 50 years (reference period).

Once the reference life **VR** is set, the two parameters **TR** (return period) and **PVR** (probability of exceedance in the reference period) can be directly expressed in relation to each other using the following expression.

$$T_R = \frac{V_R}{\ln(1 - P_{V_R})} = -\frac{Cu \cdot V_s}{\ln - (1 - P_{V_s})}$$

LIMIT STATE	PROBABILITY OF EXCEEDANCE (PVR)	RETURN PERIOD (YEARS)
SLE		
SLO – Serviceability Limit State	81%	30
SLD – Serviceability Limit State	63%	50
SLU		
SLV – Ultimate Limit State	10%	475

Table 4-2 Limit states SLO-SLD-SLV

LIMIT STATE	PROBABILITY OF EXCEEDANCE	RETURN PERIOD (YEARS)
SLC – Ultimate Limit State (Collapse Prevention)	5%	975

Table 4-3 Limit state SLC

For the site under consideration, the design structures will therefore have the following seismic parameters.

Nominal life of the structure (VN)	Reference period (VR)	Return period at SLV

50 years	50 years	475 years

Table 4-4 Nominal life of structure

4.3 SEISMIC PARAMETERS

The evaluation of the seismic hazard parameters, which according to NTC 2018 constitute the basic data for determining the design seismic actions on a structure (spectral shapes and/or inertial forces), depends—as already partially mentioned above—on the geographical location of the site, the characteristics of the structure (reference period for the evaluation of the seismic action / VR), and the reference Limit State / return period of the seismic action.

The subsoil category reported in the geotechnical report is **subsoil category E**. The topographic class is **type T1**.

Tab. 2.4.I – *Valori minimi della Vita nominale V_N di progetto per i diversi tipi di costruzioni*

	TIPI DI COSTRUZIONI	Valori minimi di V_N (anni)
1	Costruzioni temporanee e provvisorie	10
2	Costruzioni con livelli di prestazioni ordinari	50
3	Costruzioni con livelli di prestazioni elevati	100

Table 4-5 Minimum return period of structure

The case under consideration, the structures covered by this final design project will have a nominal service life of V_N = 50 years.

4.4 SLV GRAPH

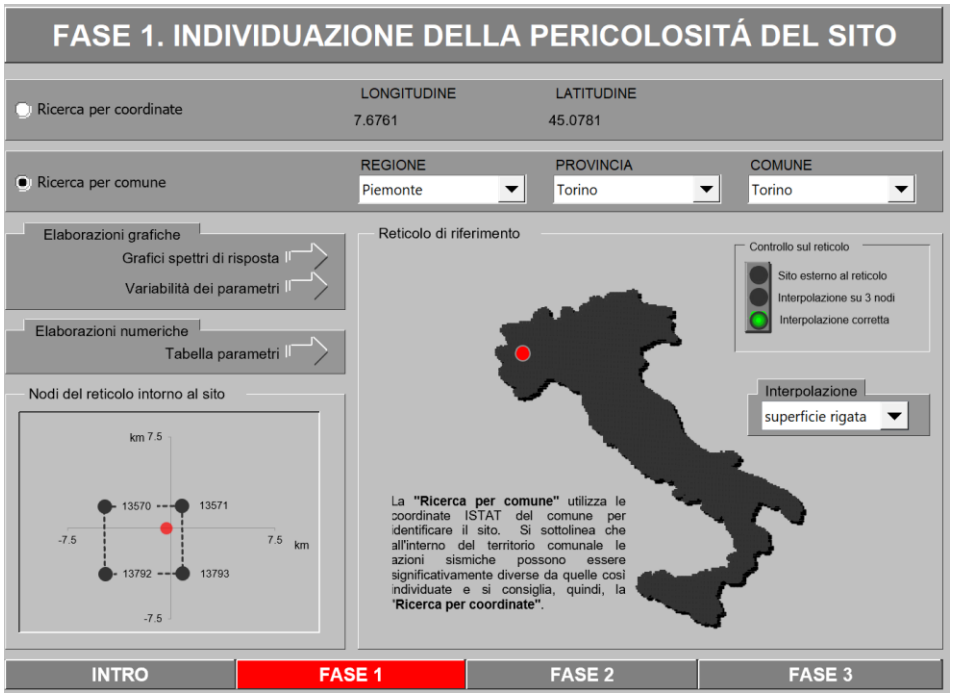

Figure 4-1 Fase 1 SLV

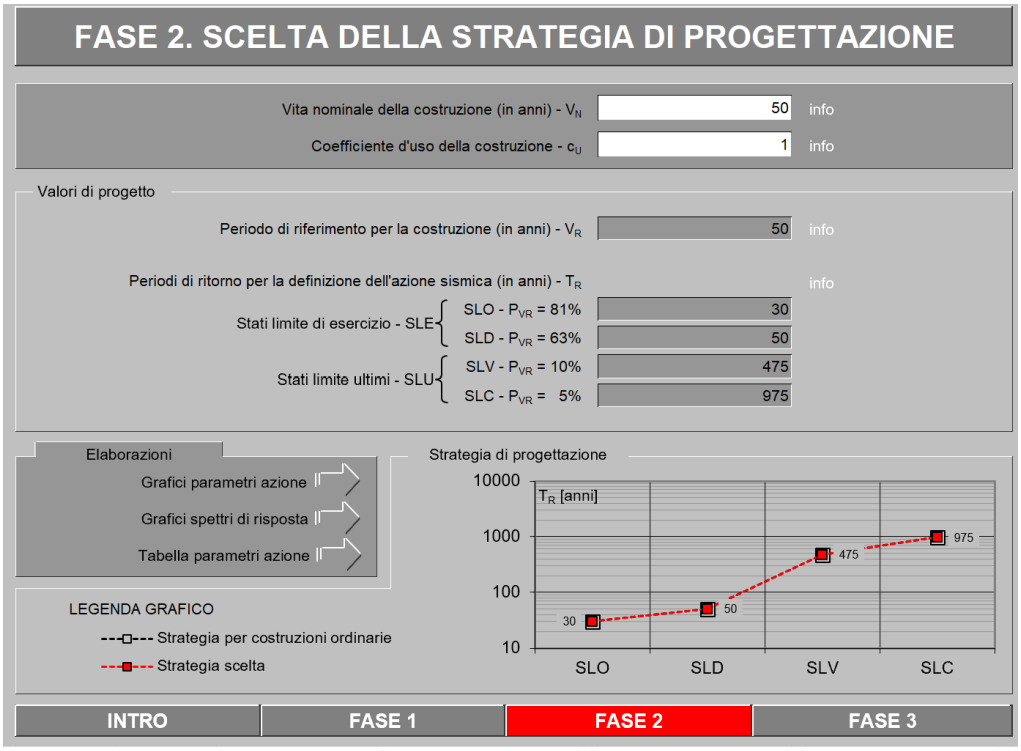

Figure 4-2 Fase 2 SLV

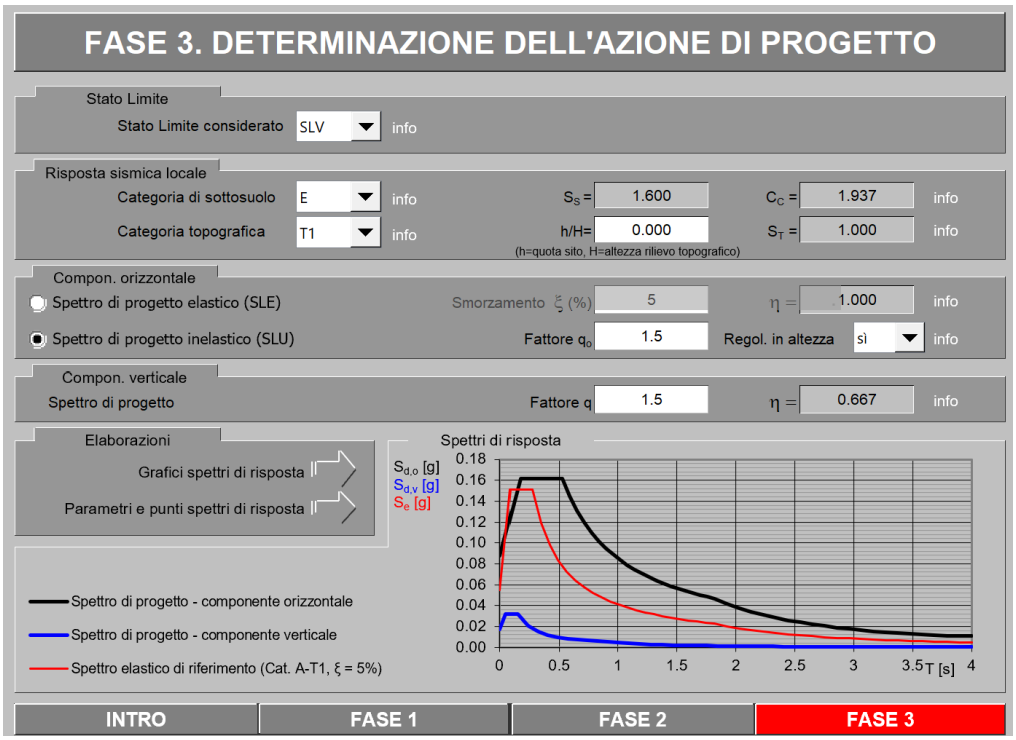

Figure 4-3 Fase 3 SLV

4.4.1 Horizontal component SLV

Parametri e punti dello spettro di risposta orizzontale per lo stato limite: SLV

Parametri indipendenti

STATO LIMITE	SLV
a_g	0.055 g
F_o	2.760
T_C^*	0.272 s
S_S	1.600
C_C	1.937
S_T	1.000
q	1.500

Parametri dipendenti

S	1.600
η	0.667
T_B	0.175 s
T_C	0.526 s
T_D	1.819 s

Espressioni dei parametri dipendenti

$S = S_S \cdot S_T$ (NTC-08 Eq. 3.2.5)

$\eta = \sqrt{10/(5+\xi)} \geq 0,55;\ \eta = 1/q$ (NTC-08 Eq. 3.2.6; §. 3.2.3.5)

$T_B = T_C/3$ (NTC-07 Eq. 3.2.8)

$T_C = C_C \cdot T_C^*$ (NTC-07 Eq. 3.2.7)

$T_D = 4,0 \cdot a_g/g + 1,6$ (NTC-07 Eq. 3.2.9)

Espressioni dello spettro di risposta (NTC-08 Eq. 3.2.4)

$0 \leq T < T_B$ $\quad S_e(T) = a_g \cdot S \cdot \eta \cdot F_o \cdot \left[\frac{T}{T_B} + \frac{1}{\eta \cdot F_o}\left(1 - \frac{T}{T_B}\right)\right]$

$T_B \leq T < T_C$ $\quad S_e(T) = a_g \cdot S \cdot \eta \cdot F_o$

$T_C \leq T < T_D$ $\quad S_e(T) = a_g \cdot S \cdot \eta \cdot F_o \cdot \left(\frac{T_C}{T}\right)$

$T_D \leq T$ $\quad S_e(T) = a_g \cdot S \cdot \eta \cdot F_o \cdot \left(\frac{T_C T_D}{T^2}\right)$

Lo spettro di progetto $S_d(T)$ per le verifiche agli Stati Limite Ultimi è ottenuto dalle espressioni dello spettro elastico $S_e(T)$ sostituendo η con 1/q, dove q è il fattore di struttura. (NTC-08 § 3.2.3.5)

Punti dello spettro di risposta

	T [s]	Se [g]
	0.000	0.088
T_B ←	0.175	0.161
T_C ←	0.526	0.161
	0.588	0.145
	0.649	0.131
	0.711	0.119
	0.772	0.110
	0.834	0.102
	0.896	0.095
	0.957	0.089
	1.019	0.083
	1.080	0.079
	1.142	0.074
	1.204	0.071
	1.265	0.067
	1.327	0.064
	1.388	0.061
	1.450	0.059
	1.511	0.056
	1.573	0.054
	1.635	0.052
	1.696	0.050
	1.758	0.048
T_D ←	1.819	0.047
	1.923	0.042
	2.027	0.038
	2.131	0.034
	2.235	0.031
	2.339	0.028
	2.442	0.026
	2.546	0.024
	2.650	0.022
	2.754	0.020
	2.858	0.019
	2.962	0.018
	3.065	0.016
	3.169	0.015
	3.273	0.014
	3.377	0.014
	3.481	0.013
	3.585	0.012
	3.688	0.011
	3.792	0.011
	3.896	0.011
	4.000	0.011

La verifica dell'idoneità del programma, l'utilizzo dei risultati da esso ottenuti sono onere e responsabilità esclusiva dell'utente. Il Consiglio Superiore dei Lavori Pubblici non potrà essere ritenuto responsabile dei danni risultanti dall'utilizzo dell

Figure 4-4 Horizontal component SLV

4.4.2 Vertical component SLV

Parametri e punti dello spettro di risposta verticale per lo stato limite: SLV

Parametri indipendenti

STATO LIMITE	SLV
a_{gv}	0.017 g
S_S	1.000
S_T	1.000
q	1.500
T_B	0.050 s
T_C	0.150 s
T_D	1.000 s

Parametri dipendenti

F_v	0.873
S	1.000
η	0.667

Espressioni dei parametri dipendenti

$S = S_S \cdot S_T$ (NTC-08 Eq. 3.2.5)

$\eta = 1/q$ (NTC-08 §. 3.2.3.5)

$F_v = 1{,}35 \cdot F_o \cdot \left(\frac{a_g}{g}\right)^{0.5}$ (NTC-08 Eq. 3.2.11)

Espressioni dello spettro di risposta (NTC-08 Eq. 3.2.10)

$0 \le T < T_B \quad S_e(T) = a_g \cdot S \cdot \eta \cdot F_v \cdot \left[\frac{T}{T_B} + \frac{1}{\eta \cdot F_o}\left(1 - \frac{T}{T_B}\right)\right]$

$T_B \le T < T_C \quad S_e(T) = a_g \cdot S \cdot \eta \cdot F_v$

$T_C \le T < T_D \quad S_e(T) = a_g \cdot S \cdot \eta \cdot F_v \cdot \left(\frac{T_C}{T}\right)$

$T_D \le T \quad S_e(T) = a_g \cdot S \cdot \eta \cdot F_v \cdot \left(\frac{T_C T_D}{T^2}\right)$

Punti dello spettro di risposta

	T [s]	Se [g]
	0.000	0.017
T_B ←	0.050	0.032
T_C ←	0.150	0.032
	0.235	0.020
	0.320	0.015
	0.405	0.012
	0.490	0.010
	0.575	0.008
	0.660	0.007
	0.745	0.006
	0.830	0.006
	0.915	0.005
T_D ←	1.000	0.005
	1.094	0.004
	1.188	0.003
	1.281	0.003
	1.375	0.003
	1.469	0.002
	1.563	0.002
	1.656	0.002
	1.750	0.002
	1.844	0.001
	1.938	0.001
	2.031	0.001
	2.125	0.001
	2.219	0.001
	2.313	0.001
	2.406	0.001
	2.500	0.001
	2.594	0.001
	2.688	0.001
	2.781	0.001
	2.875	0.001
	2.969	0.001
	3.063	0.001
	3.156	0.000
	3.250	0.000
	3.344	0.000
	3.438	0.000
	3.531	0.000
	3.625	0.000
	3.719	0.000
	3.813	0.000
	3.906	0.000
	4.000	0.000

La verifica dell'idoneità del programma, l'utilizzo dei risultati da esso ottenuti sono onere e responsabilit esclusiva dell'utente. Il Consiglio Superiore dei Lavori Pubblici non potrà essere ritenuto responsabile de danni risultanti dall'utilizzo dello stesso.

Figure 4-5 Vertical component SLV

4.5 SLD GRAPH

We adopt same procedures for SLD but change in parameters in FASE 3, Result is as follows:

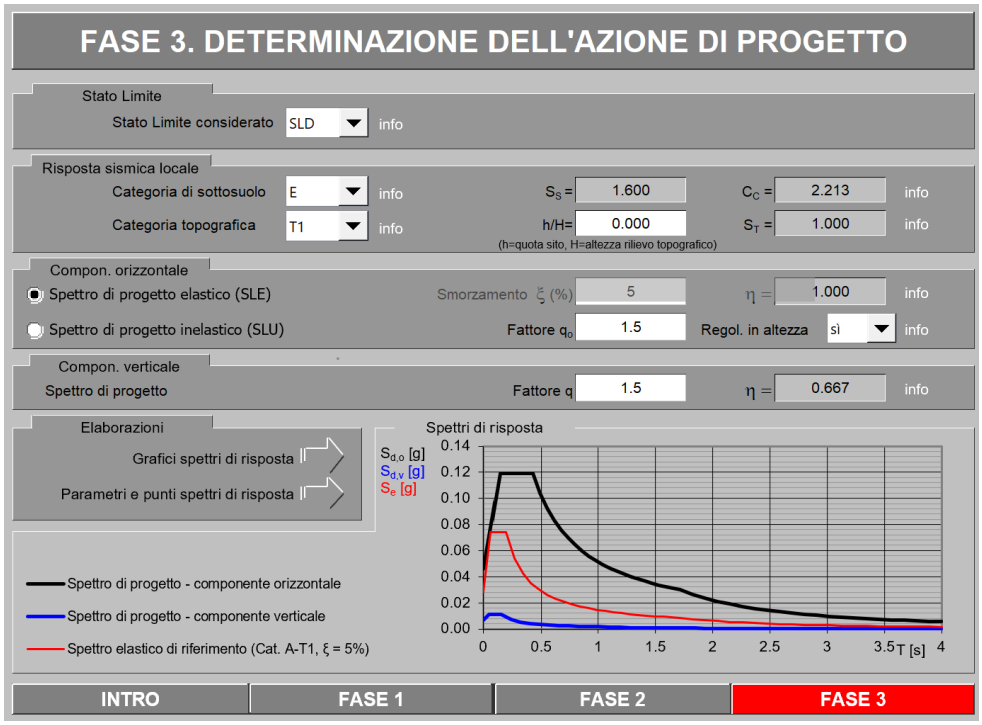

Figure 4-6 Fase 3 SLD

4.5.1 Horizontal component SLD

Parametri e punti dello spettro di risposta orizzontale per lo stato limite: SLD

Parametri indipendenti

STATO LIMITE	SLD
a_g	0.029 g
F_o	2.592
T_C^*	0.195 s
S_S	1.600
C_C	2.213
S_T	1.000
q	1.000

Parametri dipendenti

S	1.600
η	1.000
T_B	0.144 s
T_C	0.431 s
T_D	1.715 s

Espressioni dei parametri dipendenti

$S = S_S \cdot S_T$ (NTC-08 Eq. 3.2.5)

$\eta = \sqrt{10/(5+\xi)} \geq 0,55;\ \eta = 1/q$ (NTC-08 Eq. 3.2.6; §. 3.2.3.5)

$T_B = T_C/3$ (NTC-07 Eq. 3.2.8)

$T_C = C_C \cdot T_C^*$ (NTC-07 Eq. 3.2.7)

$T_D = 4,0 \cdot a_g/g + 1,6$ (NTC-07 Eq. 3.2.9)

Espressioni dello spettro di risposta (NTC-08 Eq. 3.2.4)

$0 \leq T < T_B$ $\quad S_e(T) = a_g \cdot S \cdot \eta \cdot F_o \cdot \left[\frac{T}{T_B} + \frac{1}{\eta \cdot F_o}\left(1 - \frac{T}{T_B}\right)\right]$

$T_B \leq T < T_C$ $\quad S_e(T) = a_g \cdot S \cdot \eta \cdot F_o$

$T_C \leq T < T_D$ $\quad S_e(T) = a_g \cdot S \cdot \eta \cdot F_o \cdot \left(\frac{T_C}{T}\right)$

$T_D \leq T$ $\quad S_e(T) = a_g \cdot S \cdot \eta \cdot F_o \cdot \left(\frac{T_C T_D}{T^2}\right)$

Lo spettro di progetto $S_d(T)$ per le verifiche agli Stati Limite Ultimi è ottenuto dalle espressioni dello spettro elastico $S_e(T)$ sostituendo η con 1/q, dove q è il fattore di struttura. (NTC-08 § 3.2.3.5)

Punti dello spettro di risposta

	T [s]	Se [g]
	0.000	0.046
T_B ←	0.144	0.119
T_C ←	0.431	0.119
	0.492	0.104
	0.553	0.093
	0.614	0.083
	0.675	0.076
	0.736	0.070
	0.798	0.064
	0.859	0.060
	0.920	0.056
	0.981	0.052
	1.042	0.049
	1.103	0.046
	1.164	0.044
	1.226	0.042
	1.287	0.040
	1.348	0.038
	1.409	0.036
	1.470	0.035
	1.531	0.033
	1.592	0.032
	1.654	0.031
T_D ←	1.715	0.030
	1.824	0.026
	1.932	0.024
	2.041	0.021
	2.150	0.019
	2.259	0.017
	2.368	0.016
	2.476	0.014
	2.585	0.013
	2.694	0.012
	2.803	0.011
	2.912	0.010
	3.021	0.010
	3.129	0.009
	3.238	0.008
	3.347	0.008
	3.456	0.007
	3.565	0.007
	3.674	0.007
	3.782	0.006
	3.891	0.006
	4.000	0.005

La verifica dell'idoneità del programma, l'utilizzo dei risultati da esso ottenuti sono onere e responsabilità esclusiva dell'utente. Il Consiglio Superiore dei Lavori Pubblici non potrà essere ritenuto responsabile dei danni risultanti dall'utilizzo dell

Figure 4-7 Horizontal component SLD

4.5.2 Vertical component SLD

Parametri e punti dello spettro di risposta verticale per lo stato limite: SLD

Parametri indipendenti

STATO LIMITE	SLD
a_{gv}	0.007 g
S_S	1.000
S_T	1.000
q	1.500
T_B	0.050 s
T_C	0.150 s
T_D	1.000 s

Parametri dipendenti

F_v	0.593
S	1.000
η	0.667

Espressioni dei parametri dipendenti

$S = S_S \cdot S_T$ (NTC-08 Eq. 3.2.5)

$\eta = 1/q$ (NTC-08 §. 3.2.3.5)

$F_v = 1{,}35 \cdot F_o \cdot \left(\frac{a_g}{g}\right)^{0.5}$ (NTC-08 Eq. 3.2.11)

Espressioni dello spettro di risposta (NTC-08 Eq. 3.2.10)

$0 \le T < T_B \quad S_e(T) = a_g \cdot S \cdot \eta \cdot F_v \cdot \left[\frac{T}{T_B} + \frac{1}{\eta \cdot F_o}\left(1 - \frac{T}{T_B}\right)\right]$

$T_B \le T < T_C \quad S_e(T) = a_g \cdot S \cdot \eta \cdot F_v$

$T_C \le T < T_D \quad S_e(T) = a_g \cdot S \cdot \eta \cdot F_v \cdot \left(\frac{T_C}{T}\right)$

$T_D \le T \quad S_e(T) = a_g \cdot S \cdot \eta \cdot F_v \cdot \left(\frac{T_C T_D}{T^2}\right)$

Punti dello spettro di risposta

	T [s]	Se [g]
	0.000	0.007
T_B ←	0.050	0.011
T_C ←	0.150	0.011
	0.235	0.007
	0.320	0.005
	0.405	0.004
	0.490	0.003
	0.575	0.003
	0.660	0.003
	0.745	0.002
	0.830	0.002
	0.915	0.002
T_D ←	1.000	0.002
	1.094	0.001
	1.188	0.001
	1.281	0.001
	1.375	0.001
	1.469	0.001
	1.563	0.001
	1.656	0.001
	1.750	0.001
	1.844	0.000
	1.938	0.000
	2.031	0.000
	2.125	0.000
	2.219	0.000
	2.313	0.000
	2.406	0.000
	2.500	0.000
	2.594	0.000
	2.688	0.000
	2.781	0.000
	2.875	0.000
	2.969	0.000
	3.063	0.000
	3.156	0.000
	3.250	0.000
	3.344	0.000
	3.438	0.000
	3.531	0.000
	3.625	0.000
	3.719	0.000
	3.813	0.000
	3.906	0.000
	4.000	0.000

La verifica dell'idoneità del programma, l'utilizzo dei risultati da esso ottenuti sono onere e responsabilità esclusiva dell'utente. Il Consiglio Superiore dei Lavori Pubblici non potrà essere ritenuto responsabile dei danni risultanti dall'utilizzo dello stesso.

Figure 4-8 Vertical component SLD

5 ACTIONS ON STRUCTURE AND LOAD MODELLING

5.1 INTRODUCTION

This chapter presents the actions (loads) considered in the structural design and describes how they were implemented in the finite element model (FEM). The analysis is performed in the linear-elastic field; therefore, each action is defined as an individual load case, and the structural response is obtained through superposition. Load combinations are then constructed in accordance with the relevant Ultimate Limit State (ULS) and Serviceability Limit State (SLS) requirements, including specific seismic combinations.

The numerical model applies actions through automatic self-weight based on material density, distributed and surface loads (including load-distribution areas), point and line loads where necessary, thermal actions introduced as imposed strains (uniform temperature variations), and seismic action evaluated by linear dynamic modal response-spectrum analysis.

5.2 CLASSIFICATION OF ACTIONS AND LOADS

In accordance with standard structural design practice, actions are classified into permanent, variable, environmental, and seismic actions. The project considers the following:

- **Permanent actions (G)**
  - ✓ **G1**: self-weight of the structural steel system
  - ✓ **G2**: superimposed permanent loads carried by the deck (non-structural components)
- **Variable actions (Q)**
  - ✓ pedestrian/crowd live load
  - ✓ wind action (transverse, considered with both signs)
  - ✓ thermal actions (expansion and contraction)
  - ✓ snow load (evaluated but not governing)
- **Seismic action (E)**
  - ✓ linear dynamic (modal) seismic action in the two principal horizontal directions

Each action is introduced as a dedicated load case in the FEM model, enabling clear traceability of results and consistent construction of load combinations.

5.3 PERMANENT ACTIONS

5.3.1 Structural self-weight (G1)

Self-weight is automatically computed by the FEM software by assigning density to the steel material. To account for additional weight contributions from joint plates, stiffeners, and connection details not explicitly modelled as separate components, the steel density is conservatively increased by 15%:

- ✓ Reference steel density: 7850 kg/m³
- ✓ Adopted density: 7850 × 1.15 = **9027.5 kg/m³**

This modelling choice ensures that global gravitational demand is not underestimated and that support reactions and internal forces reflect a realistic as-built weight.

5.3.2 Superimposed dead loads

In addition to self-weight, the deck system includes carried permanent components. The walking surface is modelled by considering the contribution of omega profiles and timber decking (4 cm). The adopted superimposed permanent load is:

- ✓ **50 kg/m²**

This load is applied to the deck through equivalent distributed surface actions (and/or load distribution areas) in order to reproduce the actual load transfer to the main structural members.

5.4 VARIABLE ACTIONS

5.4.1 Pedestrian load

The principal variable vertical action is the crowd load acting on the deck surface:

- ✓ **500 kg/m²**

This action represents the operational loading scenario for a fully occupied pedestrian deck and is typically the governing case for vertical bending and shear in deck members, as well as axial forces in the primary structural system.

5.4.2 Snow load

Snow action on the platform is evaluated according to the relevant national provisions. The resulting value is approximately:

- ✓ **124 kg/m²**

Since this value is lower than the crowd live load, snow is not considered governing for the main verification scenarios and is neglected in the final set of checks.

5.5 WIND ACTION

5.5.1 General assumptions and loads

Wind action is modelled as a predominantly **horizontal** action acting mainly in the **transverse direction** (crosswind) with respect to the footbridge longitudinal axis. In the FEM model, wind is introduced through two load cases in order to account for both possible directions:

- ✓ **Load Case 4: Transverse Wind +**

- ✓ **Load Case 5: Transverse Wind −**

Wind effects are evaluated separately for:

- ✓ the **deck (impalcato)**
- ✓ the **reticular/tubular structure (reticolare)**.

5.5.2 Wind action on the deck (impalcato)

The deck is located at variable elevation, from ground level up to approximately **+7.0 m**. For wind evaluation, a conservative reference height of **7.0 m** is adopted, and the pressure coefficient is assumed:

- ✓ **Cp = 2.10**

For the "isolated deck" configuration, the report defines the geometry and aerodynamic coefficients used for wind evaluation.

Geometric parameters:

- ✓ deck width: **d = 4.0 m**
- ✓ total height: **h_{tot} = 1.5 m**
- ✓ ratio: **d/h_{tot} = 10**
- ✓ distance between side beams: **3.8 m.**

Aerodynamic coefficients:

- ✓ **C_{fx} = 0.14**
- ✓ **C_{fy} = +1.2 / −1.2**
- ✓ **C_{mz} = +0.2 / −0.2**

Resulting equivalent wind actions

- ✓ **Fx = 0.75 kN/m**
- ✓ **Fy = −0.59 kN/m²** and **−1.00 kN/m²**
- ✓ **Mz = +2.68 kN·m/m** and **−2.68 kN·m/m**
- ✓ **Fz (derived from Mz) = +0.70 kN/m** and **−0.70 kN/m**

Modelling note (mesh and parapet): The Geobrugg-type mesh is characterised by a high perforation ratio; therefore, wind actions on the mesh are neglected. For the parapet, although a perforation ratio of 50% is mentioned (due to reduced density of vertical posts), the parapet is conservatively assumed as **fully solid** to account for potential local occlusions (e.g., hanging elements). The wind actions are therefore distributed equally among the parapet posts.

5.5.3 Wind action on the tubular sections (reticolare)

The reticular members consist of **circular tubular steel profiles** with diameter ranging approximately between **220 mm and 273 mm**. Wind actions on circular sections are evaluated following the recommendations of **CNR DT207**, which expresses the wind force per unit length along the flow direction through a force coefficient c_{fx0}dependent on the **Reynolds number** $Re$and the **roughness ratio** $\frac{k}{b}$.

$$c_{fx0} = \frac{0{,}11}{\left(Re/10^6\right)^{1{,}4}} \le 1{,}2 \qquad \text{(curva A)} \qquad \text{(G.22a)}$$

$$c_{fx0} = 1{,}2 + \frac{0{,}18 \cdot \log_{10}\left(10 \cdot k/b\right)}{1 + 0{,}4 \cdot \log_{10}\left(Re/10^6\right)} \ge 0{,}4 \quad \left(k/b \ge 10^{-5}\right) \qquad \text{(curva B)} \qquad \text{(G.22b)}$$

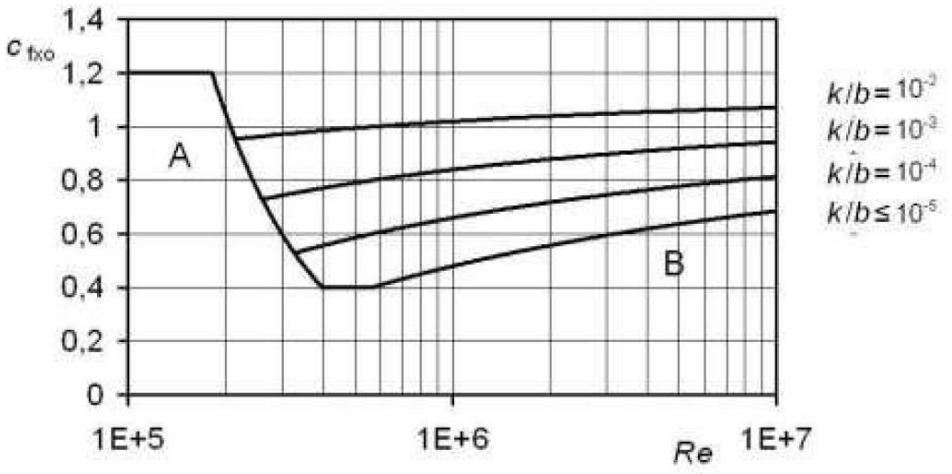

Figura G.51 – Coefficiente di forza c_{fx0} per strutture ed elementi a sezione circolare.

Figure 5-1 C_{fx0} coefficients for circular sections

Reynolds number definition (CNR DT207)

The Reynolds number at height z above ground is defined as:

$$Re(z) = \frac{l\, v_m(z)}{\nu}$$

where:

- ✓ l is a characteristic dimension of the element (for circular sections, typically the diameter),
- ✓ $v_m(z)$is the mean wind speed at height z,

- ✓ ν is the kinematic viscosity of air (reference value typically $\nu \approx 15 \cdot \frac{10^{-6}\,\mathrm{m}^2}{\mathrm{s}}$).

CNR DT207 provides curves and expressions (Curve A / Curve B) to select c_{fx0}based on $Re$and $\frac{k}{b}$.

Parameters adopted in the project

The report provides the following values adopted for the wind evaluation of the reticular members:

- ✓ Reference diameter: **B = 273 mm**
- ✓ **Re = 4,550,000**
- ✓ height range: **H_{min} = 7 m**, **H_{max} = 15 m**
- ✓ exposure coefficient: **$Ce_{,\,min}$ = 2.1**, **$Ce_{,\,max}$ = 2.65**
- ✓ exposure coefficient for diagonals: **$Ce_{,\,diagonali}$ = 2.4**

Equivalent wind line loads used in the FEM

The resulting equivalent transverse wind loads are reported as **mass per unit length**:

- ✓ **Q_w, upper chords = 42 kg/m**
- ✓ **Q_w, lower chords = 52 kg/m**
- ✓ **Q_w, diagonals = 47 kg/m**

5.6 THERMAL ACTIONS

5.6.1 Thermal scenarios

Thermal effects are introduced as imposed uniform temperature variations that generate expansion and contraction. The adopted temperature limits are:

- ✓ $Te_{,\,min}$ = −20 °C
- ✓ $Te_{,\,max}$ = 55 °C
- ✓ Reference temperature T0 = 15 °C

Resulting temperature variations:

- ✓ **Δ_{Tcon} = 45 °C** (contraction case)
- ✓ **Δ_{Texp} = 40 °C** (expansion case)

Two load cases are defined for thermal actions, corresponding to the two extremes (positive and negative temperature variations).

5.6.2 Interaction with support scheme

Thermal actions are particularly relevant for long and slender structures. The support configuration is defined to control restraint forces by allowing thermal movements where required (e.g., sliding supports at the ends) while maintaining global stability through a fixed reference support.

5.7 SEISMIC ACTIONS

5.7.1 Seismic limit states

Two seismic limit states are considered:

- ✓ **SLD (Damage Limit State)**: serviceability-oriented objective, requiring that the structure remains usable after the earthquake without significant loss of resistance and stiffness.
- ✓ **SLV (Life Safety Limit State)**: ultimate safety objective, allowing significant damage while preserving a safety margin against collapse.

5.7.1.1 Analyze method

Seismic action is evaluated through **linear dynamic (modal) analysis** using response spectra. The seismic response is assessed in the two principal horizontal directions by dedicated seismic load cases (X and Y).

A behavior factor **q = 1.5** is adopted for the SLV spectrum definition. The vertical seismic component is neglected because the design peak ground acceleration is below the adopted threshold ($a_g \leq 0.15g$). Relative support displacements are also neglected based on foundation and soil assumptions.

5.8 LOAD COMBINATION

Because the analysis is linear-elastic, internal forces and displacements from each load case are computed separately and combined by superposition. The project defines:

- ✓ **ULS combinations** for resistance and stability verifications
- ✓ **SLS combinations** for serviceability checks (e.g., deflections and stress limitations where applicable)
- ✓ **Seismic combinations (SLV)**, including variants combined with thermal extremes (SLV with $\Delta T+$ and SLV with $\Delta T-$)

5.8.1 Verification scenarios

The most relevant scenarios typically include:

- ✓ gravity-dominated combinations: G1 + G2 + crowd load
- ✓ environmental combinations: wind (±) combined with permanent actions
- ✓ thermal combinations: ΔT (±) combined with permanent actions

- ✓ seismic combinations: SLV (X/Y), including thermal extremes where required

This combination set ensures that the structure is checked under the most unfavorable arrangements of vertical, lateral, thermal, and seismic actions.

5.8.2 Loads considered in the dynamic analysis

SLS – Associated static pedestrian load case (crowd weight)

- ✓ self-weight of structure — automatically calculated
- ✓ weight of steel sheet — 16kg/m^2
- ✓ weight of parapet — 50kg/m
- ✓ pedestrian live load — 70kg/m^2

SLS – Dynamic pedestrian load case (vibration load)

- ✓ self-weight of structure — automatically calculated
- ✓ weight of steel sheet — 16kg/m^2
- ✓ weight of parapet — 50kg/m

6 DYNAMIC ANALYSIS

6.1 FOOTBRIDGE DYNAMIC ANALYSIS METHODOLOGY SÉTRA

For the purposes of Owners, prime contractors and designers, this chapter puts forward a methodology and recommendations for considering the dynamic effects caused by pedestrian traffic on footbridges.

The recommendations are the result of the inventory described in Appendices 1 to 4, on the one hand, and of the work of the Sétra-AFGC group responsible for these guidelines, on the other. Thus, they are a summary of existing knowledge and present the choices made by the group.

The methodology proposed makes it possible to limit risks of resonance of the structure caused by pedestrian footsteps. Nevertheless, it must be remembered that, apart from the resonance, very light footbridges may undergo vibrational phenomena.

At source, when deciding on his approach, the Owner needs to define the class of the footbridge as a function of the level of traffic it will undergo and determine a comfort requirement level to fulfil.

Footbridge class conditions the need, or otherwise, to determine structure natural frequency. Where they are calculated, these natural frequencies lead to the selection of one or several dynamic load cases, as a function of the frequency value ranges. These load cases are defined to represent the various possible effects of pedestrian traffic. Treatment of the load cases provides the acceleration values undergone by the structure. The comfort level obtained can be qualified by the range comprising the values. The methodology is summarized in the organization chart below.

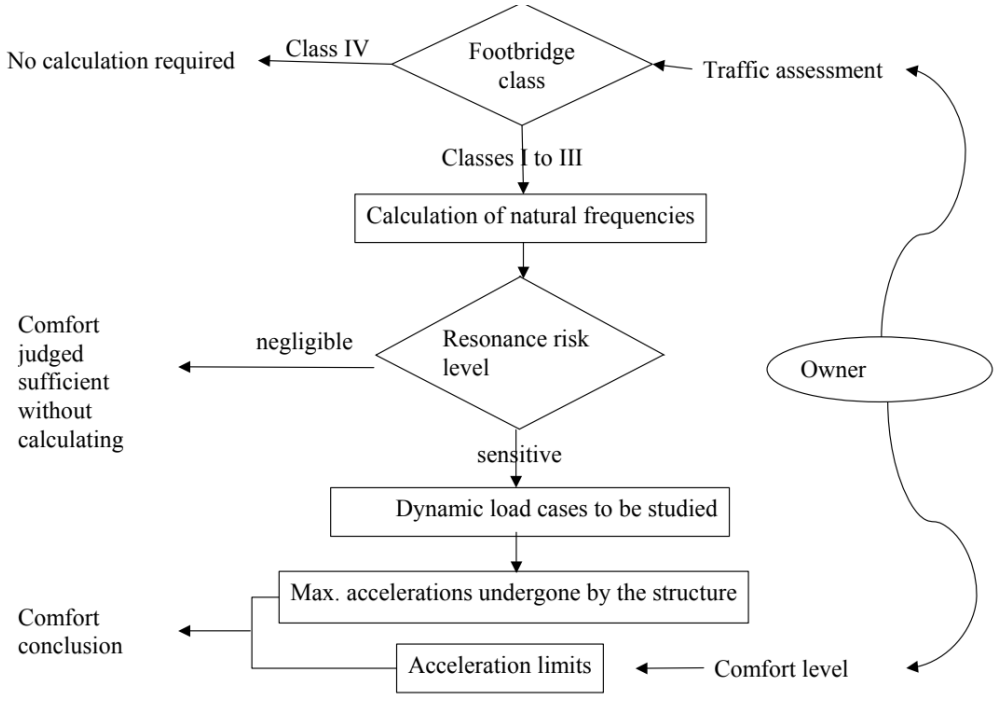

Figure 6-1 summarized scheme for dynamic analysis

This chapter also includes the specific verifications to be carried out (SLS and ULS) to take into account the dynamic behaviour of footbridges under pedestrian loading. Obviously, the standard verifications (SLS and ULS) are to be carried out in compliance with the texts in force; they are not covered by these guidelines.

6.1.1 Determination of footbridge class

Footbridge class makes it possible to determine the level of traffic it can bear:

Class IV: seldom used footbridge, built to link sparsely populated areas or to ensure continuity of the pedestrian footpath in motorway or express lane areas.

Class III: footbridge for standard use, which may occasionally be crossed by large groups of people but that will never be loaded throughout its bearing area.

Class II: urban footbridge linking populated areas, subjected to heavy traffic and that may occasionally be loaded throughout its bearing area.

Class I: urban footbridge linking up high pedestrian density areas (for instance, nearby presence of a rail or underground station) or that is frequently used by dense crowds.

(demonstrations, tourists, etc.), subjected to very heavy traffic. It is for the Owner to determine the footbridge class as a function of the above information and taking into account the possible changes in traffic level over time. His choice may also be influenced by other criteria that he decides to take into account. For instance, a higher class may be selected to increase the vibration prevention level, in view of high media expectations. On the other hand, a lower class may be accepted in order to limit construction costs or to ensure greater freedom of architectural design, bearing in mind that the risk related to selecting a lower class shall be limited to the possibility that, occasionally, when the structure is subjected to a load where traffic and intensity exceed current values, some people may feel uncomfortable.

Class IV footbridges are considered not to require any calculation to check dynamic behavior. For very light footbridges, it seems advisable to select at least Class III to ensure a minimum amount of risk control. Indeed, a very light footbridge may present high accelerations without there necessarily being any resonance**.**

In case in hand class this bridge is classified in **Class II** and calculation is considered in this regard.

6.1.2 Definition of the comfort level

The Owner determines the comfort level to bestow on the footbridge.

Maximum comfort: Accelerations undergone by the structure are practically imperceptible to the users.

Average comfort: Accelerations undergone by the structure are merely perceptible to the users.

Minimum comfort: under loading configurations that seldom occur, accelerations undergone by the structure are perceived by the users, but do not become intolerable. It should be noted that the above information cannot form absolute criteria: the concept of comfort is highly subjective, and a particular acceleration level will be experienced differently, depending on the individual. Furthermore, these guidelines

do not deal with comfort in premises either extensively or permanently occupied that some footbridges may undergo, over and above their pedestrian function.

Choice of comfort level is normally influenced by the population using the footbridge and by its level of importance. It is possible to be more demanding on behalf of particularly sensitive users (schoolchildren, elderly or disabled people), and more tolerant in case of short footbridges (short transit times).

In cases where the risk of resonance is considered negligible after calculating structure natural frequencies, comfort level is automatically considered sufficient.

6.1.3 Acceleration range associated with the comfort level

The level of comfort achieved is assessed through reference to the acceleration undergone by the structure, determined through calculation, using different dynamic load cases. Thus, it is not directly a question of the acceleration perceived by the users of the structure. Given the subjective nature of the comfort concept, it has been judged preferable to reason in terms of ranges rather than thresholds. Figures 6-2 and 6-3 define 4 value ranges, noted 1, 2, 3 and 4, for vertical and horizontal accelerations, respectively. In ascending order, the first 3 correspond to the maximum, mean and minimum comfort levels described in the previous paragraph. The 4th range corresponds to uncomfortable acceleration levels that are not acceptable.

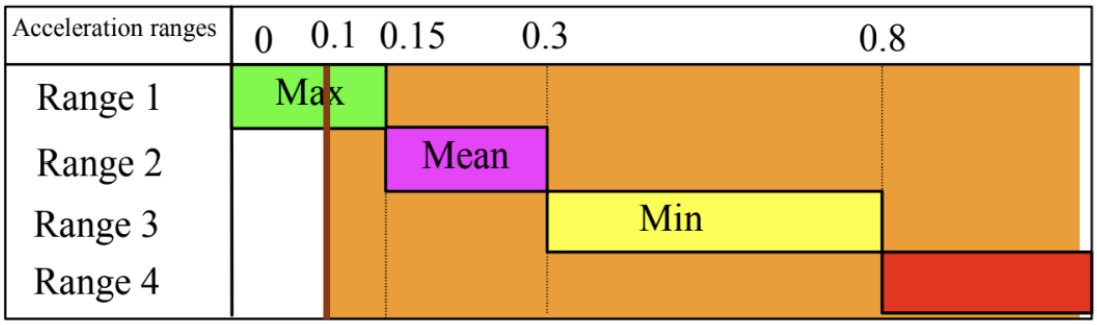

Figure 6-2 Acceleration Range-Lateral and Longitudinal direction

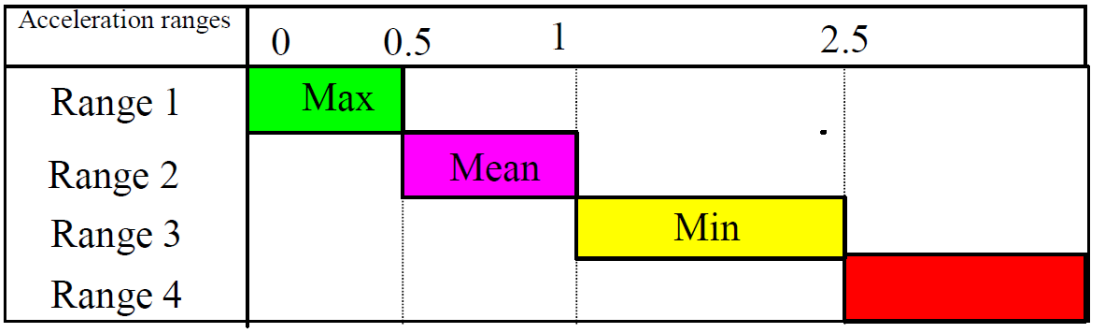

Figure 6-3 Acceleration-Vertical direction

6.1.4 Determination of frequencies and of the need to perform dynamic load case calculations or not

For Class I to III footbridges, it is necessary to determine the natural vibration frequency of the structure. These frequencies concern vibrations in each of 3 directions: vertical, transverse horizontal and longitudinal horizontal. They are determined by 2 mass assumptions: empty footbridge and footbridge loaded throughout its bearing area, to the tune of one 700 N pedestrian per square meter (70 kg/m2).

The ranges in which these frequencies are situated make it possible to assess the risk of resonance entailed by pedestrian traffic and, as a function of this, the dynamic load cases to study in order to verify the comfort criteria.

6.1.5 Frequency range classification

In both vertical and horizontal directions, there are four frequency ranges, corresponding to a decreasing risk of resonance:

Range 1: maximum risk of resonance.

Range 2: medium risk of resonance.

Range 3: low risk of resonance for standard loading situations.

Range 4: negligible risk of resonance.

Figure 6-4 defines the frequency ranges for vertical vibrations and for longitudinal horizontal vibrations. Figure 6-5 concerns transverse horizontal vibrations.

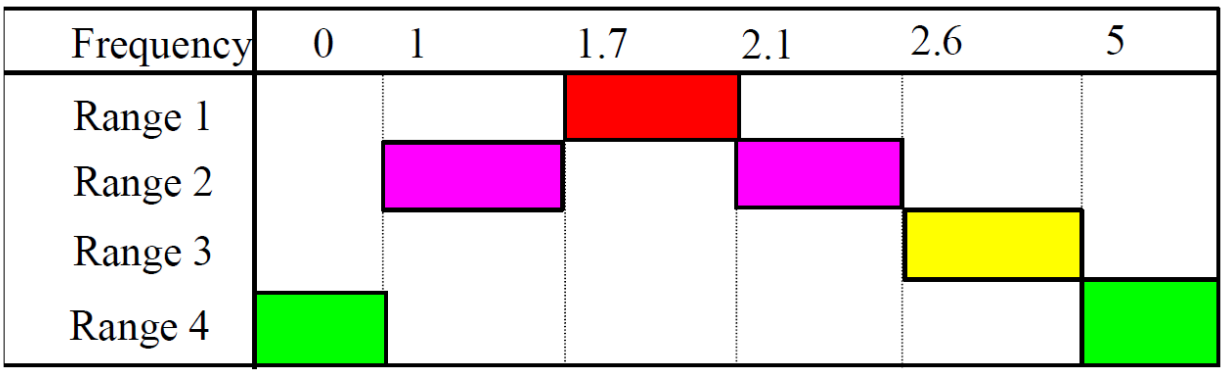

Figure 6-4 frequency ranges Longitudinal and Vertical directions

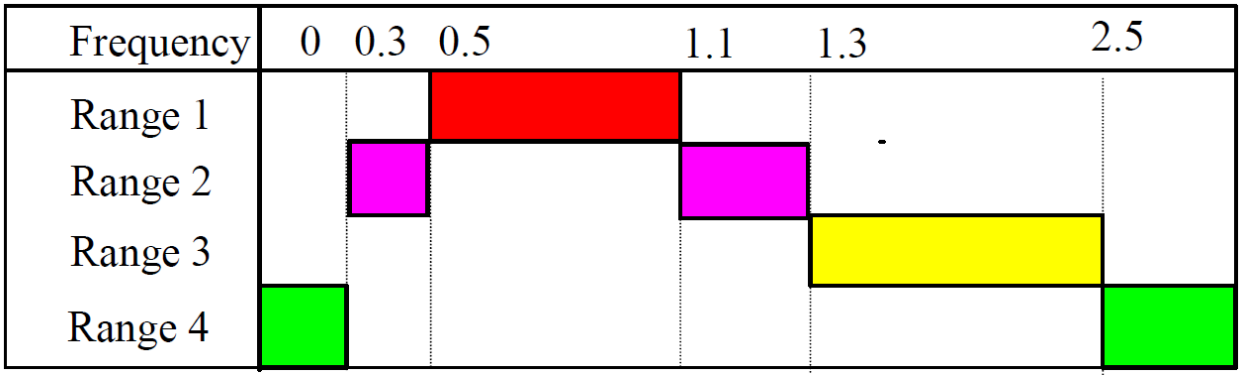

Figure 6-5 Frequency ranges - lateral direction

6.1.6 Definition of the required dynamic calculations

Depending on footbridge class and on the ranges within which its natural frequencies are situated, it is necessary to carry out dynamic structure calculations for all or part of a set of 3 load cases:

Case 1: sparse and dense crowd

Case 2: very dense crowd

Case 3: complement for an evenly distributed crowd (2nd harmonic effect)

Table 6-1 clearly defines the calculations to be performed in each case.

		Load cases to select for acceleration checks		
		Natural frequency range		
Traffic	Class	1	2	3
Sparse	III	Case1	Nil	Nil
Dense	II		Case 1	Case 3
Very dense	I	Case 2	Case 2	Case 3

Case No. 1: Sparse and dense crowd
Case No. 2: Very dense crowd
Case No. 3: Crowd complement (2nd harmonic)

Table 6-1 Footbridge classification

if necessary: calculation with dynamic load cases.

If the previous stage concludes that dynamic calculations are needed, these calculations shall enable:

- ✓ checking the comfort level criteria in paragraph 6.1.3 required by the Owner, under working conditions, under the dynamic load cases as defined hereafter,
- ✓ traditional SLS and ULS type checks, including the dynamic load cases.

6.1.7 Dynamic load cases

The load cases defined hereafter have been set out to represent, in a simplified and practicable way, the effects of fewer or more pedestrians on the footbridge. They have been constructed for each natural vibration mode, the frequency of which has been identified within a range of risk of resonance. Indications of the way these loads are to be taken into account and to be incorporated into structural calculation software, and the way the constructions are to be modelized are given in the next chapter.

Case 1: sparse and dense crowds

This case is only to be considered for category III (sparse crowd) and II (dense crowd) footbridges. The density d of the pedestrian crowd is to be considered according to the footbridge class:

Class	Density *d* of the crowd
III	0.5 pedestrians/m^2
II	0.8 pedestrians/m^2

Equation 6-1 Density of footbridge

This crowd is considered to be uniformly distributed over the total area of the footbridge S. The number of pedestrians involved is therefore: N = S × d. The number of equivalent pedestrians, in other words the number of pedestrians who, being all at the same frequency and in phase, would produce the same effects as random pedestrians,

in frequency and in phase is: $10{,}8 \times (\xi \times N)^{1/2}$. The load that is to be taken into account is modified by a minus factor ψ which makes allowance for the fact that the risk of resonance in a footbridge becomes less likely the further away from the range 1.7 Hz – 2.1 Hz for vertical accelerations, and 0.5 Hz – 1.1 Hz for horizontal accelerations. This factor falls to 0 when the footbridge frequency is less than 1 Hz for the vertical action and 0.3 Hz for the horizontal action. In the same way, beyond 2.6 Hz for the vertical action and 1.3 Hz for the horizontal action, the factor cancels itself out. In this case, however, the second harmonic of pedestrian walking must be examined.

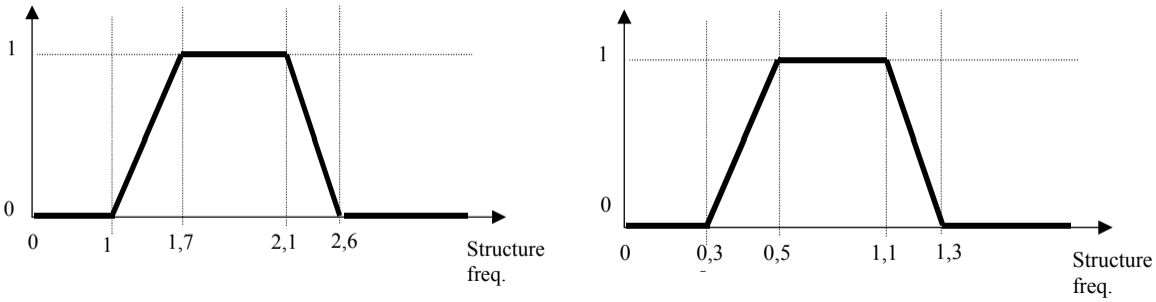

Figure 6-6 Spare and dense crowds coefficient ψ

The table below summarizes the load per unit area to be applied for each direction of vibration, for any random crowd, if one is interested in the vertical and longitudinal modes. ξ represents the critical damping ratio (no unit), and the number of pedestrians on the footbridge (d x S).

Direction	Load per m²
Vertical (v)	$d \times (280\text{N}) \times \cos(2\pi f_v t) \times 10.8 \times (\xi/n)^{1/2} \times \psi$
Longitudinal (l)	$d \times (140\text{N}) \times \cos(2\pi f_l t) \times 10.8 \times (\xi/n)^{1/2} \times \psi$
Transversal (t)	$d \times (35\text{N}) \times \cos(2\pi f_v t) \times 10.8 \times (\xi/n)^{1/2} \times \psi$

Equation 6-2 Vibration load cases spare and dense

The loads are to be applied to the whole of footbridge, and the sign of the vibration amplitude must, at any point, be selected to produce the maximum effect: the direction of application of the load must therefore be the same as the direction of the mode shape, and must be inverted each time the mode shape changes direction, when passing through a node.

Comment 1: in order to obtain these values, the number of equivalent pedestrians is calculated using the formula $10.8 \times (\xi \times n)^{1/2}$, then divided by the loaded area S, which is replaced by n/d (reminder n = S × d), which gives $d \times 10.8 \times (\xi / n)^{1/2}$, to be multiplied by the individual action of these equivalent pedestrians ($F0 \cos(\omega t)$) and by the minus factor ψ.

Comment 2: It is very obvious that these load cases are not to be applied simultaneously. The vertical load case is applied for each vertical mode at risk, and the longitudinal load case for each longitudinal mode at risk, adjusting on each occasion the frequency of the load to the natural frequency is concerned.

Comment 3: The load cases above do not show the static part of the action of pedestrians, G_0. This component has no influence on acceleration; however, it shall be borne in mind that the mass of each of the pedestrians must be incorporated within the mass of the footbridge.

Comment 4: These loads are to be applied until the maximum acceleration of the resonance is obtained. Remember that the number of equivalent pedestrians was constructed so as to compare real pedestrians with fewer fictitious pedestrians having perfect resonance.

Case 2: very dense crowd

This load case is only to be taken into account for class I footbridges.

The pedestrian crowd density to be considered is set at 1 pedestrian per m^2. This crowd is considered to be uniformly distributed over area S as previously defined. It is considered that the pedestrians are all at the same frequency and have random phases. In this case, the number of pedestrians all in phase equivalent to the number of pedestrians in random phases (n) is 1.85 n.

The second minus factor, ψ, because of the uncertainty of the coincidence between the frequency of stresses created by the crowd and the natural frequency of the construction, is defined by figure 6-7 according to the natural frequency of the mode under consideration, for vertical and longitudinal vibrations on the one hand, and transversal on the other. The following table summarizes the load to be applied per unit of area for each vibration direction. The same comments apply as those for the previous paragraph:

Direction	Load per m^2
Vertical (v)	$1.0 \times (280N) \times \cos(2\pi f_v t) \times 1.85\ (1/n)^{1/2} \times \psi$
Longitudinal (l)	$1.0 \times (140N) \times \cos(2\pi f_v t) \times 1.85\ (1/n)^{1/2} \times \psi$
Transversal (t)	$1.0 \times \ (35N) \times \cos(2\pi f_v t) \times 1.85\ (1/n)^{1/2} \times \psi$

Equation 6-3 Vibration load cases very dense crowed

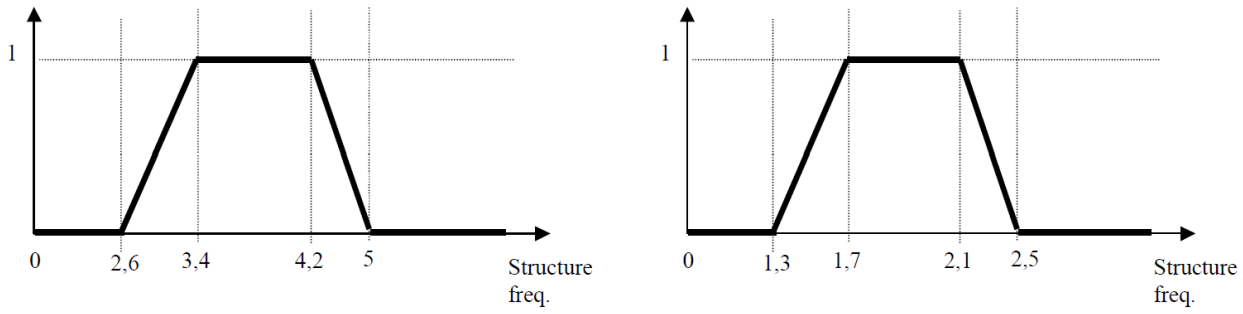

Figure 6-7 Second harmonic ψ factor

Case 3: effect of the second harmonic of the crowd

This case is similar to cases 1 and 2 but considers the second harmonic of the stresses caused by pedestrians walking, located, on average, at double the frequency of the first harmonic. It is only to be taken into account for footbridges of categories I and II.

The density of the pedestrian crowd to be considered is 0.8 pedestrians per m^2 for category II, and 1.0 for category I.

This crowd is considered to be uniformly distributed. The individual force exerted by a pedestrian is reduced to 70N vertically, 7N transversally and 35N longitudinally. For category II footbridges, allowance is made for the random character of the frequencies and of the pedestrian phases, as for load case No. 1.

For category I footbridges, allowance is made for the random character of the pedestrian phases only, as for load case No. 2.

The second minus factor, ψ, because of the uncertainty of the coincidence between the frequency of stresses created by the crowd and the natural frequency of the construction, is given by figure 6-7

according to the natural frequency of the mode under consideration, for vertical and longitudinal vibrations on the one hand, and transversal on the other.

6.2 DYNAMIC ANALYSIS

6.2.1 Eigenvalue analysis

in the Midas dynamic loads with RS FUNCTION, information that is taken from excel file that is based on SPETTRI-NTC is inserted, and here we are not considering 5 percent damping ratio because already included.

6.2.1.1 Normalized acceleration horizontal component SLV

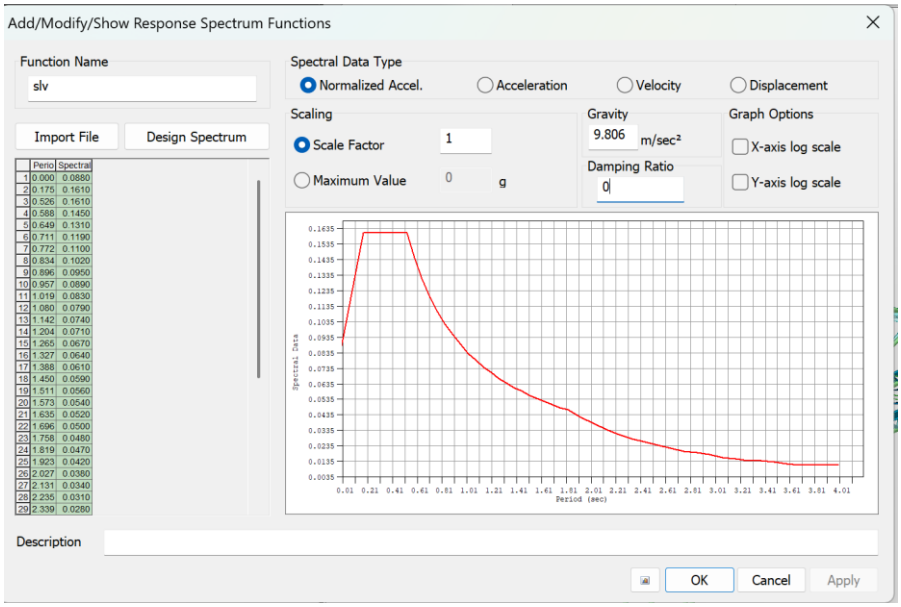

Figure 6-8 Normalized acceleration horizontal SLV

6.2.1.2 Normalized acceleration vertical component SLV

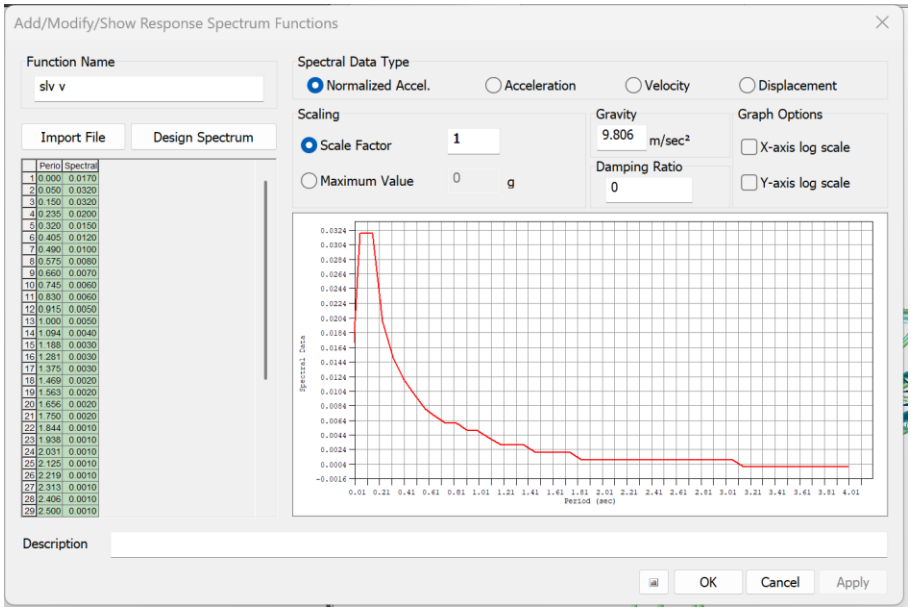

Figure 6-9 Normalized acceleration vertical SLV

6.2.1.3 Normalized acceleration horizontal component SLD

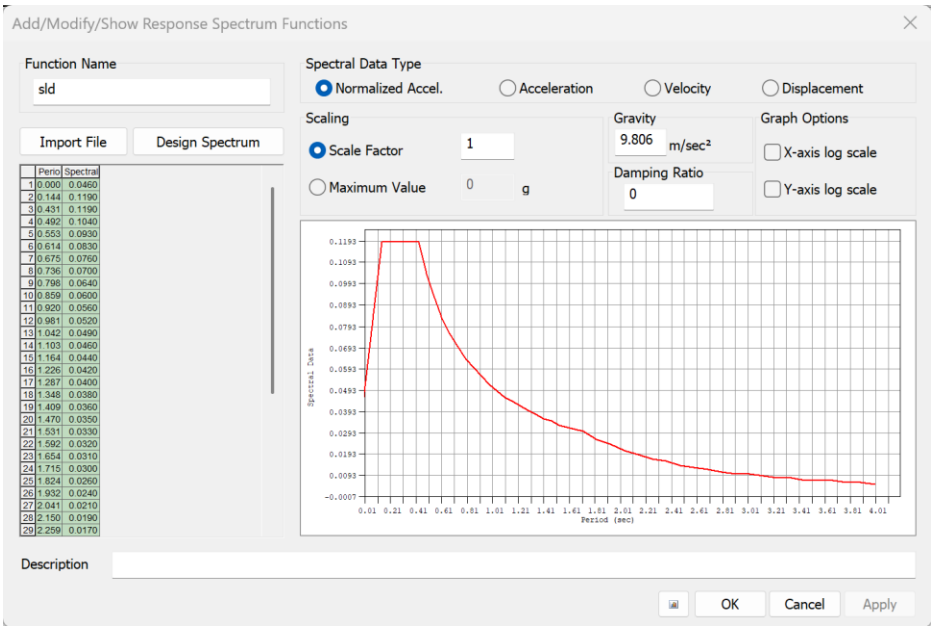

Figure 6-10 Normalized acceleration horizontal SLD

6.2.1.4 Normalized acceleration vertical component SLD

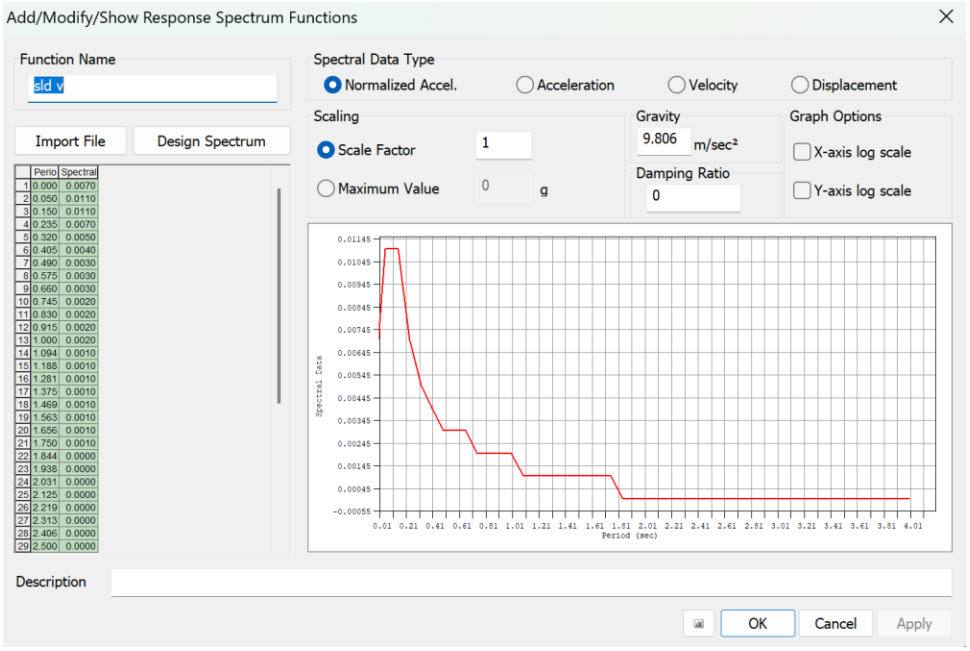

Figure 6-11 Normalized acceleration vertical SLD

6.2.2 Dynamic analysis SLS – Associated static pedestrian load case (crowd weight)

By referring to the standard we can see that we do not need to do the dynamic analysis for vertical direction, but we need to do that for horizontal and longitudinal direction what we need to obtain is sinusoidal function based on input we have by referring to the standard Setra.

In the case in hand, we need to examine second harmonic effect function that needs to be determined as following table.

Note: **This crowd is considered to be uniformly distributed. The individual force exerted by a pedestrian is reduced to 70N vertically, 7N transversally and 35N longitudinally. For category II footbridges, allowance is made for the random character of the frequencies and of the pedestrian phases, as for load case No. 1**.

Direction	Load per m^2
Vertical (v)	$1.0 \times (280\text{N}) \times \cos(2\pi f_v t) \times 1.85\ (1/n)^{1/2} \times \psi$
Longitudinal (l)	$1.0 \times (140\text{N}) \times \cos(2\pi f_v t) \times 1.85\ (1/n)^{1/2} \times \psi$
Transversal (t)	$1.0 \times \ (35\text{N}) \times \cos(2\pi f_v t) \times 1.85\ (1/n)^{1/2} \times \psi$

Equation 6-4 Dynamic load cases very dense

DYNAMIC PROPERTY	
AREA	155.4m^2
L	42m
B	3.7m
d	0.8
ψ SLS L	0.612
ψ SLS LA	0.675
ψ SLS LA	0.075
ξ	0.4%
Numbers of points	38
n	124.3

Table 6-2 Time history input

Numbers of points in FEM model is obtained as follows:

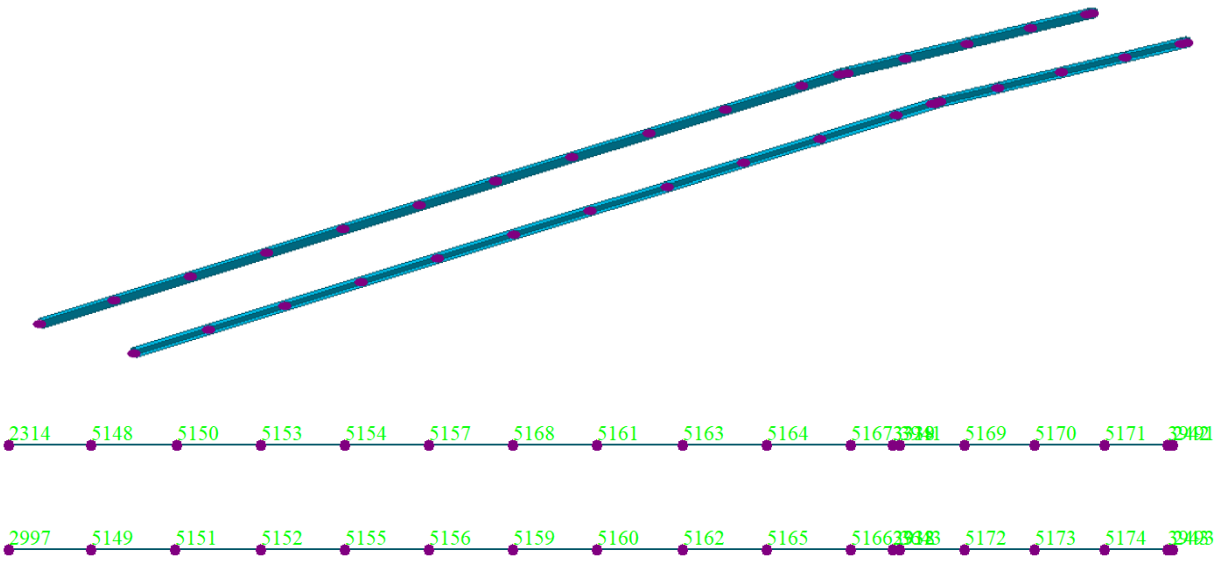

Figure 6-12 Number of nods on the deck

In Midas two dynamic load cases are created for two directions which are longitudinal and horizontal (lateral), analyzing type is linear, analyzing method is modal and time history type is transient.

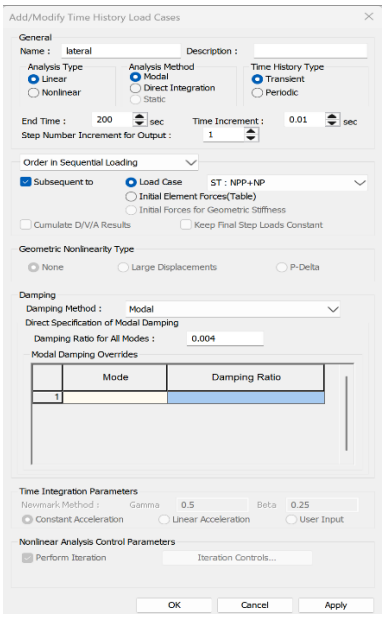

Figure 6-13 Lateral load case in Midas

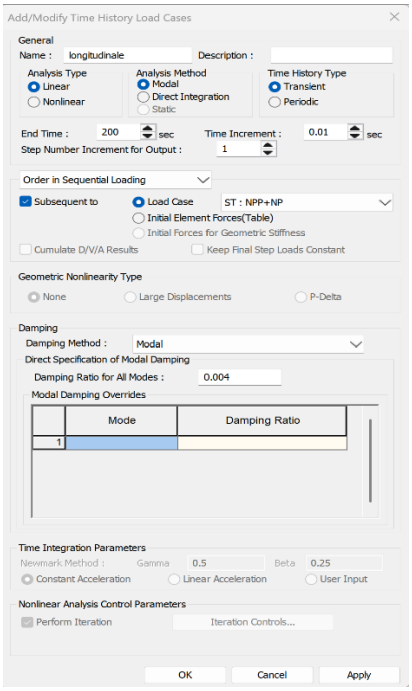

Figure 6-14 Longitudinal load case Midas

6.2.3 Time history input

Time history function is defined based on time history input as follows in Midas

Longitudinal direction function:

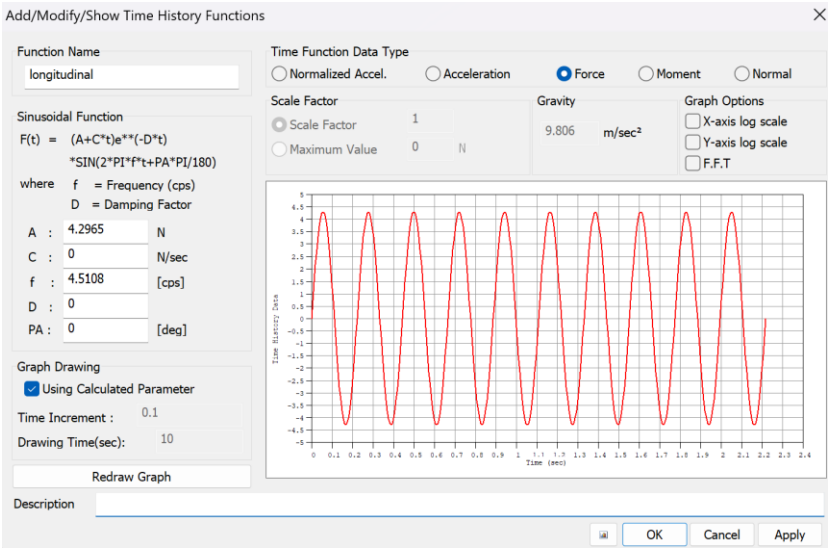

Figure 6-15 Longitudinal Time history function SLS (crowd weight)

Lateral direction function:

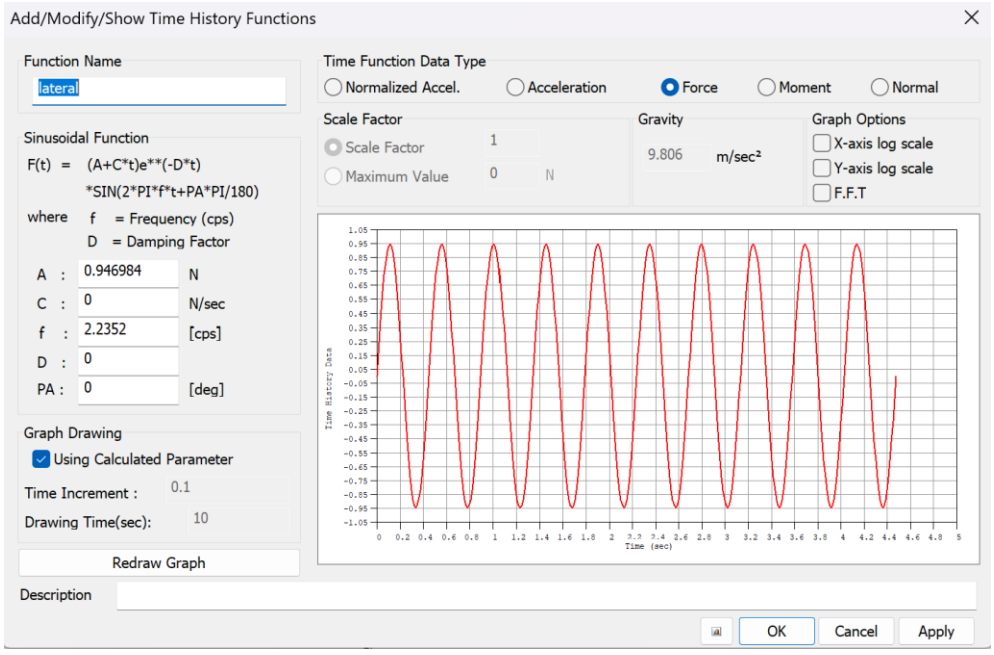

Figure 6-16 Lateral time history function (crowd weight)

Now we apply the loads on nodes that is provided in the section above and in this case we need to have 0.1m/s^2 acceleration in all nodes that we have on the deck.

6.2.4 Dynamic analysis SLS – Dynamic pedestrian load case (vibration load)

Taking same procedures for applying the load but in this case, we do not apply pedestrian load on the bridge 70kg/m^2, also in this case we need to have result upper that Setra standard limit.

6.2.4.1 Time history input

Longitudinal direction function:

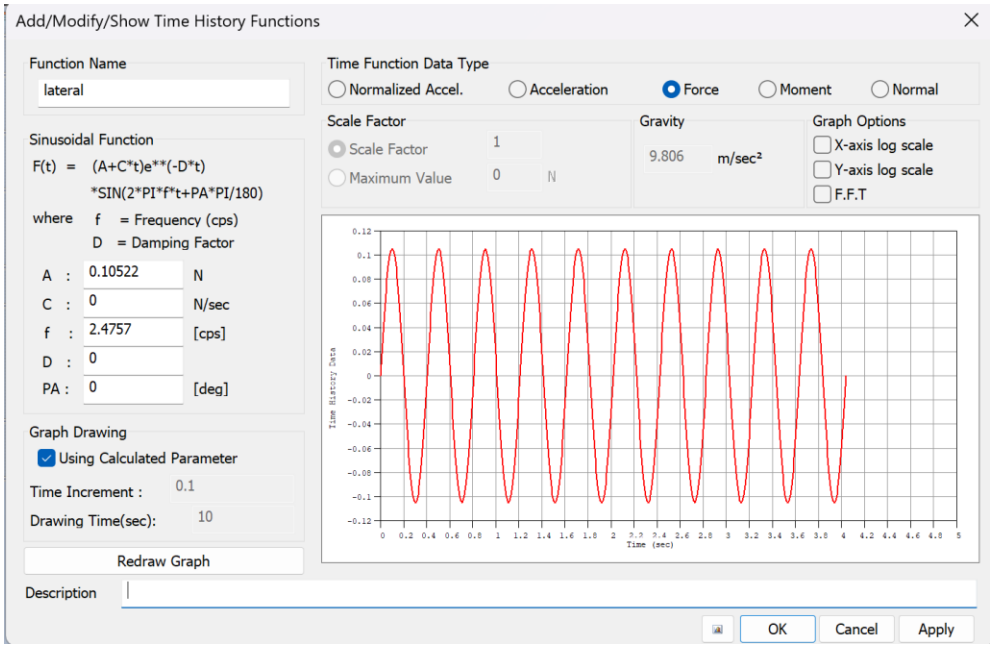

Figure 6-17 Lateral time history function SLS (vibration load)

Lateral direction function: Don't need to perform.

Now we apply the loads on nodes that is provided in the section above and in this case we need to have 0.1m/s^2 acceleration in all nodes that we have on the deck.

7 RESULTS

7.1 RESULTS OF EIGENVALUE ANALYSIS SLS – ASSOCIATED STATIC PEDESTRIAN LOAD CASE (CROWD WEIGHT)

After running the Model, we can analyse the risk of resonance by considering fundamental mode, which is first value in each direction, lateral (red), vertical (orange), and longitudinal (green).

Mode	UX	UY	UZ	RX	RY		RZ	
EIGENVALUE ANALYSIS								
Mode No	Frequency (rad/sec)	Frequency (cycle/sec)	Period (sec)	Tolerance				
1	14,04	2,24	0,45	0,00				
2	20,95	3,33	0,30	0,00				
3	28,34	4,51	0,22	0,00				
4	31,12	4,95	0,20	0,00				
5	37,76	6,01	0,17	0,00				
6	42,54	6,77	0,15	0,00				
7	46,07	7,33	0,14	0,00				
8	57,59	9,17	0,11	0,00				
9	61,62	9,81	0,10	0,00				
10	62,09	9,88	0,10	0,00				
11	71,88	11,44	0,09	0,00				
12	77,56	12,34	0,08	0,00				
13	79,37	12,63	0,08	0,00				
14	92,96	14,79	0,07	0,00				
15	125,62	19,99	0,05	0,00				
16	128,42	20,44	0,05	0,00				
17	172,19	27,41	0,04	0,00				
18	175,29	27,90	0,04	0,00				
19	215,69	34,33	0,03	0,00				
20	286,97	45,67	0,02	0,00				
21	354,24	56,38	0,02	0,00				

MODAL PARTICIPATION MASSES PRINTOUT												
Mode No	TRAN-X		TRAN-Y		TRAN-Z		ROTN-X		ROTN-Y		ROTN-Z	
	MASS(%)	SUM(%)	MASS(%)	SUM(%)	MASS(%)	SUM(%)	MASS(%)	SUM(%)	MASS(%)	SUM(%)	MASS(%)	SUM(%)
1	0,05	0,05	80,19	80,19	0,00	0,00	5,51	5,51	0,00	0,00	9,32	9,32
2	0,02	0,07	10,77	90,96	0,00	0,00	0,12	5,63	0,00	0,00	80,07	89,39
3	91,42	91,49	0,00	90,96	1,50	1,51	0,38	6,01	0,17	0,17	0,00	89,39
4	0,80	92,29	4,13	95,09	0,17	1,67	31,18	37,19	0,02	0,19	3,35	92,74
5	2,00	94,29	0,00	95,09	38,35	40,03	0,03	37,22	11,95	12,14	0,01	92,76
6	0,00	94,29	0,59	95,68	0,00	40,03	13,45	50,67	0,00	12,14	0,06	92,82
7	0,01	94,30	0,92	96,60	0,00	40,03	0,86	51,53	0,00	12,14	3,82	96,63

8	0,00	94,30	0,00	96,60	0,00	40,03	0,04	51,58	0,08	12,22	0,01	96,64
9	0,00	94,30	0,37	96,97	0,11	40,14	0,85	52,43	0,01	12,23	0,05	96,69
10	0,07	94,37	0,01	96,98	6,26	46,40	0,03	52,46	2,39	14,62	0,00	96,69
11	0,00	94,37	0,49	97,47	0,00	46,40	0,27	52,73	0,01	14,63	0,01	96,70
12	0,00	94,37	0,30	97,77	0,02	46,42	0,44	53,16	0,14	14,77	0,37	97,07
13	0,12	94,49	0,01	97,78	1,53	47,95	0,03	53,19	6,70	21,47	0,01	97,08
14	0,01	94,50	0,09	97,87	0,00	47,95	0,73	53,92	0,00	21,48	0,22	97,30
15	0,00	94,50	0,27	98,14	0,01	47,96	0,47	54,39	0,09	21,57	0,15	97,44
16	0,02	94,52	0,00	98,14	2,09	50,05	0,01	54,40	2,88	24,45	0,00	97,44
17	0,68	95,20	0,01	98,16	17,90	67,95	0,06	54,46	14,68	39,13	0,00	97,44
18	2,35	97,55	0,01	98,16	4,11	72,06	0,02	54,48	10,54	49,68	0,01	97,46
19	0,00	97,55	1,53	99,70	0,03	72,09	19,87	74,35	0,01	49,69	0,19	97,65
20	2,02	99,57	0,00	99,70	0,01	72,09	0,00	74,35	2,81	52,50	0,01	97,66
21	0,14	99,71	0,00	99,70	18,53	90,62	0,08	74,42	1,36	53,85	0,00	97,66

Table 7-1 Eigenvalue analysis SLS (crowd weight)

Result shows lateral and longitudinal frequencies are below the threshold of the S`ETRA limit and need to perform vibration check in case of acceleration.

7.1.1 Risk of resonance

Based on standard and results that is obtained in modal analyses we need to check frequency range classification due to risk of resonance, referring to the table result is as follows based on direction of vibration.

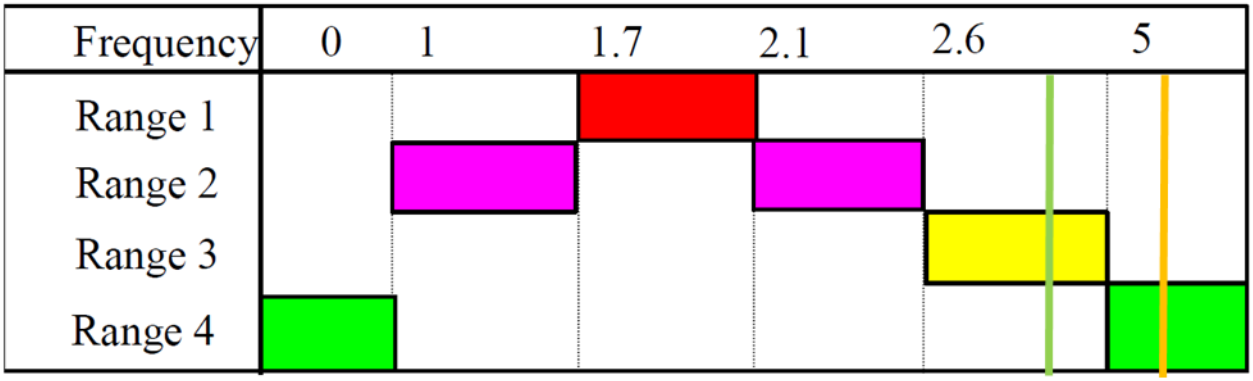

Figure 7-1 Risk of resonance-vertical and longitudinal SLS (crowd weight)

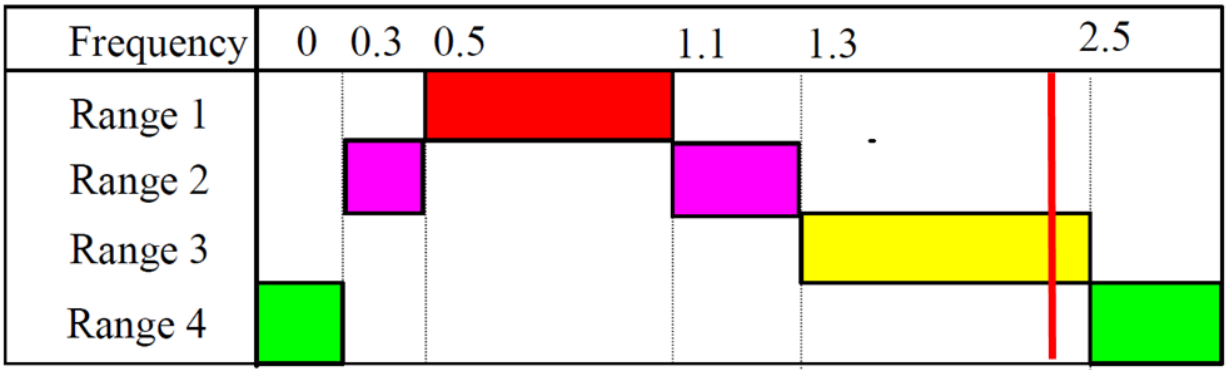

Figure 7-2 Risk of resonance-lateral direction SLS (crowd weight)

Figure 7-2 and Figure 7-1 show lateral and longitudinal directions, we need to perform dynamic analysis for verification of acceleration.

7.1.2 Result of acceleration in longitudinal direction

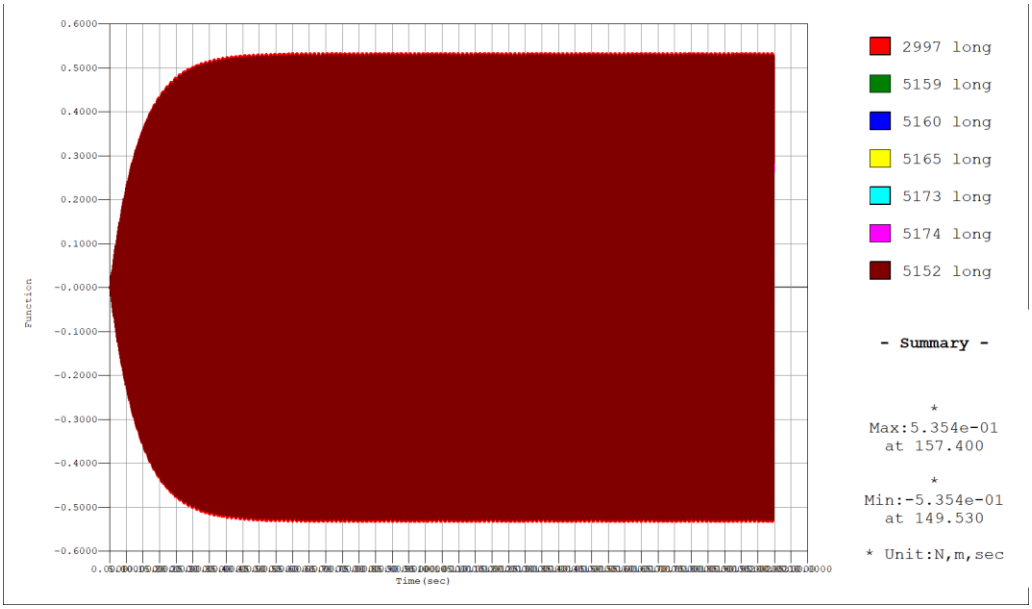

Figure 7-3 Longitudinal acceleration of points SLS (crowd weight)

7.1.3 Result of acceleration in lateral direction

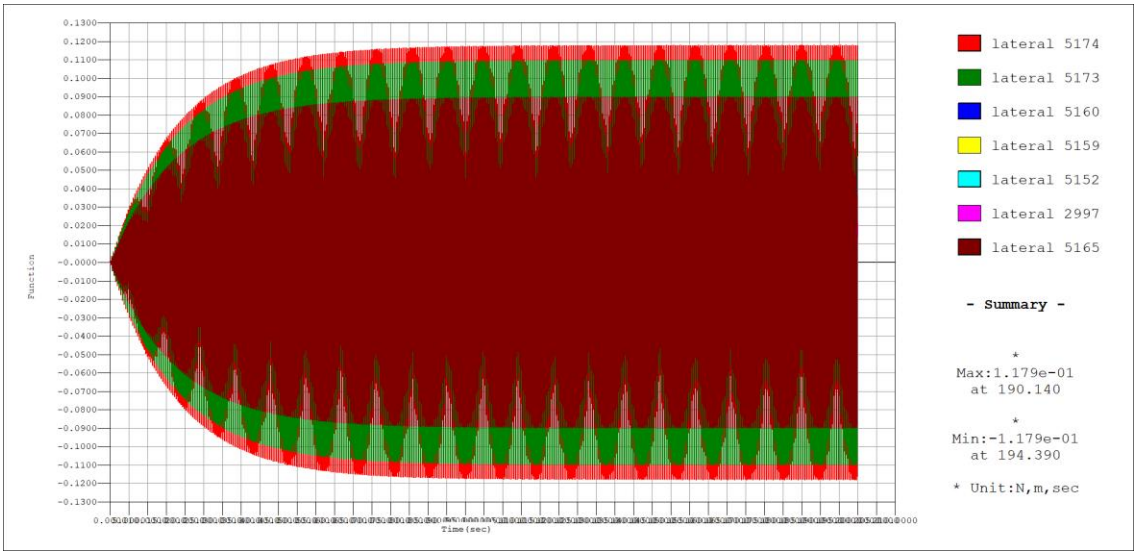

Figure 7-4 Lateral acceleration of points (crowd weight)

As we can see from graphs limited value for lateral and longitudinal is 0.1m/s^2.

Direction	Max value m/s^2
Lateral	0.11
Longitudinal	0.53

Table 7-2 Summary of acceleration SLS (crowd weight)

7.2 RESULT OF EIGENVALUE ANALYSIS SLS – DYNAMIC PEDESTRIAN LOAD CASE (VIBRATION LOAD)

After running the Model we can analyses the risk of resonance by considering fundamental mode which is first value in each direction, horizontal, vertical and longitudinal. And they are shown with lateral(red), longitudinal (green) and vertical (orange).

EIGENVALUE ANALYSIS								
Mode No	Frequency		Period	Tolerance				
	(rad/sec)	(cycle/sec)	(sec)					
1	15,56	2,48	0,40	0,00				
2	24,68	3,93	0,25	0,00				
3	33,16	5,28	0,19	0,00				
4	33,73	5,37	0,19	0,00				
5	38,17	6,07	0,16	0,00				
6	42,61	6,78	0,15	0,00				
7	53,66	8,54	0,12	0,00				
8	57,48	9,15	0,11	0,00				
9	62,09	9,88	0,10	0,00				

10	62,54	9,95	0,10	0,00				
11	75,52	12,02	0,08	0,00				
12	79,35	12,63	0,08	0,00				
13	79,54	12,66	0,08	0,00				
14	100,24	15,95	0,06	0,00				
15	128,10	20,39	0,05	0,00				
16	137,94	21,95	0,05	0,00				
17	173,07	27,55	0,04	0,00				
18	178,02	28,33	0,04	0,00				
19	220,02	35,02	0,03	0,00				
20	297,71	47,38	0,02	0,00				
21	356,20	56,69	0,02	0,00				

MODAL PARTICIPATION MASSES PRINTOUT

Mode No	TRAN-X		TRAN-Y		TRAN-Z		ROTN-X		ROTN-Y		ROTN-Z	
	MASS(%)	SUM(%)	MASS(%)	SUM(%)	MASS(%)	SUM(%)	MASS(%)	SUM(%)	MASS(%)	SUM(%)	MASS(%)	SUM(%)
1	0,03	0,03	73,78	73,78	0,00	0,00	10,14	10,14	0,00	0,00	10,43	10,43
2	0,01	0,04	12,13	85,91	0,00	0,01	0,01	10,15	0,00	0,00	78,42	88,85
3	48,01	48,05	3,09	89,00	2,78	2,78	11,55	21,69	0,69	0,69	0,76	89,60
4	32,67	80,73	4,91	93,91	4,28	7,06	14,63	36,32	1,03	1,72	1,35	90,95
5	11,32	92,05	0,03	93,94	32,83	39,89	0,11	36,42	11,80	13,52	0,04	90,99
6	0,00	92,05	0,74	94,69	0,00	39,89	13,46	49,89	0,00	13,52	0,02	91,01
7	0,02	92,07	0,61	95,29	0,00	39,89	0,64	50,53	0,00	13,52	3,87	94,88
8	0,00	92,07	0,00	95,29	0,00	39,89	0,00	50,53	0,07	13,59	0,00	94,88
9	0,13	92,20	0,00	95,30	6,31	46,20	0,01	50,54	2,59	16,19	0,00	94,88
10	0,01	92,20	0,36	95,66	0,04	46,24	2,31	52,84	0,04	16,23	0,29	95,17
11	0,00	92,20	0,32	95,98	0,01	46,25	0,69	53,53	0,01	16,24	0,35	95,52
12	0,13	92,34	0,01	95,99	1,45	47,70	0,00	53,53	6,23	22,47	0,00	95,52
13	0,03	92,37	0,38	96,37	0,08	47,79	0,17	53,71	0,35	22,82	0,00	95,52
14	0,01	92,38	0,80	97,18	0,00	47,79	0,79	54,49	0,00	22,82	0,00	95,53
15	0,03	92,41	0,00	97,18	2,04	49,82	0,04	54,53	2,84	25,66	0,00	95,53
16	0,06	92,47	0,07	97,25	0,03	49,85	0,95	55,48	0,28	25,94	0,00	95,53
17	0,08	92,55	0,01	97,26	21,82	71,67	0,06	55,55	20,95	46,89	0,00	95,53
18	4,06	96,61	0,06	97,32	0,24	71,91	0,43	55,98	2,48	49,37	0,01	95,54
19	0,06	96,66	2,22	99,53	0,05	71,96	18,67	74,65	0,04	49,41	0,65	96,18
20	2,84	99,50	0,00	99,54	0,03	71,99	0,00	74,65	2,34	51,75	0,01	96,19
21	0,13	99,64	0,00	99,54	18,39	90,38	0,04	74,69	1,23	52,97	0,00	96,20

Table 7-3 Eigenvalue analysis SLS (vibration load)

From result of modal analysis it can be evident that only lateral direction needs to be checked.

7.2.1 Result of risk of resonance

Based on standard and results that is obtained in modal analyses we need to check frequency range classification due to risk of resonance, referring to the table result is as follows based on direction of vibration.

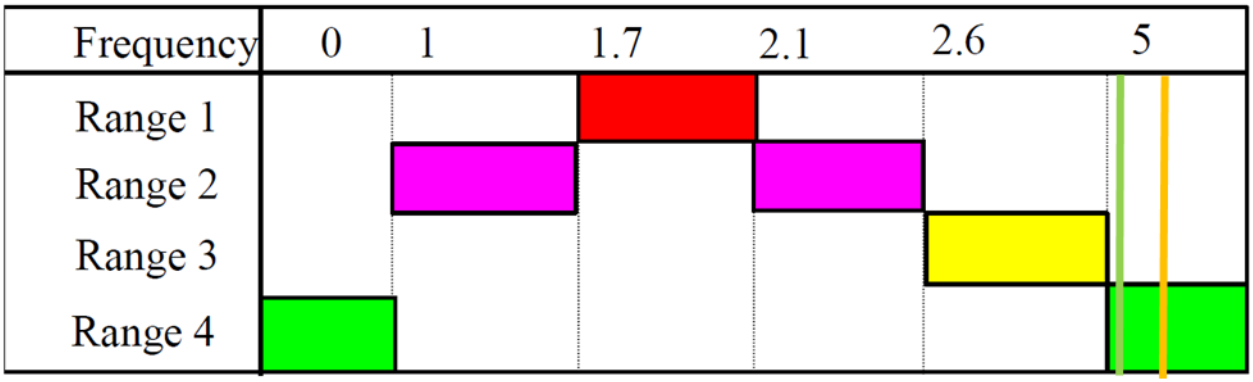

Figure 7-5 Risk of resonance-longitudinal and vertical directions SLS (vibration load)

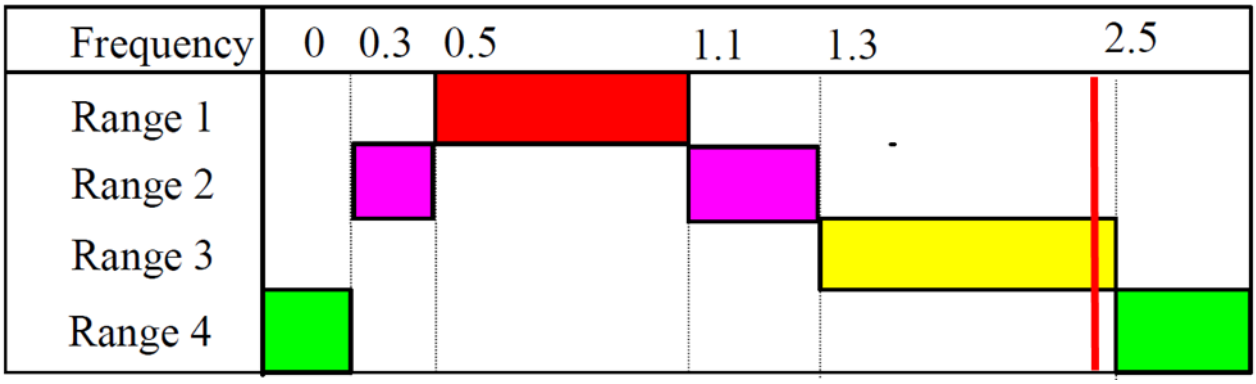

Figure 7-6Risk of resonance-lateral direction SLS (vibration load)

7.2.2 Result of acceleration in longitudinal direction

Because it passes the limit of Setra do not need to check.

7.2.3 Result of acceleration in lateral direction

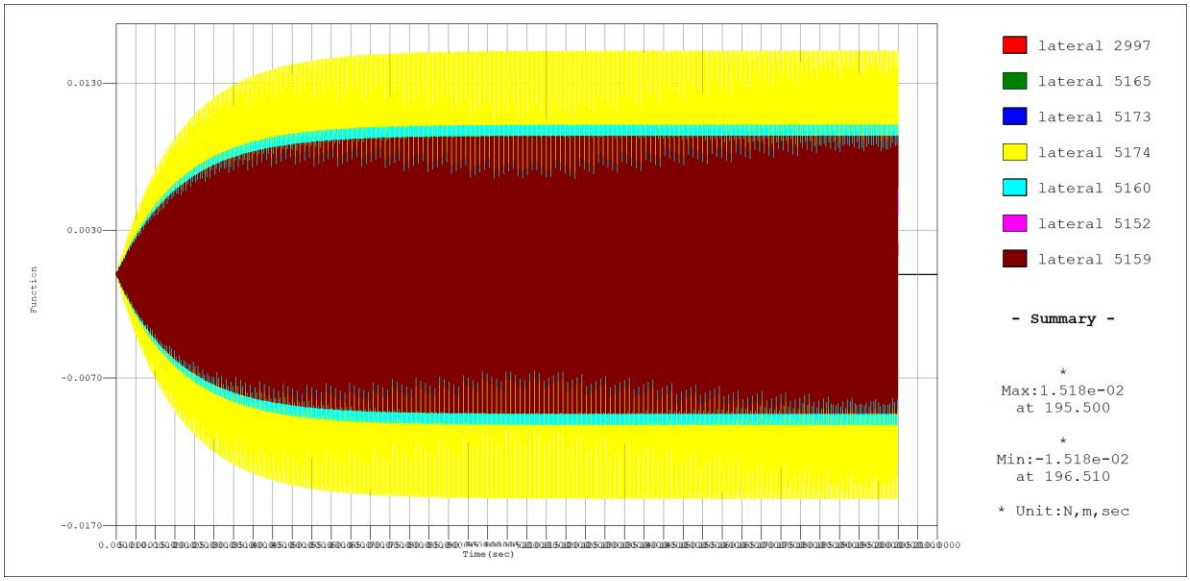

Figure 7-7 Lateral acceleration of points SLS (vibration load)

As we can see in the graphs result of acceleration in SLS – Dynamic pedestrian load case (vibration load) condition for two directions are verified.

Direction	Max value m/s^2
Lateral	0.015

Table 7-4 Summary of lateral acceleration

8 VERIFICATION

8.1 SUMMARY OF VERIFICATION OF STEEL PROFILE

Verification of steel profiles are satisfied and summary of verification is as follows for each profile in table:

The following correspondence between the report “Properties” and the profile names adopted in this thesis is used:

- ✓ **Property 1 → CHS 219.15 mm**
- ✓ **Property 2 → CHS 273×5 mm**
- ✓ **Property 7 → C400×200×12 mm**
- ✓ **Property 8 → 2C200×5 mm**
- ✓ **Property 10 → L60×6 mm**

The governing utilization factors for the selected profiles are reported below (together with the governing beam element Trave and the governing load combination L.C.).

Profile	Utilization	Governing Trave	Governing L.C.	Class	Fatt.Inst	Governing Trave	Combination	Class
CHS 219.1×5 mm	0.69	1076	Cmb 22	2	0.53	773	Cmb 21	2
CHS 273×5 mm	0.62	1106	Cmb 22	3	0.63	722	Cmb 21	3
C400×200×12 mm	0.68	664	Cmb 14	4	0.67	1323	Cmb 22	4
2C200×5 mm	0.67	705	Cmb 13	3	0.76	705	Cmb 13	3
L60×6 mm	0.38	518	Cmb 14	4	0.00*	—	—	—

Table 8-1 Summary of verification of profiles SLU

8.1.1 Profile verification

CHS 219.1×5 mm (Property 1): The circular hollow section CHS 219.1×5 mm satisfies both resistance and stability requirements. The governing resistance utilization is **Fatt.Res = 0.69** (Cmb 22), while the governing stability utilization is **Fatt.Inst = 0.53** (Cmb 21). Both values remain below unity, confirming adequate safety margins.

CHS 273×5 mm (Property 2): The CHS 273×5 mm profile is verified under the governing combinations. The maximum resistance utilization is **Fatt.Res = 0.62** (Cmb 22) and the maximum stability utilisation is **Fatt.Inst = 0.63** (Cmb 21), both indicating compliance with the prescribed criteria.

C400×200×12 mm (Property 7): For the C400×200 profile family, the governing utilization factors are **Fatt.Res = 0.68** (Cmb 14) and **Fatt.Inst = 0.67** (Cmb 22), with the section reported as **Class 4** in the

summary. The results confirm verification in both resistance and stability under the governing ULS/SLV combinations.

2C200×5 mm (Property 8): The built-up profile 2C200×5 mm is verified, with the governing scenario occurring in **Cmb 13** for both checks. The maximum resistance utilization is **Fatt.Res = 0.67**, while the maximum stability utilization is **Fatt.Inst = 0.76**. Among the selected profiles, this is the highest stability demand, but it remains below unity and therefore compliant.

L60×6 mm (Property 10): The equal angle L60×6 mm is verified with a governing resistance utilization of **Fatt.Res = 0.38** (Cmb 14). In the summary table, stability is not governing for this profile, and the profile remains well within the admissible limits for the design combinations considered.

Concluding statement for the verification chapter

The verification results confirm that the selected profiles used in the project satisfy the requirements in both **resistance** and **stability** under the governing ULS/SLV combinations. For the examined subset, the maximum utilization factors are **0.69–0.68** in resistance (depending on profile) and **0.76** in stability (2C200×5 mm), all remaining below the limit value of 1.00.

8.2 VERIFICATION OF THE COMFORT LEVEL

8.2.1 Dynamic comfort verification (SETRA) – interpretation of deck accelerations

The dynamic comfort check according to the **SETRA footbridge guideline** is based on comparing the **deck acceleration** produced by pedestrian excitation with **admissible horizontal acceleration limits**, which are commonly expressed through comfort classes (maximum/medium/minimum/unacceptable). In SETRA-type assessments, horizontal (lateral and longitudinal) comfort is typically judged using peak acceleration ranges where, for example, **< 0.10 m/s²** corresponds to very good comfort and **> 0.80 m/s²** corresponds to unacceptable discomfort for horizontal vibrations.

8.2.2 verification of comfort level SLS – Associated static pedestrian load case (crowd weight)

In the numerical model, accelerations were extracted at representative deck nodes. The time histories show a rapid increase of response at the beginning, followed by a plateau (steady amplitude). This behavior is typical of a forced vibration close to resonance, where the response grows until it is limited by the assumed damping and the steady-state harmonic balance is reached.

8.2.2.1 Lateral direction

The graph of acceleration in the points that mentioned shows that in lateral direction, maximum lateral acceleration obtained **0.11m/s²** which is still not verified.

8.2.2.2 Longitudinal direction

For the longitudinal direction (nodes 2997, 5152, 5159, 5160, 5165, 5173, 5171), the response is significantly larger. The maximum recorded longitudinal acceleration is:

- **a_{max} = 0.53 m/s²**

This value is **greater than 0.10 m/s²**, which not verified acceleration in any case limited to value that is mentioned.

Why the longitudinal points are not verified:
The longitudinal direction is **not verified** because the computed peak acceleration (**0.53 m/s²**) exceeds even the upper bound of the "minimum comfort" range and enters the **unacceptable** domain. This is typically associated with one (or more) of the following mechanisms:

- ✓ **Resonance proximity:** the dominant longitudinal natural frequency is close to a pedestrian excitation harmonic, producing strong amplification and a steady-state plateau.
- ✓ **Low effective damping in the longitudinal mode:** small damping leads to higher steady-state amplitudes under harmonic forcing.
- ✓ **High modal participation along the bridge axis:** the longitudinal mode shape mobilizes a large part of the deck mass at the extracted points, so many nodes show similar peak levels.

8.2.3 verification of comfort level SLS – Dynamic pedestrian load case (vibration load)

Dynamic time-history analyses were performed without including pedestrian live load/mass, and the acceleration response was extracted at the selected deck control points (IDs 2997, 5152, 5159, 5160, 5165, 5173, 5174). The time histories show an initial transient phase followed by a stabilized response, indicating that the vibration amplitude reaches a steady level governed by the structural damping and the proximity between excitation frequencies and the bridge natural frequencies.

8.2.3.1 Lateral direction

The maximum acceleration obtained from the plot summary is:

$$a_{lat,\max} = 0.015 \text{m/s}^2$$

This value corresponds to max comfort criteria, so it is verified under SLS conditions.

8.2.3.2 Longitudinal direction

Under SLS condition based on modal analysis result frequency of longitudinal direction is 5.28Hz which shows that value is greater than 5Hz and verification of acceleration do not need to be carried out.

9 CONCLUSION

9.1 AIM AND ADOPTED STANDARD

This chapter concludes the vibration assessment of the reference footbridge using the **Sétra (Sétra–AFGC) guideline** procedure for pedestrian-induced vibrations. The objective is to evaluate the **risk of resonance** and, where required, verify that the **deck accelerations** remain within acceptable comfort limits for users.

The Sétra approach is applied following the standard workflow:

- ✓ classify the footbridge (traffic class),
- ✓ define comfort requirement,
- ✓ perform **modal (eigenvalue) analysis** to screen resonance risk,
- ✓ when screening indicates sensitivity, perform **dynamic calculations (time-history)** and compare **peak accelerations** to comfort thresholds.

Inputs used in the dynamic model

The dynamic verification uses the same structural numerical model adopted in previous chapters and includes the loads explicitly listed for the dynamic analysis:

- ✓ self-weight (automatic),
- ✓ steel sheet weight (16 kg/m²),
- ✓ parapet weight (50 kg/m),
- ✓ pedestrian live load (70 kg/m²).

The pedestrian excitation is introduced using Sétra-type simplified harmonic functions and implemented in MIDAS as **time-history dynamic load cases** in the two horizontal directions:

- ✓ **longitudinal** (along the bridge axis),
- ✓ **lateral/transverse** (across the bridge width).

The time-history function parameters reported in the thesis (deck area, geometry, coefficients and number of loaded nodes) are those used to build the excitation functions and apply them to the deck nodes in the FEM model.

9.2 RESONANCE SCREENING

The eigenvalue analysis is used as a **screening step** to decide whether comfort verification requires time-history calculations.

From the reference-model eigenvalue results, the bridge has low-frequency horizontal modes that fall inside the Sétra sensitivity ranges, meaning a **risk of resonance** under pedestrian excitation and therefore the need to check accelerations in the horizontal directions.

In the thesis, it is also stated that **vertical direction checks are not required** under the adopted Sétra rule in this case, while horizontal directions (lateral and longitudinal) remain relevant for comfort verification.

9.3 COMFORT CRITERIA

The comfort verification is based on comparing **peak deck acceleration** to the adopted limit:

- ✓ $\mathbf{a_{lim} = 0.10\ m/s^2}$ (horizontal comfort threshold used as the governing criterion in the thesis).

Accelerations are extracted at representative deck nodes (control points). For ULS checks, two sets are used in the lateral direction and one set in longitudinal direction; in SLS the same deck points are monitored.

The time histories show a typical forced response: **initial growth and then a steady plateau**, which indicates that the excitation is close to a structural frequency and the steady amplitude is mainly controlled by damping and modal participation.

9.4 VERIFICATION OUTCOME

9.4.1 verification SLS – Associated static pedestrian load case (crowd weight)

- ✓ **Lateral direction:** the maximum lateral acceleration is approximately **0.11 m/s²**, slightly above the 0.10 m/s² limit → **NOT VERIFIED** (at least for the most demanding set of points).
- ✓ **Longitudinal direction:** the maximum longitudinal acceleration reaches approximately **0.53 m/s²** → clearly above the comfort limit → **NOT VERIFIED**.

So, in SLS – Associated static pedestrian load case (crowd weight) the comfort requirement is not satisfied, and the **governing failure is longitudinal**.

Important correction for consistency: one earlier “Results” table swaps the max values between lateral and longitudinal, but the later verification section and explanation clearly identify **0.11 m/s² as lateral** and **0.53 m/s² as longitudinal**, which is the consistent interpretation adopted here.

9.4.2 verification SLS-dynamic pedestrian load case (vibration load)

For SLS, the thesis reports time-history analyses at the same deck points and indicates:

- ✓ **Lateral direction:** verified (accelerations fall in the acceptable comfort range).
- ✓ **Longitudinal direction:** the thesis states that based on the modal result (**5.28 Hz**), the longitudinal frequency exceeds the adopted threshold and therefore a time-history acceleration verification is not required under the screening rule.

Even with this screening argument for SLS – Dynamic pedestrian load case (vibration load), the overall dynamic behaviour remains dominated by the longitudinal sensitivity highlighted in static pedestrian load case (crowd weight).

9.5 INTERPRETATION AND FINAL STATEMENT

The non-verification is mainly associated with **resonance-type amplification** in horizontal modes:

- ✓ the response builds up and stabilizes (plateau), typical of excitation close to a natural frequency,
- ✓ the longitudinal direction shows high peaks at multiple deck points, meaning a **global longitudinal mode** participates strongly, not a local vibration only.

In practical terms, the reference configuration behaves like a structure with **insufficient longitudinal dynamic robustness** under pedestrian excitation: either the longitudinal stiffness is too low, the damping is too low, or the boundary conditions (supports/bearings) allow too much longitudinal participation—so the steady-state vibration becomes large.

Based on the Sétra-based procedure applied:

- ✓ the modal screening indicates **horizontal sensitivity** and requires dynamic checks,
- ✓ the comfort criterion **a_lim = 0.10 m/s²** is **not satisfied** in the reference model, especially in the **longitudinal direction** (0.53 m/s² SLS – Associated static pedestrian load case),
- ✓ therefore, **mitigation measures are necessary**, and they must primarily target **reducing longitudinal accelerations** (by increasing stiffness, increasing damping, and/or improving the support/bearing behaviour).

This conclusion motivates the next chapter, where interventions are proposed and compared specifically to shift frequencies away from pedestrian excitation and reduce resonance amplification.

10 PROPOSED INTERVENTIONS TO MITIGATE EXCESSIVE VIBRATIONS

10.1 INTRODUCTION

The dynamic verification of the footbridge highlighted that, under pedestrian excitation, the structural response is strongly influenced by the proximity between the bridge natural frequencies and the dominant walking-induced frequencies. In the critical cases, this frequency matching leads to resonance phenomena, which amplify the vibration response and may cause acceleration levels to exceed the comfort/safety thresholds adopted for serviceability checks. In this work, in line with the SETRA-based approach and the conservative requirement to keep peak accelerations below **0.1 m/s²** to avoid resonance-related discomfort, a set of practical structural interventions is proposed to shift the natural frequencies away from excitation ranges, reduce vibration amplitudes, and improve overall robustness and durability.

The proposed interventions target the two main drivers of the observed dynamic behavior: **global stiffness (and therefore natural frequencies)** and **energy dissipation (damping)**. From a structural mechanics perspective, increasing stiffness generally increases natural frequencies and reduces displacement/acceleration amplification under pedestrian loads; increasing damping reduces the resonance peak and limits acceleration even when frequency separation is not fully achievable. The following measures are therefore introduced as design-oriented solutions to mitigate the identified vibration issues while keeping the interventions feasible for construction and retrofitting.

10.1.1 Increasing the opening between the legs of the central columns

The central support configuration has a key role in controlling the global lateral and longitudinal stiffness of the deck–support system. Increasing the spacing (opening) between the legs of the central columns enhances the effective lever arm and the lateral stability of the support, increasing the frame's resistance to sway and reducing flexibility in the most vibration-sensitive direction. This intervention is intended to improve the structural restraint provided at midspan, modify the mode shapes, and shift critical frequencies away from the pedestrian excitation band.

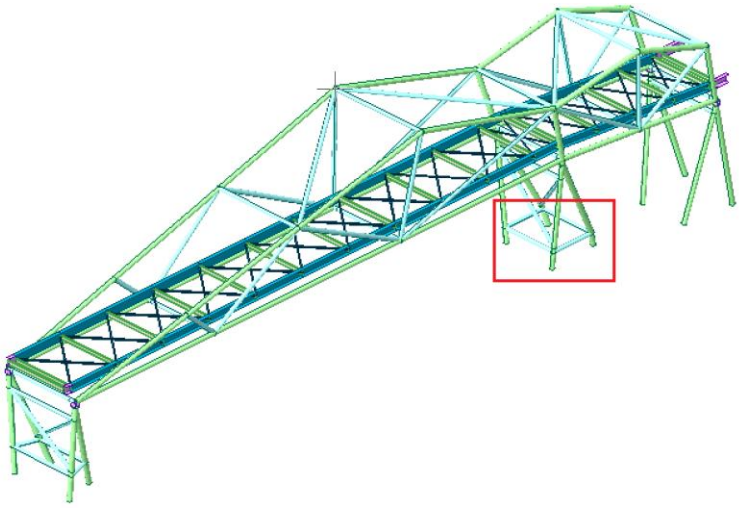

Figure 10-1 scheme of proposed increasing of legs

10.1.2 Increasing the cross-section of the central columns

Enlarging the cross-section (or thickness) of the central columns increases bending and torsional stiffness and reduces the deformation demand at the support region. Since the bridge dynamic response is highly sensitive to support flexibility, a stiffer central support typically results in higher natural frequencies and lower modal participation in the critical modes. This measure directly addresses the lack of stiffness that contributes to high accelerations under pedestrian loading.

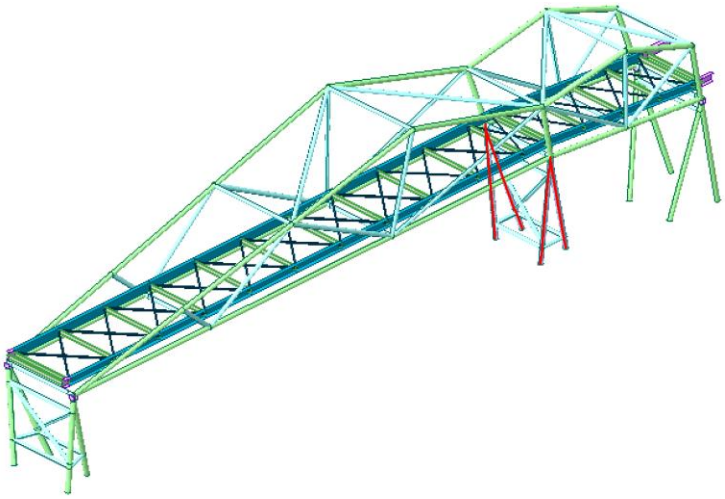

Figure 10-2 Scheme of proposed changing cross section

10.1.3 Adding bracing to the final portion currently without bracing

The unbraced end segment behaves more flexibly, creating a local “soft” zone that can contribute to large vibration amplitudes and unfavorable mode shapes. Introducing bracing in this region increases the lateral stiffness, improves load redistribution, and reduces torsional and transverse deformations of the deck-

support system. In dynamic terms, the bracing reduces modal displacements in the flexible zone and helps avoid localized vibration concentration at the end of the bridge.

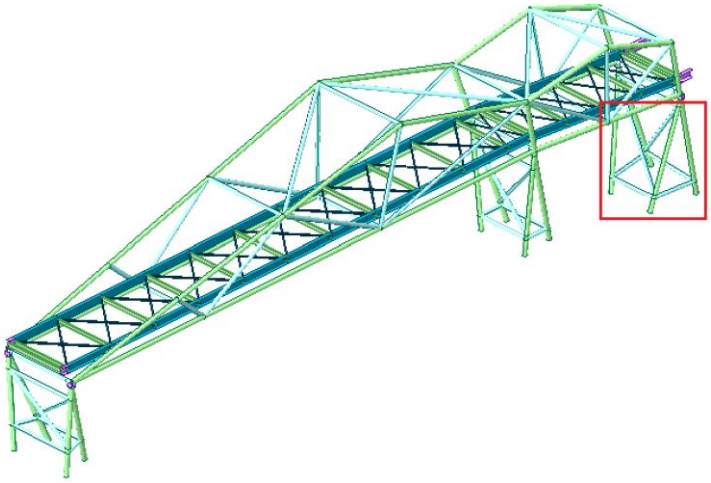

Figure 10-3 Scheme of proposed adding bracing

10.1.4 Replacing Teflon bearings with rubber bearings

Beyond stiffness, damping is crucial in vibration serviceability. Teflon-based bearings typically provide very low damping and allow smoother sliding, which can reduce energy dissipation and increase the risk of resonance amplification. Rubber bearings, in contrast, introduce **additional damping** through material hysteresis and also provide a more controlled stiffness in translation/rotation. The replacement is therefore aimed at reducing acceleration peaks by dissipating vibrational energy more effectively, improving user comfort and limiting resonance effects even when complete frequency separation is difficult to achieve.

Overall, these interventions are selected to act in a complementary way: **stiffness-oriented measures** (geometry adjustment of supports, larger column sections, added bracing) primarily aim to **increase natural frequencies and reduce flexibility**, while the **bearing replacement** primarily aims to **increase damping and reduce resonance amplification**. The combined objective is to ensure that both longitudinal and lateral vibration checks satisfy the adopted acceleration limits, improving the bridge's comfort performance and operational reliability under pedestrian use.

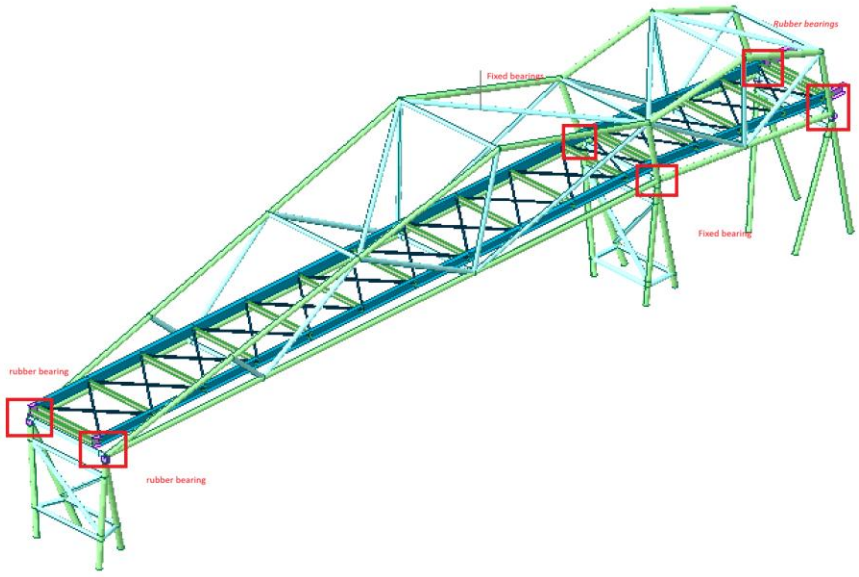

Figure 10-4 Scheme of proposed changing of bearings

In order to ensure that the proposed interventions are not only conceptually effective but also quantitatively justified, the effect of each modification will be assessed and reported separately. For every intervention (increase of the opening between the central column legs, increase of the central column cross-section, addition of bracing in the unbraced end segment, and replacement of Teflon bearings with rubber bearings), the structural model will be updated and re-analysed under the same pedestrian excitation scenarios adopted in the verification phase.for this phase using rubber bearings of 480mm x 230mm with thickness of 10mm result of stiffnes are reported below that is intered on Midas with elastic links .

No	Node	Node2	Type	B Angle	RIGID	SDx	SDy	SDz	SRx	SRy	SRz	Shear Spring Location	Distance Ratio SD	Distance Ratio SDz	Group
1	5283	2314	GEN	0.00	11100	0.00	0.00	0.00	0.00	0.00	0.00	☐	0.50	0.50	Default
2	5284	2997	GEN	0.00	11100	0.00	0.00	0.00	0.00	0.00	0.00	☐	0.50	0.50	Default
3	5316	2493	GEN	0.00	11100	0.00	0.00	0.00	0.00	0.00	0.00	☐	0.50	0.50	Default
4	5315	2491	GEN	0.00	11100	0.00	0.00	0.00	0.00	0.00	0.00	☐	0.50	0.50	Default
5	1676	3281	GEN	0.00	00100	1270	9936	0.00	0.00	0.00	0.00	☐	0.50	0.50	Default
6	1673	2659	GEN	0.00	00100	1270	9936	0.00	0.00	0.00	0.00	☐	0.50	0.50	Default
7	2508	5321	GEN	0.00	00100	1270	9936	0.00	0.00	0.00	0.00	☐	0.50	0.50	Default
8	3554	5322	GEN	0.00	00100	1270	9936	0.00	0.00	0.00	0.00	☐	0.50	0.50	Default
45	5289	5152	GEN	0.00	11100	0.00	0.00	0.00	0.00	0.00	0.00	☐	0.50	0.50	Default
46	5290	5153	GEN	0.00	11100	0.00	0.00	0.00	0.00	0.00	0.00	☐	0.50	0.50	Default
53	5300	5161	GEN	0.00	11100	0.00	0.00	0.00	0.00	0.00	0.00	☐	0.50	0.50	Default
54	5299	5160	GEN	0.00	11100	0.00	0.00	0.00	0.00	0.00	0.00	☐	0.50	0.50	Default
61	5308	3318	RIGID	0.00	00000	0.00	0.00	0.00	0.00	0.00	0.00	☐	0.50	0.50	Default
62	5307	3932	RIGID	0.00	00000	0.00	0.00	0.00	0.00	0.00	0.00	☐	0.50	0.50	Default
65	5311	5170	GEN	0.00	11100	0.00	0.00	0.00	0.00	0.00	0.00	☐	0.50	0.50	Default
66	5312	5173	GEN	0.00	11100	0.00	0.00	0.00	0.00	0.00	0.00	☐	0.50	0.50	Default

Figure 10-5 Elastic link property

Trelleborg Elastomeric Bearing Pads & Strips

Part No.	Strip Dimensions mm x mm	Working Load per Metre kN/m	Compressive Stiffness kN/mm/m	Shear Stiffness kN/mm/m	Shear Capacity +/- mm	Rotation Capacity rad
Type O 5 x 50	5 x 50	200	550	9.0	2	0.022
Type O 5 x 75	5 x 75	300	1163	13.5	2	0.010
Type O 5 x 100	5 x 100	400	2001	18.0	2	0.006
Type O 5 x 125	5 x 125	500	3061	22.5	2	0.004
Type O 5 x 150	5 x 150	600	4348	27.0	2	0.003
Type O 5 x 200	5 x 200	800	7599	36.0	2	0.002
Type O 10 x 50	10 x 50	100	138	4.5	5	0.044
Type O 10 x 75	10 x 75	225	309	6.8	5	0.029
Type O 10 x 100	10 x 100	400	550	9.0	5	0.022
Type O 10 x 125	10 x 125	500	828	11.3	5	0.014
Type O 10 x 150	10 x 150	600	1163	13.5	5	0.010
Type O 10 x 200	10 x 200	800	2001	18.0	5	0.006
Type O 15 x 75	15 x 75	150	138	4.5	8	0.044
Type O 15 x 100	15 x 100	265	244	6.0	8	0.033
Type O 15 x 125	15 x 125	415	381	7.5	8	0.026
Type O 15 x 150	15 x 150	600	550	9.0	8	0.022
Type O 15 x 200	15 x 200	800	933	12.0	8	0.013
Type O 20 x 75	20 x 75	110	77	3.4	10	0.058
Type O 20 x 100	20 x 100	200	138	4.5	10	0.044
Type O 20 x 125	20 x 125	315	215	5.6	10	0.035
Type O 20 x 150	20 x 150	450	309	6.8	10	0.029
Type O 20 x 200	20 x 200	800	550	9.0	10	0.022
Type O 20 x 250	20 x 250	1000	828	11.3	10	0.014
Type O 25 x 100	25 x 100	160	88	3.6	13	0.055
Type O 25 x 125	25 x 125	250	138	4.5	13	0.044
Type O 25 x 150	25 x 150	360	198	5.4	13	0.036
Type O 25 x 200	25 x 200	640	352	7.2	13	0.027
Type O 25 x 250	25 x 250	1000	550	9.0	13	0.022

Other sizes available upon request

1. Calculations based on AS5100.4 Bearings
2. Maximum Total Load = Working Load as stated in table + 25%
3. Parameters for rubber: Hardness SDH 60, Shear Modulus (MN/m^2)=0.9
4. For thicknesses over 5mm shear deflection is 50%. For 5mm thickness shear deflection is 40%
5. Maximum Rotation = Rotation as stated in table + 30% (table value includes 0.0035 radians for construction tolerances).
6. Tolerance on calculated stiffness value +/-20%
7. Calculations based on bearing strip mounted between wood float finished concrete surfaces

Figure 10-6 Rubber bearing property

Rubber bearing stiffness used in MIDAS (elastic links)

A rubber pad with plan dimensions **480×230 mm** and thickness **10 mm** was considered. Starting from catalogue stiffness values provided per metre length, stiffness was scaled to the target width and then converted to pad stiffness using the actual pad length.

- ✓ Width scaling ratio:

$$r = \frac{230}{200} = 1.15$$

- ✓ Shear stiffness scaling (∝ width):

$$k_{s,230} = 18.0 \cdot 1.15 = 20.7 \text{ kN/mm/m}$$

- ✓ Compressive stiffness scaling (∝ width²):

$$k_{c,230} = 2001 \cdot (1.15)^2 = 2646.3 \text{ kN/mm/m}$$

- ✓ Conversion from "per metre" to pad stiffness using pad length $L = 0.48$m:

$$K_h = k_{s,230} \cdot L = 20.7 \cdot 0.48 = 9.936 \text{ kN/mm}$$
$$K_v = k_{c,230} \cdot L = 2646.3 \cdot 0.48 = 1270.2 \text{ kN/mm}$$

Implementation in MIDAS: model the rubber bearing as an **elastic link** with translational stiffness:

- ✓ **Kx = Ky = 9.936 kN/mm** (horizontal shear)
- ✓ **Kz = 1270.2 kN/mm** (vertical compression)

10.1.5 Combination of adding bracing to the final portion currently without bracing , change Teflon to Rubber bearing and change the cross section

Because vibration behaviour is governed by both stiffness and damping, a combined retrofit strategy may be more robust than a single modification. In this thesis, a combined configuration is considered by simultaneously:

- ✓ Increasing the central column cross-section (stiffness increase),
- ✓ Adding bracing in the previously unbraced end segment (local stiffness increase),
- ✓ Replacing Teflon bearings with rubber bearings (damping increase + boundary modification).

The purpose is to obtain a configuration where the governing fundamental frequencies are moved above the adopted screening thresholds and where resonance amplification is reduced, so that comfort verification is either satisfied directly or time-history checks become unnecessary.

11 RESULT OF PROPOSED INTERVENSIONS

11.1 DYNAMIC ANALYSIS

For each intervention, an eigenvalue analysis was performed for **SLS – Associated static pedestrian load case (crowd weight)** and **SLS – Dynamic pedestrian load case (vibration load)** mass configurations. The governing modal frequency for each direction was identified using the **dominant translational modal participation mass**:

- ✓ **Longitudinal mode** → highest **TRAN-X** participation (X, green)
- ✓ **Lateral mode** → highest **TRAN-Y** participation (Y, red)
- ✓ **Vertical mode** → highest **TRAN-Z** participation (Z, orange)

SÉTRA screening used in this thesis:

- if $f_Y > 2.5\ Hz$, lateral resonance risk is low → lateral time-history check may be omitted.
- if $f_Z > 5\ Hz$, vertical and longitudinal resonance risk is low → vertical time-history check may be omitted.

11.1.1 Eigenvalue analysis of Increasing the opening between the legs of the central columns

11.1.1.1 Eigenvalue analysis SLS – Associated static pedestrian load case (crowd weight)

Mode	UX	UY	UZ	RX	RY	RZ		
EIGENVALUE ANALYSIS								
Mode No	Frequency		Period	Tolerance				
	(rad/sec)	(cycle/sec)	(sec)					
1	13,62	2,17	0,46	0,00				
2	21,22	3,38	0,30	0,00				
3	31,04	4,94	0,20	0,00				
4	32,97	5,25	0,19	0,00				
5	38,23	6,09	0,16	0,00				
6	42,53	6,77	0,15	0,00				
7	46,13	7,34	0,14	0,00				
8	57,58	9,16	0,11	0,00				
9	61,50	9,79	0,10	0,00				
10	62,13	9,89	0,10	0,00				
11	70,42	11,21	0,09	0,00				
12	76,49	12,17	0,08	0,00				
13	79,41	12,64	0,08	0,00				
14	94,27	15,00	0,07	0,00				
15	126,46	20,13	0,05	0,00				

16	128,59		20,47		0,05		0,00					
17	171,48		27,29		0,04		0,00					
18	176,97		28,17		0,04		0,00					
19	212,85		33,88		0,03		0,00					
20	257,83		41,04		0,02		0,00					
21	352,28		56,07		0,02		0,00					
MODAL PARTICIPATION MASSES PRINTOUT												
Mode No	TRAN-X		TRAN-Y		TRAN-Z		ROTN-X		ROTN-Y		ROTN-Z	
	MASS(%)	SUM(%)	MASS(%)	SUM(%)	MASS(%)	SUM(%)	MASS(%)	SUM(%)	MASS(%)	SUM(%)	MASS(%)	SUM(%)
1	0,04	0,04	80,16	80,16	0,00	0,00	5,59	5,59	0,00	0,00	9,57	9,57
2	0,01	0,05	11,19	91,35	0,00	0,00	0,16	5,75	0,00	0,00	79,56	89,14
3	1,91	1,96	3,48	94,84	0,01	0,01	30,52	36,27	0,00	0,00	3,54	92,67
4	80,13	82,09	0,16	94,99	7,46	7,47	0,49	36,76	1,20	1,20	0,14	92,81
5	12,07	94,15	0,01	95,00	32,50	39,96	0,04	36,79	11,00	12,21	0,02	92,83
6	0,00	94,16	0,56	95,57	0,00	39,96	13,25	50,04	0,00	12,21	0,04	92,87
7	0,02	94,17	1,00	96,57	0,00	39,96	0,96	51,01	0,00	12,21	3,51	96,39
8	0,01	94,18	0,00	96,57	0,00	39,96	0,03	51,04	0,08	12,29	0,00	96,39
9	0,00	94,18	0,34	96,91	0,07	40,03	1,03	52,07	0,00	12,29	0,08	96,46
10	0,20	94,38	0,00	96,91	6,28	46,31	0,02	52,09	2,47	14,76	0,00	96,47
11	0,00	94,39	0,31	97,22	0,00	46,31	0,68	52,77	0,00	14,76	0,00	96,47
12	0,00	94,39	0,46	97,68	0,00	46,31	0,56	53,33	0,08	14,83	0,36	96,83
13	0,27	94,66	0,00	97,68	1,57	47,88	0,02	53,35	6,67	21,50	0,00	96,83
14	0,01	94,67	0,06	97,74	0,00	47,89	0,46	53,81	0,00	21,50	0,30	97,14
15	0,01	94,68	0,23	97,98	0,37	48,25	0,36	54,17	0,40	21,90	0,10	97,23
16	0,04	94,72	0,06	98,03	1,81	50,06	0,31	54,48	2,66	24,56	0,02	97,26
17	0,18	94,90	0,01	98,04	20,74	70,81	0,01	54,49	18,84	43,40	0,00	97,26
18	3,22	98,12	0,01	98,05	1,53	72,34	0,04	54,53	5,84	49,23	0,02	97,28
19	0,00	98,12	1,65	99,70	0,01	72,34	20,88	75,41	0,01	49,24	0,35	97,63
20	1,53	99,65	0,01	99,71	0,02	72,36	0,06	75,47	3,50	52,74	0,02	97,65
21	0,09	99,74	0,00	99,71	18,09	90,45	0,07	75,54	1,55	54,29	0,00	97,65

Table 11-1 Eigenvalue analysis of Increasing the opening between the legs of the central columns SLS (crowd weight)

From the modal participation results:

- ✓ **Lateral (Y, red):** Mode 1, $f_Y = 2.17Hz$ (TRAN-Y = 80%)
- ✓ **Longitudinal (X, green):** Mode 4, $f_X = 5.25\ Hz$ (dominant TRAN-X = 80%)
- ✓ **Vertical (Z, orange):** Mode 5, $f_Z = 6.09\ Hz$ (TRAN-Z= 32.5%)

According to the adopted SÉTRA screening, **vertical verification is not required** because $\boldsymbol{f_Z > 5\ Hz}$. The **lateral frequency remains below 2.5 Hz**, therefore **lateral resonance risk remains,** and a dynamic acceleration verification is required in Y. Longitudinal behavior is close to the screening limit but still is verified.

Risk of resonance:

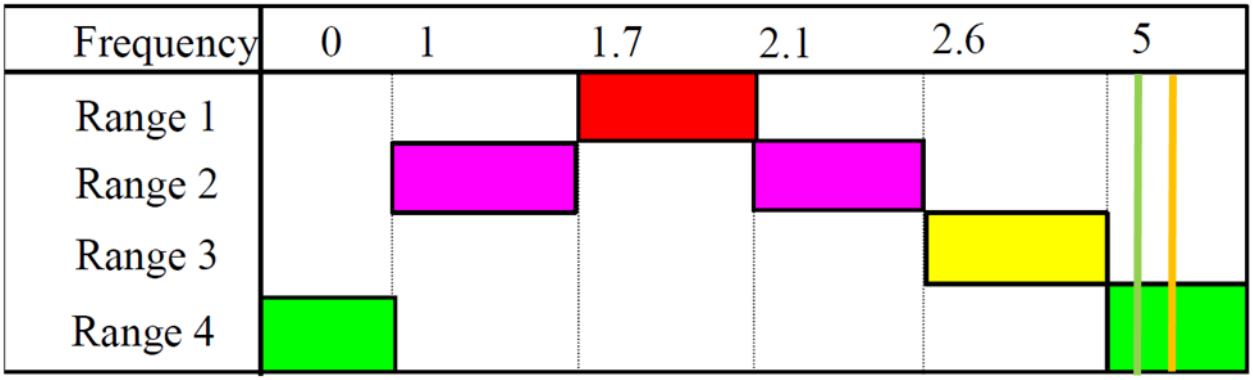

Figure 11-1 Risk of resonance- vertical and longitudinal Increasing the opening between the legs of the central columns SLS (crowd weight)

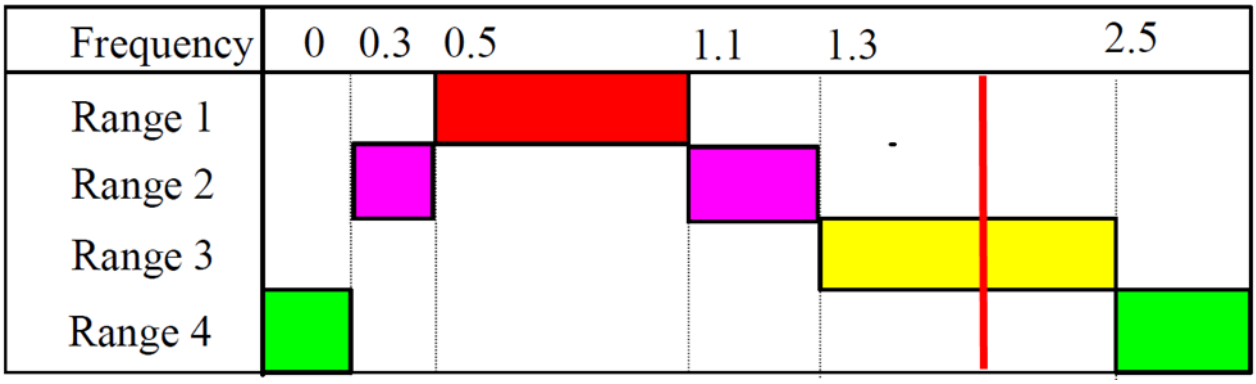

Figure 11-2 Risk of resonance- lateral direction - Increasing the opening between the legs of the central columns SLS (crowd weight)

The resonance screening plot confirms that the **red (lateral, Y)** component remains within the critical range because $f_Z = 6.09\ Hz < 2.5\ Hz$. The **green (longitudinal, X)** component is shifted upward compared to the reference model. The **orange (vertical, Z)** component is above the **5 Hz** threshold and does not trigger further checks.

11.1.1.2 Eigenvalue analysis SLS – Dynamic pedestrian load case (vibration load)

Mode	UX	UY	UZ	RX	RY	RZ		
EIGENVALUE ANALYSIS								
Mode No	Frequency		Period	Tolerance				
	(rad/sec)	(cycle/sec)	(sec)					
1	15,11	2,40	0,42	0,00				
2	24,99	3,98	0,25	0,00				

3	33,38	5,31	0,19	0,00				
4	36,35	5,78	0,17	0,00				
5	40,95	6,52	0,15	0,00				
6	42,60	6,78	0,15	0,00				
7	53,68	8,54	0,12	0,00				
8	57,49	9,15	0,11	0,00				
9	62,16	9,89	0,10	0,00				
10	62,50	9,95	0,10	0,00				
11	77,31	12,30	0,08	0,00				
12	79,43	12,64	0,08	0,00				
13	80,81	12,86	0,08	0,00				
14	98,75	15,72	0,06	0,00				
15	127,69	20,32	0,05	0,00				
16	140,76	22,40	0,04	0,00				
17	172,05	27,38	0,04	0,00				
18	179,08	28,50	0,04	0,00				
19	213,41	33,96	0,03	0,00				
20	272,20	43,32	0,02	0,00				
21	354,09	56,36	0,02	0,00				

MODAL PARTICIPATION MASSES PRINTOUT

Mode No	TRAN-X		TRAN-Y		TRAN-Z		ROTN-X		ROTN-Y		ROTN-Z	
	MASS(%)	SUM(%)	MASS(%)	SUM(%)	MASS(%)	SUM(%)	MASS(%)	SUM(%)	MASS(%)	SUM(%)	MASS(%)	SUM(%)
1	0,03	0,03	74,45	74,45	0,01	0,01	9,74	9,74	0,00	0,00	10,63	10,63
2	0,01	0,03	12,46	86,91	0,00	0,01	0,00	9,74	0,00	0,00	78,30	88,93
3	0,41	0,44	7,07	93,98	0,01	0,02	26,79	36,53	0,00	0,00	2,46	91,40
4	24,24	24,68	0,03	94,01	32,69	32,71	0,00	36,54	9,56	9,56	0,00	91,40
5	67,19	91,87	0,04	94,05	7,29	40,00	0,03	36,57	3,97	13,54	0,04	91,44
6	0,06	91,93	0,72	94,77	0,00	40,00	13,69	50,26	0,01	13,54	0,01	91,45
7	0,03	91,96	0,66	95,43	0,00	40,00	0,69	50,94	0,00	13,55	3,58	95,03
8	0,01	91,98	0,00	95,43	0,00	40,00	0,00	50,94	0,07	13,62	0,01	95,03
9	0,40	92,38	0,00	95,43	6,26	46,25	0,02	50,96	2,68	16,30	0,00	95,03
10	0,01	92,39	0,36	95,79	0,07	46,33	2,34	53,30	0,06	16,36	0,34	95,38
11	0,00	92,39	0,63	96,42	0,03	46,35	0,15	53,45	0,08	16,44	0,25	95,62
12	0,41	92,80	0,01	96,43	1,53	47,89	0,01	53,47	6,38	22,82	0,00	95,62
13	0,00	92,80	0,00	96,44	0,02	47,91	0,34	53,80	0,04	22,86	0,35	95,97
14	0,02	92,82	0,77	97,21	0,00	47,91	1,06	54,87	0,00	22,86	0,00	95,97
15	0,06	92,88	0,00	97,21	2,07	49,98	0,05	54,91	2,87	25,73	0,00	95,97
16	0,07	92,95	0,12	97,33	0,03	50,01	1,07	55,98	0,22	25,95	0,13	96,10
17	0,00	92,95	0,02	97,35	22,27	72,28	0,07	56,05	21,48	47,43	0,01	96,12
18	4,72	97,68	0,09	97,44	0,12	72,40	0,57	56,62	1,81	49,24	0,00	96,12
19	0,07	97,75	2,16	99,59	0,06	72,46	18,00	74,61	0,07	49,30	0,52	96,64
20	1,84	99,59	0,00	99,60	0,12	72,58	0,01	74,63	3,29	52,60	0,00	96,64
21	0,09	99,68	0,00	99,60	17,90	90,48	0,04	74,66	1,51	54,11	0,01	96,65

Table 11-2 Eigenvalue analysis of Increasing the opening between the legs of the central columns SLS (Vibration load)

From the modal participation results:

- ✓ **Lateral (Y, red):** Mode 1, $f_Y = 2.40Hz$
- ✓ **Longitudinal (X, green):** Mode 5, $f_X = 6.52\ Hz$
- ✓ **Vertical (Z, orange):** Mode 4, $f_Z = 5.78\ Hz$

In SLS the frequencies increase slightly compared to ULS, improving separation, but $\boldsymbol{f_Y}$ **remains below 2.5 Hz**, therefore a lateral dynamic verification remains required. Vertical verification remains unnecessary because $\boldsymbol{f_Z > 5\ Hz}$.

Risk of resonance:

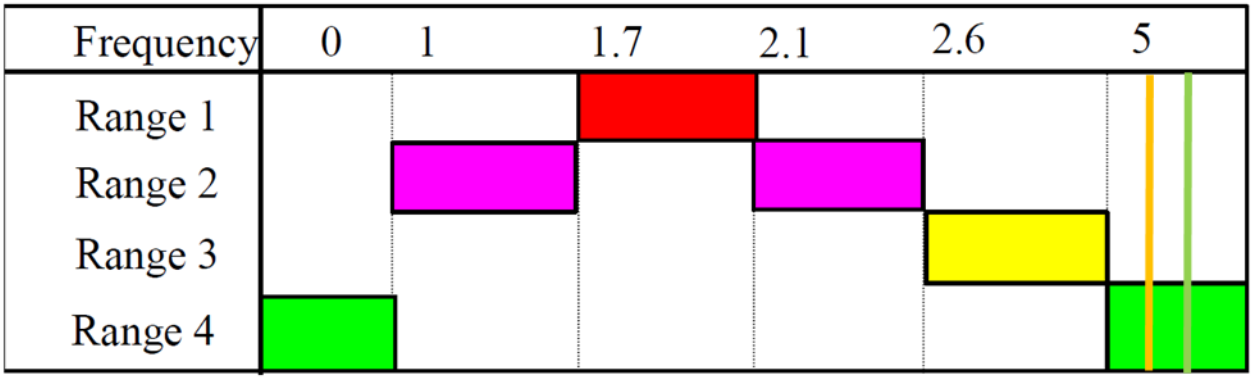

Figure 11-3 Risk of resonance- vertical and longitudinal directions - Increasing the opening between the legs of the central columns SLS (vibration load)

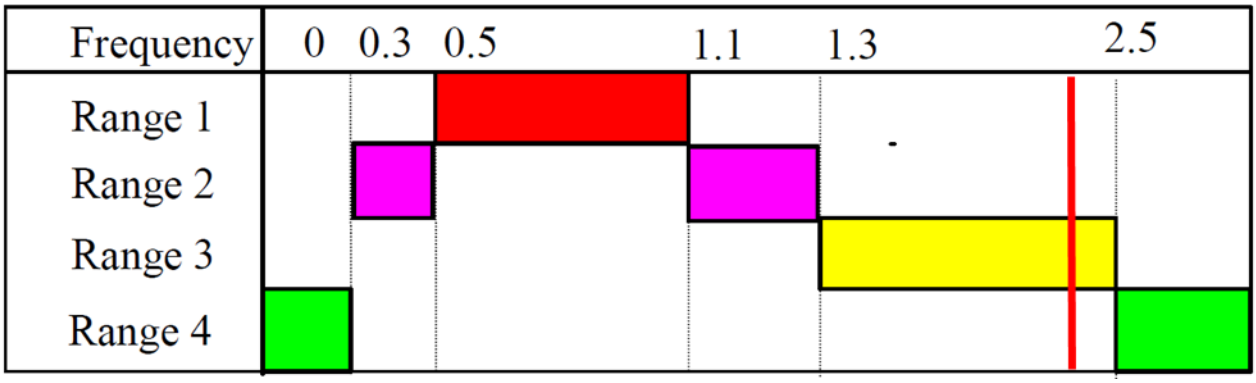

Figure 11-4 Risk of resonance- lateral direction - Increasing the opening between the legs of the central columns SLS (vibration load)

The resonance screening confirms that the lateral direction (red, Y) still governs the dynamic risk because $f_Y = 2.40Hz$ is marginally below the SÉTRA threshold. Longitudinal and vertical directions are improved and do not govern resonance risk in SLS.

11.1.2 Eigenvalue result of Increasing the cross-section of the central columns

11.1.2.1 Eigenvalue analysis SLS – Associated static pedestrian load case (crowd weight):

Mode	UX	UY	UZ	RX	RY		RZ	
EIGENVALUE ANALYSIS								
Mode No	Frequency (rad/sec)	Frequency (cycle/sec)	Period (sec)	Tolerance				
1	16,30	2,59	0,39	0,00				
2	21,61	3,44	0,29	0,00				
3	31,95	5,09	0,20	0,00				
4	35,35	5,63	0,18	0,00				
5	38,74	6,17	0,16	0,00				
6	42,66	6,79	0,15	0,00				
7	46,31	7,37	0,14	0,00				
8	57,65	9,18	0,11	0,00				
9	61,75	9,83	0,10	0,00				
10	62,21	9,90	0,10	0,00				
11	69,42	11,05	0,09	0,00				
12	77,31	12,30	0,08	0,00				
13	79,80	12,70	0,08	0,00				
14	89,98	14,32	0,07	0,00				
15	121,01	19,26	0,05	0,00				
16	130,19	20,72	0,05	0,00				
17	174,55	27,78	0,04	0,00				
18	178,99	28,49	0,04	0,00				
19	220,48	35,09	0,03	0,00				
20	270,74	43,09	0,02	0,00				
21	386,02	61,44	0,02	0,00				

MODAL PARTICIPATION MASSES PRINTOUT												
Mode No	TRAN-X		TRAN-Y		TRAN-Z		ROTN-X		ROTN-Y		ROTN-Z	
	MASS(%)	SUM(%)	MASS(%)	SUM(%)	MASS(%)	SUM(%)	MASS(%)	SUM(%)	MASS(%)	SUM(%)	MASS(%)	SUM(%)
1	0,04	0,04	81,75	81,75	0,00	0,00	10,36	10,36	0,00	0,00	2,23	2,23
2	0,01	0,05	4,82	86,57	0,00	0,00	0,49	10,85	0,00	0,00	83,03	85,27
3	0,77	0,82	6,34	92,91	0,01	0,01	23,47	34,32	0,00	0,00	6,13	91,40
4	63,90	64,71	0,09	93,01	13,57	13,59	0,07	34,39	4,32	4,32	0,06	91,45
5	27,56	92,28	0,03	93,04	23,23	36,82	0,05	34,45	8,85	13,17	0,05	91,50
6	0,00	92,28	0,67	93,71	0,00	36,82	11,58	46,03	0,00	13,17	0,02	91,52
7	0,04	92,32	0,64	94,35	0,00	36,82	0,54	46,57	0,00	13,17	4,07	95,60
8	0,01	92,32	0,00	94,35	0,00	36,82	0,03	46,60	0,07	13,24	0,01	95,61
9	0,00	92,33	0,51	94,85	0,06	36,88	0,99	47,59	0,00	13,24	0,01	95,61
10	0,20	92,53	0,01	94,86	5,78	42,66	0,02	47,60	2,78	16,02	0,00	95,62
11	0,01	92,54	0,62	95,48	0,00	42,66	0,72	48,33	0,01	16,03	0,04	95,66
12	0,00	92,54	0,89	96,37	0,03	42,70	0,56	48,89	0,28	16,30	0,16	95,81

13	0,23	92,77	0,03	96,40	1,34	44,03	0,04	48,93	5,54	21,84	0,00	95,82
14	0,01	92,78	0,19	96,58	0,00	44,03	0,53	49,46	0,00	21,84	0,46	96,28
15	0,00	92,78	0,71	97,29	0,05	44,08	0,34	49,80	0,08	21,93	0,59	96,87
16	0,03	92,81	0,06	97,35	1,69	45,77	0,00	49,80	2,53	24,46	0,04	96,91
17	1,85	94,66	0,01	97,35	9,23	55,00	0,02	49,83	4,90	29,36	0,01	96,92
18	1,24	95,90	0,01	97,37	9,72	64,72	0,17	49,99	16,33	45,69	0,04	96,96
19	0,13	96,03	2,06	99,42	0,10	64,82	23,47	73,46	0,03	45,72	0,34	97,29
20	3,26	99,29	0,03	99,46	0,21	65,03	0,56	74,02	3,69	49,41	0,00	97,29
21	0,22	99,51	0,00	99,46	20,45	85,48	0,01	74,03	1,47	50,89	0,00	97,30

Table 11-3 Eigenvalue result of Increasing the cross-section of the central columns SLS (crowd weight)

Modal identification gives:

- ✓ **Lateral (Y, red):** Mode 1, $f_Y = 2.59Hz$
- ✓ **Longitudinal (X, green):** Mode 4, $f_X = 5.63Hz$
- ✓ **Vertical (Z, orange):** Mode 5, $f_Z = 6.17\ Hz$

This intervention produces a marked stiffness increase. Both **lateral and vertical frequencies exceed the SÉTRA thresholds**, therefore lateral and vertical time-history checks can be omitted. The longitudinal mode is improved and above 5 Hz; however, because longitudinal vibration was critical for the reference model, a longitudinal acceleration verification is retained to confirm comfort compliance.

Risk of resonance:

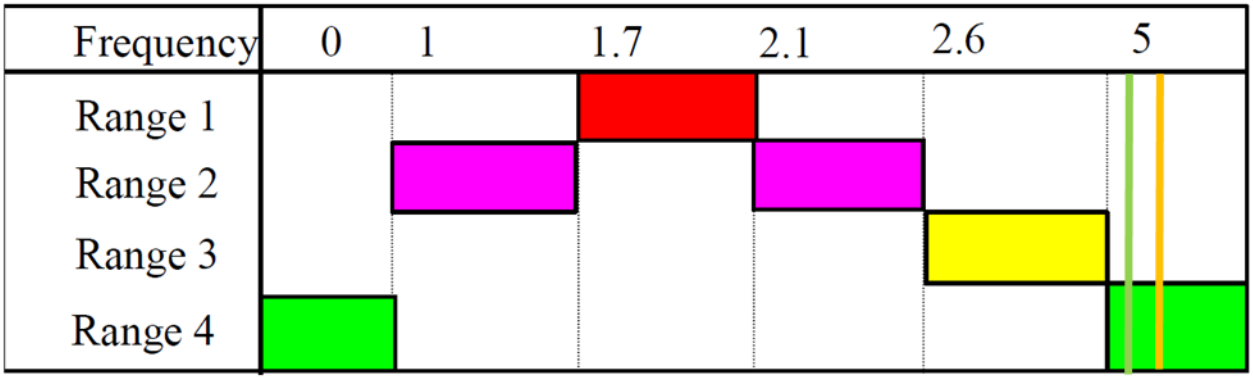

Figure 11-5 Risk of resonance- vertical and longitudinal directions - Increasing the cross-section of the central columns (crowd weight)

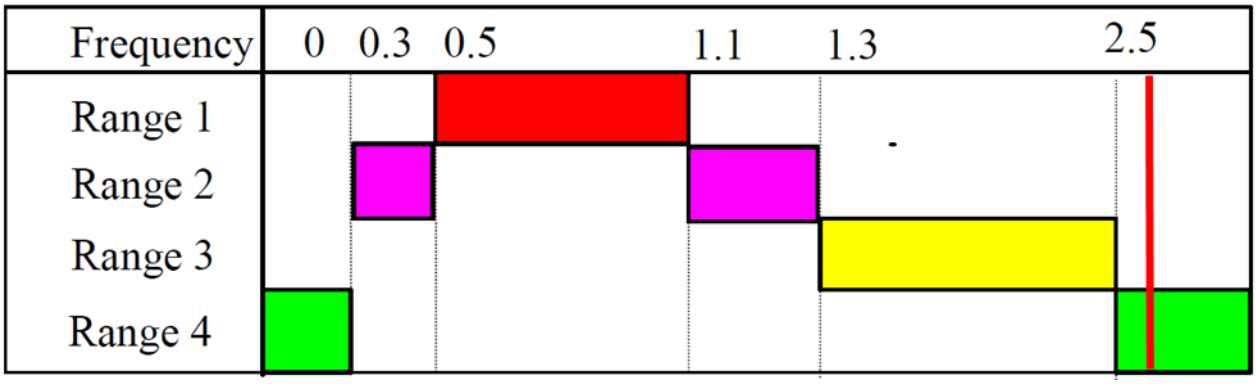

Figure 11-6 Figure 11 5 Risk of resonance- lateral direction - Increasing the cross-section of the central columns (crowd weight)

The screening chart indicates that the lateral (red) and vertical (orange) components move into the safe zone (above 2.5 Hz and 5 Hz). The longitudinal component (green) is also shifted above 5 Hz, significantly reducing resonance likelihood and motivating the expected reduction of peak accelerations.

11.1.2.2 Eigenvalue analysis SLS-dynamic pedestrian load case (vibration load)

Mode	UX	UY	UZ	RX	RY		RZ	
EIGENVALUE ANALYSIS								
Mode No	Frequency (rad/sec)	Frequency (cycle/sec)	Period (sec)	Tolerance				
1	18,40	2,93	0,34	0,00				
2	25,34	4,03	0,25	0,00				
3	35,17	5,60	0,18	0,00				
4	37,17	5,92	0,17	0,00				
5	42,76	6,80	0,15	0,00				
6	43,49	6,92	0,14	0,00				
7	54,11	8,61	0,12	0,00				
8	57,65	9,17	0,11	0,00				
9	62,25	9,91	0,10	0,00				
10	62,72	9,98	0,10	0,00				
11	71,80	11,43	0,09	0,00				
12	79,66	12,68	0,08	0,00				
13	81,27	12,93	0,08	0,00				
14	91,43	14,55	0,07	0,00				
15	114,92	18,29	0,05	0,00				
16	130,16	20,72	0,05	0,00				
17	175,84	27,99	0,04	0,00				
18	179,16	28,51	0,04	0,00				
19	230,04	36,61	0,03	0,00				

20	298,65		47,53		0,02		0,00					
21	391,73		62,35		0,02		0,00					
MODAL PARTICIPATION MASSES PRINTOUT												
Mode No	TRAN-X		TRAN-Y		TRAN-Z		ROTN-X		ROTN-Y		ROTN-Z	
	MASS(%)	SUM(%)	MASS(%)	SUM(%)	MASS(%)	SUM(%)	MASS(%)	SUM(%)	MASS(%)	SUM(%)	MASS(%)	SUM(%)
1	0,0	0,0	69,5	69,5	0,0	0,0	17,3	17,3	0,0	0,0	3,2	3,2
2	0,0	0,0	8,0	77,5	0,0	0,0	0,1	17,4	0,0	0,0	80,3	83,5
3	0,3	0,3	12,1	89,6	0,1	0,1	15,8	33,2	0,0	0,0	5,3	88,8
4	8,0	8,3	0,0	89,6	34,6	34,7	0,0	33,2	14,2	14,3	0,0	88,8
5	0,5	8,8	1,0	90,6	0,0	34,7	11,5	44,7	0,0	14,3	0,0	88,8
6	79,7	88,5	0,1	90,8	1,6	36,3	0,2	45,0	0,9	15,2	0,0	88,8
7	0,1	88,6	0,2	91,0	0,0	36,3	0,3	45,2	0,0	15,2	4,4	93,2
8	0,0	88,6	0,0	91,0	0,0	36,3	0,0	45,2	0,1	15,2	0,0	93,2
9	0,4	89,0	0,0	91,0	5,7	42,0	0,0	45,2	3,1	18,3	0,0	93,2
10	0,0	89,0	0,4	91,4	0,0	42,1	1,7	46,9	0,1	18,4	0,2	93,5
11	0,0	89,0	0,4	91,8	0,0	42,1	0,4	47,3	0,0	18,4	0,5	94,0
12	0,3	89,3	0,0	91,9	1,3	43,3	0,0	47,3	5,3	23,7	0,0	94,0
13	0,0	89,3	0,7	92,6	0,1	43,4	0,0	47,3	0,2	23,9	0,5	94,5
14	0,0	89,4	1,1	93,7	0,0	43,4	1,1	48,5	0,0	23,9	0,0	94,6
15	0,0	89,4	1,5	95,2	0,0	43,4	0,3	48,8	0,1	24,0	0,9	95,4
16	0,0	89,4	0,0	95,2	1,7	45,2	0,0	48,8	2,4	26,4	0,0	95,5
17	2,7	92,1	0,0	95,2	7,9	53,0	0,1	48,9	3,3	29,7	0,0	95,5
18	1,5	93,6	0,0	95,2	11,1	64,1	0,0	48,9	16,1	45,8	0,0	95,5
19	0,0	93,6	3,9	99,2	0,0	64,2	23,1	72,0	0,0	45,8	1,0	96,5
20	5,3	98,9	0,0	99,2	0,2	64,3	0,0	72,0	3,9	49,7	0,0	96,5
21	0,3	99,2	0,0	99,2	20,4	84,8	0,1	72,0	1,0	50,8	0,0	96,5

Table 11-4 Eigenvalue result of Increasing the cross-section of the central columns SLS (vibration load)

Modal identification gives:

- ✓ **Lateral (Y, red):** Mode 1, $f_Y = 2.93Hz$
- ✓ **Longitudinal (X, green):** Mode 6, $f_X = 6.92Hz$
- ✓ **Vertical (Z, orange):** Mode 4, $f_Z = 5.92\ Hz$

In SLS-dynamic pedestrian load case (vibration load) all governing frequencies are comfortably above screening thresholds; therefore, resonance risk is low in all directions.

Risk of resonance:

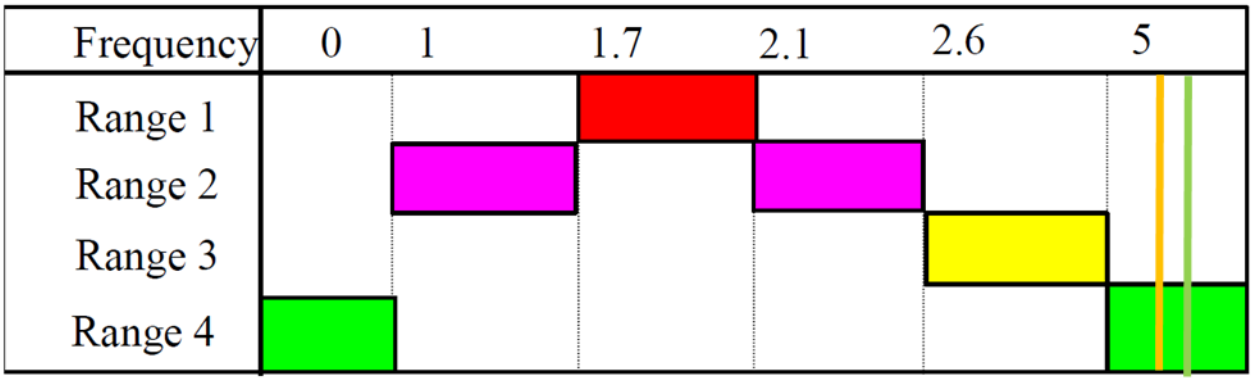

Figure 11-7 Risk of resonance- vertical and longitudinal directions - Increasing the cross-section of the central columns SLS (vibration load)

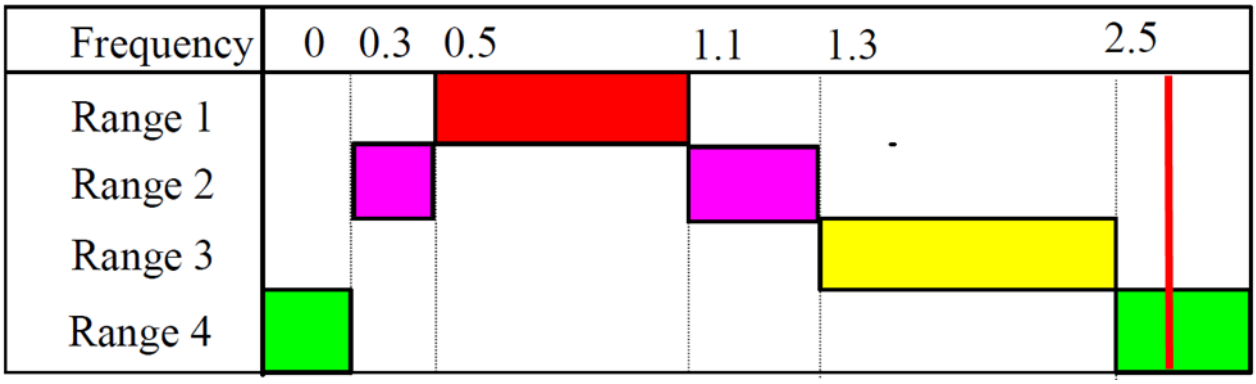

Figure 11-8 Figure 11 7 Risk of resonance- lateral direction - Increasing the cross-section of the central columns SLS (vibration load)

The dynamic pedestrian load case (vibration load) resonance plot s showed all three frequencies are in the safe zone: **green (X)** $f_X > 5$ **Hz, red (Y)** $f_Y > 2.5\ Hz$, **orange (Z)** $f_Z > 5\ Hz$ This confirms that the cross-section enlargement is effective as a stand-alone mitigation measure.

11.1.3 Eigenvalue analysis of Adding bracing to the final portion currently without bracing

11.1.3.1 Eigenvalue analysis SLS – Associated static pedestrian load case (crowd weight):

Mode	UX	UY	UZ	RX	RY		RZ	
EIGENVALUE ANALYSIS								
Mode No	Frequency (rad/sec)	Frequency (cycle/sec)	Period (sec)	Tolerance				
1	17,02	2,71	0,37	0,00				
2	25,57	4,07	0,25	0,00				
3	29,37	4,67	0,21	0,00				

4	35,40	5,63	0,18	0,00				
5	37,87	6,03	0,17	0,00				
6	42,60	6,78	0,15	0,00				
7	50,13	7,98	0,13	0,00				
8	58,49	9,31	0,11	0,00				
9	62,07	9,88	0,10	0,00				
10	62,22	9,90	0,10	0,00				
11	69,76	11,10	0,09	0,00				
12	77,49	12,33	0,08	0,00				
13	79,42	12,64	0,08	0,00				
14	88,09	14,02	0,07	0,00				
15	126,06	20,06	0,05	0,00				
16	149,27	23,76	0,04	0,00				
17	171,39	27,28	0,04	0,00				
18	176,44	28,08	0,04	0,00				
19	235,48	37,48	0,03	0,00				
20	284,66	45,31	0,02	0,00				
21	350,88	55,84	0,02	0,00				

MODAL PARTICIPATION MASSES PRINTOUT

Mode No	TRAN-X		TRAN-Y		TRAN-Z		ROTN-X		ROTN-Y		ROTN-Z	
	MASS(%)	SUM(%)	MASS(%)	SUM(%)	MASS(%)	SUM(%)	MASS(%)	SUM(%)	MASS(%)	SUM(%)	MASS(%)	SUM(%)
1	0,28	0,28	81,34	81,34	0,01	0,01	9,87	9,87	0,00	0,00	4,68	4,68
2	6,33	6,61	0,00	81,35	0,09	0,10	10,63	20,50	0,02	0,02	53,94	58,63
3	77,16	83,76	0,21	81,56	1,35	1,45	4,14	24,65	0,41	0,43	0,07	58,70
4	4,76	88,52	7,00	88,55	2,51	3,96	7,07	31,72	0,76	1,19	31,69	90,39
5	3,52	92,04	0,22	88,77	34,41	38,37	0,18	31,90	11,32	12,51	1,43	91,81
6	0,02	92,07	0,71	89,48	0,00	38,37	10,61	42,50	0,00	12,51	0,08	91,89
7	0,43	92,49	5,61	95,09	0,00	38,38	2,54	45,04	0,01	12,52	0,40	92,29
8	0,00	92,49	0,01	95,10	0,00	38,38	0,37	45,41	0,07	12,58	0,03	92,32
9	0,10	92,60	0,10	95,21	5,70	44,08	0,06	45,47	2,17	14,75	0,02	92,33
10	0,01	92,61	1,22	96,42	0,41	44,48	0,85	46,32	0,25	15,00	0,12	92,46
11	0,00	92,61	0,15	96,57	0,00	44,48	0,69	47,01	0,02	15,03	0,37	92,82
12	0,04	92,64	0,00	96,58	0,07	44,56	0,08	47,10	0,36	15,39	1,10	93,93
13	0,10	92,74	0,00	96,58	1,41	45,96	0,01	47,11	5,69	21,08	0,05	93,98
14	0,01	92,74	0,04	96,61	0,00	45,96	0,08	47,19	0,09	21,17	0,15	94,12
15	0,03	92,77	0,00	96,61	1,64	47,60	0,00	47,19	2,18	23,34	0,00	94,12
16	0,03	92,80	0,95	97,57	0,02	47,63	4,83	52,02	0,07	23,41	0,83	94,95
17	0,24	93,04	0,00	97,57	19,68	67,31	0,00	52,02	16,16	39,57	0,02	94,97
18	2,61	95,65	0,06	97,63	1,57	68,88	0,26	52,28	5,56	45,13	0,23	95,20
19	0,94	96,59	1,67	99,29	0,00	68,88	17,46	69,74	0,44	45,57	1,16	96,36
20	2,86	99,44	0,30	99,60	0,05	68,93	6,18	75,91	3,15	48,71	0,07	96,43
21	0,16	99,61	0,00	99,60	18,80	87,73	0,14	76,05	1,51	50,22	0,00	96,43

Table 11-5 Eigenvalue analysis of Adding bracing to the final portion currently without bracing SLS (crowd weight)

Modal identification gives:

- ✓ **Lateral (Y, red):** Mode 1, $f_Y = 2.71Hz$
- ✓ **Longitudinal (X, green):** Mode 3, $f_X = 4.67\ Hz$
- ✓ **Vertical (Z, orange):** Mode 5, $f_Z = 6.03\ Hz$

The added bracing increases the stiffness of the previously flexible end segment and shifts the **lateral mode above 2.5 Hz**, reducing lateral resonance risk. The **longitudinal mode remains below 5 Hz**, therefore longitudinal dynamic acceleration verification remains necessary. Vertical verification is not required because $\boldsymbol{f_Z > 5\ Hz}$.

Risk of resonance:

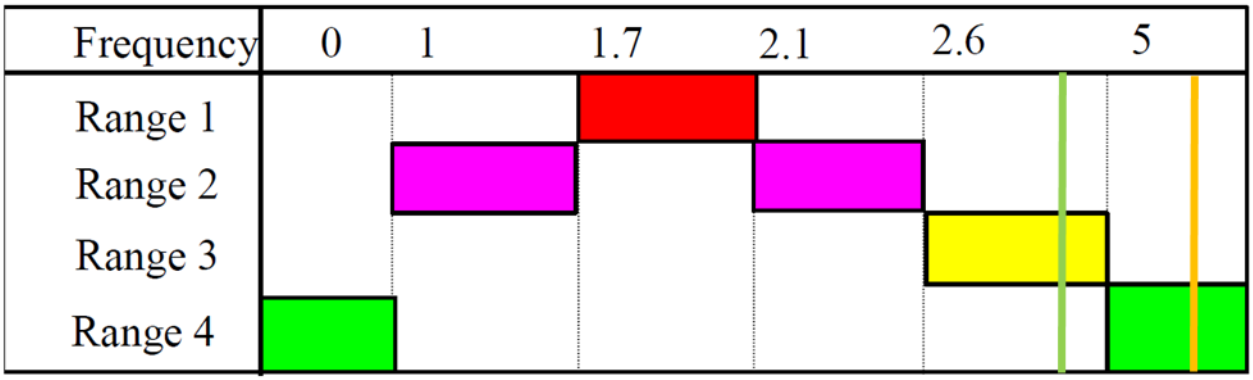

Figure 11-9 Risk of resonance- vertical and longitudinal directions - Adding bracing to the final portion currently without bracing SLS (crowd weight)

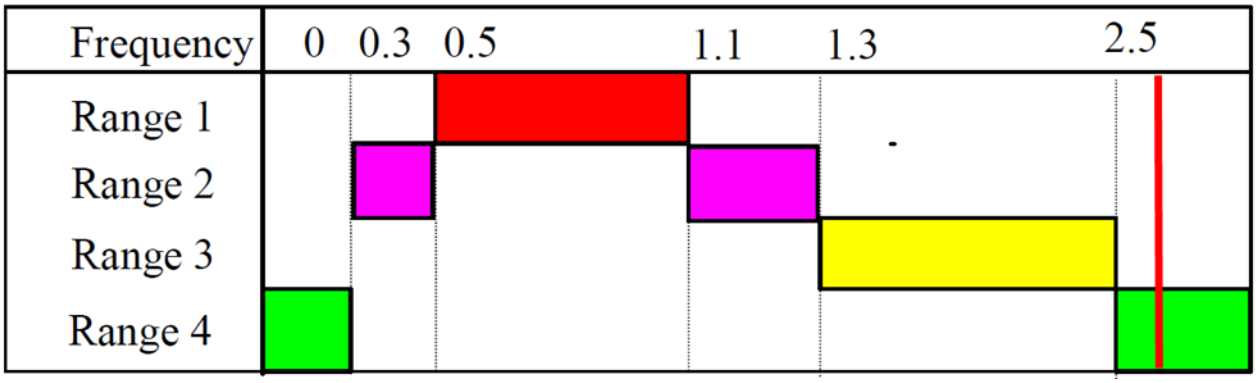

Figure 11-10 Risk of resonance- lateral direction - Adding bracing to the final portion currently without bracing SLS (crowd weight)

The resonance screening confirms that the dominant risk remains in the **longitudinal direction (green)** because $f_X = 4.67\ Hz$ remains close to the excitation content. The **lateral direction (red)** improves and exceeds 2.5 Hz; therefore it is expected to govern comfort.

11.1.3.2 Eigenvalue analysis dynamic SLS-dynamic pedestrian load case (vibration load)

Mode	UX	UY	UZ	RX	RY		RZ	
EIGENVALUE ANALYSIS								
Mode No	Frequency (rad/sec)	Frequency (cycle/sec)	Period (sec)	Tolerance				
1	19,17	3,05	0,33	0,00				
2	28,52	4,54	0,22	0,00				
3	33,93	5,40	0,19	0,00				
4	37,84	6,02	0,17	0,00				
5	40,70	6,48	0,15	0,00				
6	42,95	6,84	0,15	0,00				
7	56,44	8,98	0,11	0,00				
8	58,48	9,31	0,11	0,00				
9	62,10	9,88	0,10	0,00				
10	64,82	10,32	0,10	0,00				
11	66,48	10,58	0,09	0,00				
12	73,18	11,65	0,09	0,00				
13	79,33	12,63	0,08	0,00				
14	96,46	15,35	0,07	0,00				
15	126,73	20,17	0,05	0,00				
16	158,39	25,21	0,04	0,00				
17	172,21	27,41	0,04	0,00				
18	177,58	28,26	0,04	0,00				
19	243,97	38,83	0,03	0,00				
20	287,31	45,73	0,02	0,00				
21	355,93	56,65	0,02	0,00				

MODAL PARTICIPATION MASSES PRINTOUT												
Mode No	TRAN-X		TRAN-Y		TRAN-Z		ROTN-X		ROTN-Y		ROTN-Z	
	MASS(%)	SUM(%)	MASS(%)	SUM(%)	MASS(%)	SUM(%)	MASS(%)	SUM(%)	MASS(%)	SUM(%)	MASS(%)	SUM(%)
1	0,25	0,25	74,28	74,28	0,01	0,01	16,00	16,00	0,00	0,00	1,96	1,96
2	1,67	1,93	2,65	76,93	0,06	0,07	9,58	25,58	0,01	0,01	53,29	55,26
3	68,49	70,42	0,90	77,83	6,22	6,29	2,21	27,78	2,15	2,16	0,91	56,17
4	4,40	74,82	1,54	79,37	30,16	36,44	0,87	28,65	11,36	13,52	4,37	60,54
5	13,43	88,24	5,97	85,35	1,89	38,34	0,79	29,44	0,78	14,30	25,35	85,89
6	1,30	89,55	3,39	88,73	0,05	38,39	13,88	43,32	0,04	14,34	3,91	89,80
7	0,22	89,77	2,84	91,57	0,00	38,39	1,11	44,43	0,00	14,34	0,00	89,80
8	0,00	89,77	0,14	91,72	0,00	38,39	0,59	45,02	0,09	14,43	0,00	89,81
9	0,15	89,91	0,00	91,72	6,11	44,50	0,00	45,02	2,75	17,18	0,00	89,81
10	0,03	89,94	1,22	92,94	0,00	44,50	2,14	47,16	0,01	17,19	0,14	89,95
11	0,10	90,04	1,29	94,23	0,00	44,50	0,63	47,80	0,00	17,19	1,95	91,89
12	0,03	90,08	1,35	95,58	0,00	44,50	0,07	47,86	0,02	17,21	0,04	91,93
13	0,17	90,25	0,00	95,58	1,48	45,98	0,00	47,87	5,86	23,07	0,00	91,93
14	0,01	90,26	0,06	95,64	0,00	45,98	0,08	47,94	0,04	23,12	0,88	92,81

15	0,04	90,29	0,00	95,64	1,73	47,71	0,01	47,95	2,11	25,23	0,00	92,82
16	0,11	90,40	1,28	96,92	0,03	47,74	6,01	53,96	0,50	25,73	1,40	94,21
17	0,36	90,77	0,00	96,92	19,64	67,38	0,02	53,98	14,52	40,26	0,00	94,21
18	3,47	94,24	0,12	97,05	1,77	69,16	0,50	54,48	5,33	45,59	0,42	94,63
19	1,46	95,70	1,97	99,02	0,01	69,17	15,90	70,38	0,57	46,16	0,88	95,51
20	3,52	99,22	0,47	99,49	0,20	69,37	6,65	77,03	3,18	49,33	0,06	95,57
21	0,28	99,49	0,00	99,49	18,51	87,88	0,02	77,05	0,87	50,20	0,01	95,58

Table 11-6 Eigenvalue analysis of Adding bracing to the final portion currently without bracing SLS (vibration load)

Modal identification gives:

- ✓ **Lateral (Y, red):** Mode 1, $f_Y = 3.05\ Hz$
- ✓ **Longitudinal (X, green):** Mode 3, $f_X = 5.40\ Hz$
- ✓ **Vertical (Z, orange):** Mode 4, $f_Z = 6.02\ Hz$

In associated static pedestrian load case (crowd weight), bracing increases frequencies further and the lateral mode is clearly above threshold. Longitudinal behavior improves.

Risk of resonance:

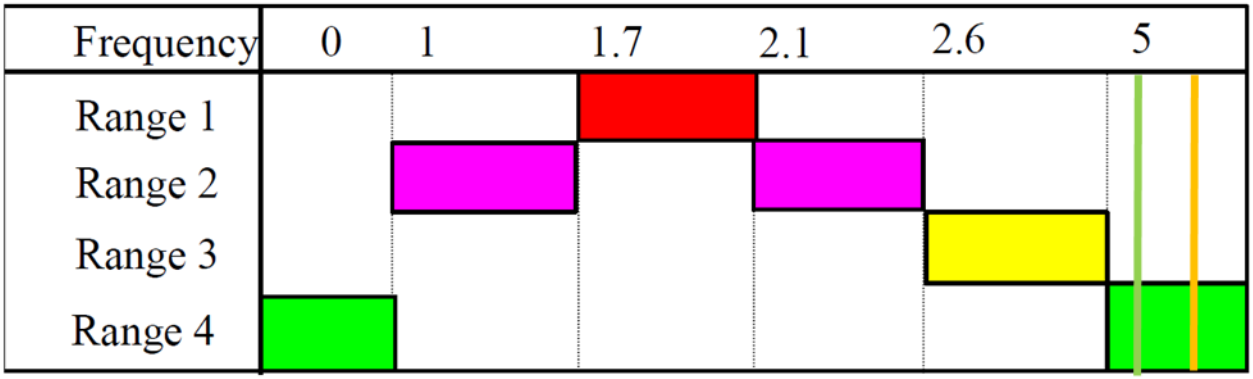

Figure 11-11 Risk of resonance- vertical and longitudinal directions - Adding bracing to the final portion currently without bracing SLS(vibration load)

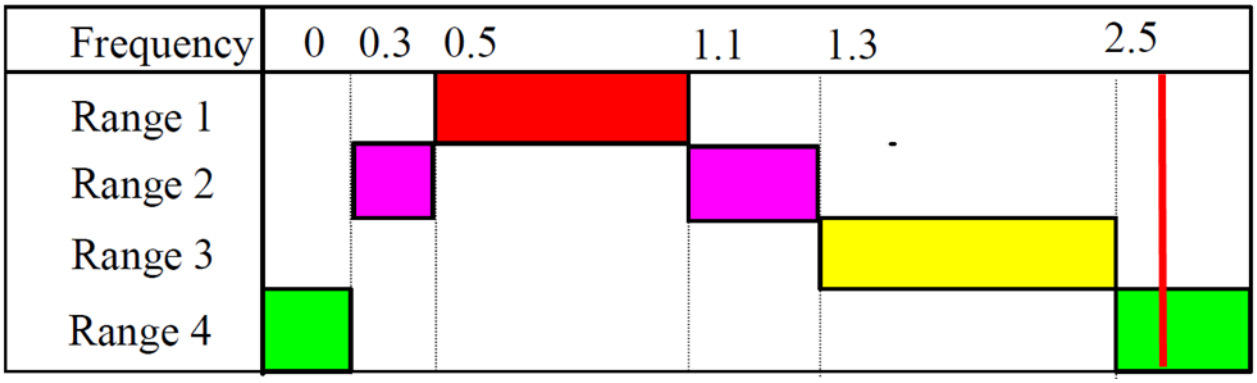

Figure 11-12 Risk of resonance- lateral direction - Adding bracing to the final portion currently without bracing SLS (vibration load)

In SLS the resonance plot shows improved separation in all directions, with the remaining sensitivity associated mainly with the longitudinal direction if excitation content overlaps but it goes over 5Hz and check is not required.

11.1.4 Eigenvalue analysis of Replacing Teflon bearings with rubber bearings

11.1.4.1 Eigenvalue analysis SLS – Associated static pedestrian load case (crowd weight)

Mode	UX	UY	UZ	RX	RY		RZ	
EIGENVALUE ANALYSIS								
Mode No	Frequency (rad/sec)	Frequency (cycle/sec)	Period (sec)	Tolerance				
1	14,27	2,27	0,44	0,00				
2	21,54	3,43	0,29	0,00				
3	31,13	4,95	0,20	0,00				
4	33,49	5,33	0,19	0,00				
5	37,85	6,02	0,17	0,00				
6	42,53	6,77	0,15	0,00				
7	46,46	7,39	0,14	0,00				
8	58,80	9,36	0,11	0,00				
9	61,42	9,78	0,10	0,00				
10	62,07	9,88	0,10	0,00				
11	66,30	10,55	0,09	0,00				
12	75,15	11,96	0,08	0,00				
13	79,34	12,63	0,08	0,00				
14	99,36	15,81	0,06	0,00				
15	112,46	17,90	0,06	0,00				
16	126,65	20,16	0,05	0,00				
17	169,75	27,02	0,04	0,00				
18	197,71	31,47	0,03	0,00				
19	212,67	33,85	0,03	0,00				

20	312,75		49,78		0,02		0,00					
21	338,12		53,81		0,02		0,00					
MODAL PARTICIPATION MASSES PRINTOUT												
Mode No	TRAN-X		TRAN-Y		TRAN-Z		ROTN-X		ROTN-Y		ROTN-Z	
	MASS(%)	SUM(%)	MASS(%)	SUM(%)	MASS(%)	SUM(%)	MASS(%)	SUM(%)	MASS(%)	SUM(%)	MASS(%)	SUM(%)
1	0,04	0,04	77,29	77,29	0,00	0,00	5,68	5,68	0,00	0,00	11,96	11,96
2	0,04	0,08	13,21	90,50	0,00	0,01	0,02	5,70	0,00	0,00	77,14	89,11
3	0,61	0,69	4,17	94,67	0,02	0,02	31,33	37,03	0,00	0,00	3,13	92,24
4	88,19	88,87	0,14	94,81	4,36	4,39	0,11	37,14	0,80	0,80	0,00	92,24
5	6,62	95,49	0,01	94,82	35,71	40,10	0,03	37,17	11,41	12,21	0,01	92,25
6	0,01	95,49	0,60	95,42	0,00	40,10	13,39	50,56	0,00	12,21	0,06	92,31
7	0,00	95,49	1,19	96,61	0,00	40,10	0,92	51,49	0,00	12,21	4,24	96,55
8	0,00	95,49	0,00	96,61	0,00	40,10	0,26	51,75	0,02	12,24	0,01	96,56
9	0,00	95,50	0,34	96,95	0,01	40,12	1,72	53,46	0,00	12,24	0,09	96,65
10	0,13	95,63	0,00	96,95	6,28	46,39	0,02	53,48	2,37	14,60	0,00	96,65
11	0,00	95,63	0,21	97,16	0,01	46,41	1,10	54,58	0,04	14,64	0,02	96,68
12	0,01	95,64	0,73	97,89	0,00	46,41	0,21	54,79	0,02	14,65	0,40	97,08
13	0,09	95,73	0,00	97,89	1,55	47,96	0,00	54,79	6,79	21,45	0,00	97,08
14	0,00	95,73	0,05	97,94	0,00	47,96	0,13	54,92	0,07	21,51	0,48	97,55
15	0,00	95,74	0,18	98,12	0,11	48,07	0,49	55,41	0,29	21,80	0,02	97,58
16	0,02	95,75	0,04	98,16	1,51	49,58	0,32	55,73	2,08	23,88	0,03	97,60
17	0,01	95,77	0,00	98,16	21,58	71,16	0,01	55,74	24,79	48,67	0,00	97,61
18	2,29	98,06	0,00	98,16	0,01	71,16	0,01	55,75	0,18	48,85	0,01	97,61
19	0,01	98,07	1,51	99,67	0,06	71,22	20,32	76,07	0,07	48,92	0,32	97,93
20	1,34	99,40	0,01	99,68	1,01	72,23	0,32	76,39	3,22	52,14	0,01	97,94
21	0,37	99,78	0,00	99,69	17,93	90,16	0,14	76,53	0,65	52,79	0,00	97,94

Table 11-7 Eigenvalue analysis of Replacing Teflon bearings with rubber bearings SLS (crowd weight)

Modal identification gives:

- ✓ **Lateral (Y, red):** Mode 1, $f_Y = 2.27Hz$
- ✓ **Longitudinal (X, green):** Mode 4, $f_X = 5.33Hz$
- ✓ **Vertical (Z, orange):** Mode 5, $f_Z = 6.02Hz$

The bearing replacement primarily increases damping and modifies boundary conditions, while global stiffness changes are limited. The lateral frequency remains **below 2.5 Hz**; therefore, a lateral dynamic verification remains required. Vertical verification remains unnecessary because $\boldsymbol{f_Z > 5\ Hz}$**.**

Risk of resonance:

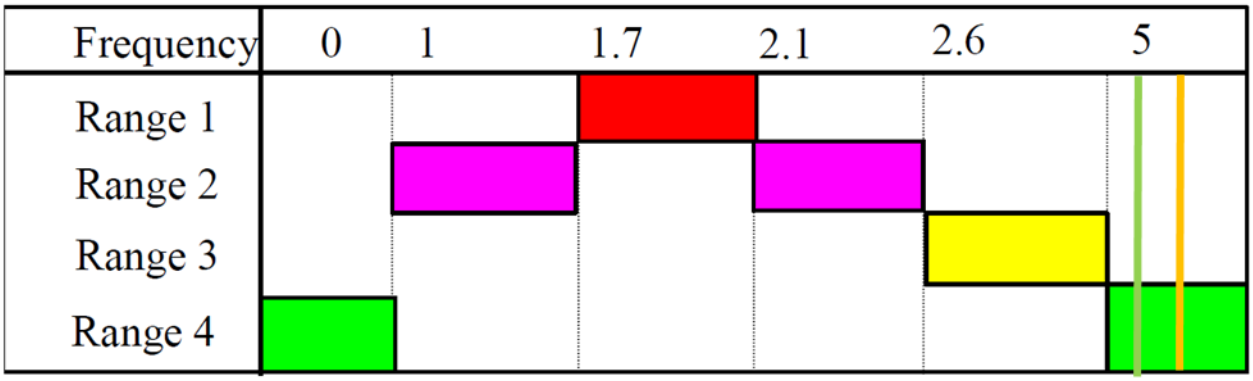

Figure 11-13 Risk of resonance- vertical and longitudinal directions - Replacing Teflon bearings with rubber bearings SLS (crowd weight)

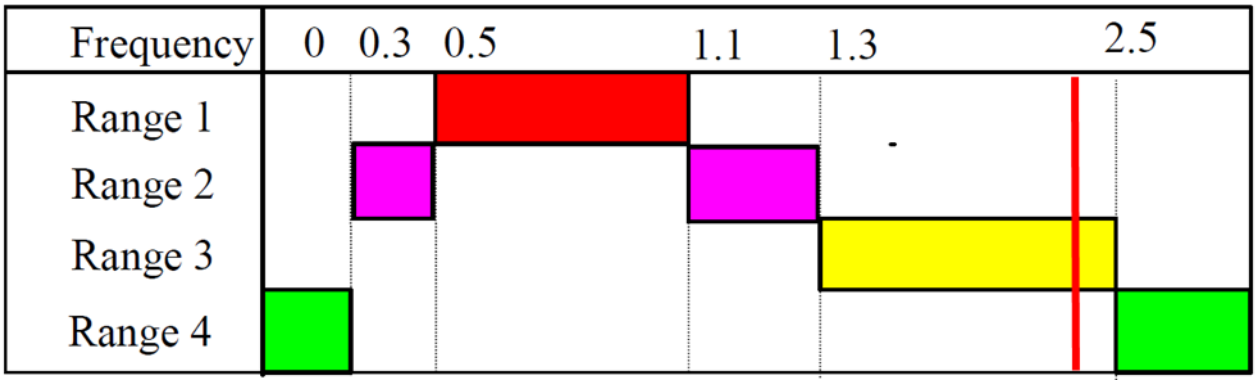

Figure 11-14 Risk of resonance- lateral direction - Replacing Teflon bearings with rubber bearings SLS (crowd weight)

Still verification of acceleration needs to be performed in lateral based on result of resonance and eigenvalue analysis.

11.1.4.2 Eigenvalue analysis dynamic SLS-dynamic pedestrian load case (vibration load)

Mode	UX	UY	UZ	RX	RY		RZ	
EIGENVALUE ANALYSIS								
Mode No	Frequency		Period	Tolerance				
	(rad/sec)	(cycle/sec)	(sec)					
1	15,76	2,51	0,40	0,00				
2	25,33	4,03	0,25	0,00				
3	32,63	5,19	0,19	0,00				
4	33,89	5,39	0,19	0,00				
5	37,98	6,05	0,17	0,00				
6	42,60	6,78	0,15	0,00				
7	53,99	8,59	0,12	0,00				

8	57,78	9,20	0,11	0,00				
9	62,09	9,88	0,10	0,00				
10	62,33	9,92	0,10	0,00				
11	72,60	11,55	0,09	0,00				
12	79,34	12,63	0,08	0,00				
13	87,32	13,90	0,07	0,00				
14	101,11	16,09	0,06	0,00				
15	129,31	20,58	0,05	0,00				
16	162,87	25,92	0,04	0,00				
17	172,22	27,41	0,04	0,00				
18	184,67	29,39	0,03	0,00				
19	244,67	38,94	0,03	0,00				
20	269,21	42,85	0,02	0,00				
21	353,52	56,26	0,02	0,00				

MODAL PARTICIPATION MASSES PRINTOUT

Mode No	TRAN-X		TRAN-Y		TRAN-Z		ROTN-X		ROTN-Y		ROTN-Z	
	MASS(%)	SUM(%)	MASS(%)	SUM(%)	MASS(%)	SUM(%)	MASS(%)	SUM(%)	MASS(%)	SUM(%)	MASS(%)	SUM(%)
1	0,02	0,02	71,52	71,52	0,00	0,00	10,01	10,01	0,00	0,00	12,80	12,80
2	0,07	0,09	13,50	85,02	0,00	0,00	0,14	10,15	0,00	0,00	76,41	89,21
3	64,23	64,32	2,36	87,37	2,63	2,63	7,74	17,89	0,82	0,82	0,12	89,33
4	20,65	84,97	6,52	93,89	2,73	5,36	18,91	36,81	0,76	1,58	1,43	90,75
5	7,81	92,78	0,04	93,93	34,71	40,07	0,15	36,96	11,96	13,54	0,07	90,82
6	0,01	92,79	0,75	94,69	0,00	40,07	13,79	50,75	0,00	13,54	0,02	90,84
7	0,07	92,86	0,81	95,50	0,00	40,07	0,66	51,41	0,00	13,55	4,28	95,12
8	0,00	92,87	0,00	95,50	0,00	40,07	0,00	51,41	0,06	13,60	0,00	95,12
9	0,17	93,04	0,00	95,50	6,31	46,37	0,00	51,42	2,59	16,19	0,00	95,12
10	0,00	93,04	0,39	95,88	0,01	46,39	3,01	54,43	0,01	16,20	0,37	95,49
11	0,00	93,04	0,47	96,35	0,00	46,39	0,71	55,13	0,03	16,23	0,19	95,69
12	0,10	93,14	0,00	96,35	1,57	47,96	0,00	55,14	6,69	22,92	0,00	95,69
13	0,00	93,14	0,72	97,07	0,00	47,96	1,25	56,38	0,01	22,93	0,11	95,79
14	0,04	93,18	0,36	97,43	0,00	47,96	0,00	56,39	0,01	22,94	0,04	95,84
15	0,00	93,18	0,00	97,43	2,45	50,41	0,07	56,46	3,61	26,55	0,00	95,84
16	0,03	93,21	0,68	98,11	0,28	50,69	3,65	60,10	0,23	26,78	0,22	96,06
17	0,02	93,23	0,00	98,11	21,48	72,17	0,01	60,11	22,73	49,51	0,00	96,06
18	2,71	95,94	0,00	98,11	0,07	72,24	0,01	60,13	0,37	49,89	0,04	96,10
19	0,40	96,34	1,44	99,55	0,08	72,32	19,39	79,52	0,01	49,90	0,36	96,46
20	3,04	99,38	0,14	99,68	0,01	72,33	2,57	82,09	0,78	50,69	0,00	96,46
21	0,18	99,56	0,00	99,68	18,43	90,76	0,00	82,09	0,64	51,33	0,00	96,47

Table 11-8 Eigenvalue analysis of Replacing Teflon bearings with rubber bearings SLS (vibration load)

Modal identification gives:

- ✓ **Lateral (Y, red):** Mode 1, $f_Y = 2.51Hz$
- ✓ **Longitudinal (X, green):** Mode 3, $f_X = 5.19Hz$
- ✓ **Vertical (Z, orange):** Mode 5, $f_Z = 6.05Hz$

In SLS the lateral frequency is only **marginally above 2.5 Hz**, so this configuration remains sensitive and but still passes the limit.

Risk of resonance:

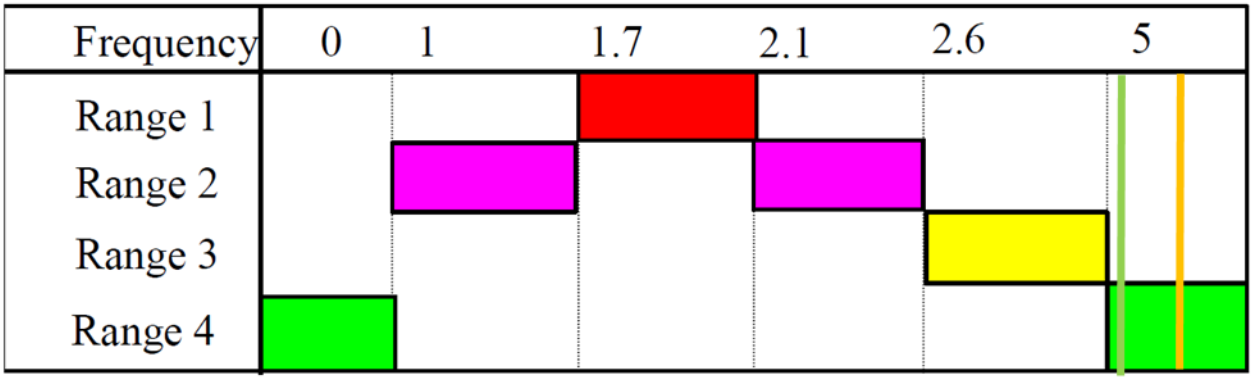

Figure 11-15 Risk of resonance - vertical and longitudinal directions - Replacing Teflon bearings with rubber bearings SLS (vibration load)

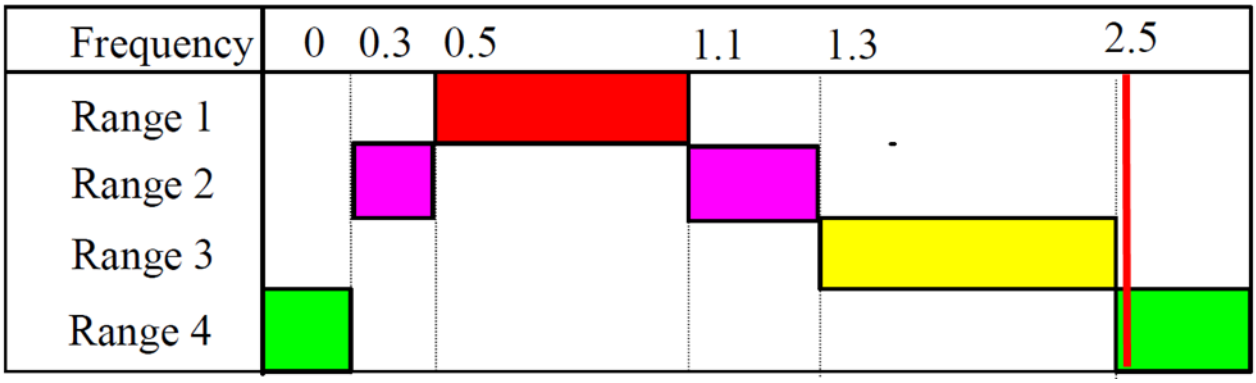

Figure 11-16 Risk of resonance - lateral direction - Replacing Teflon bearings with rubber bearings SLS (vibration load)

Result shows that longitudinal and lateral are barely passing the limit and verification of acceleration is not required.

11.1.5 Eigenvalue analysis of Combination of adding bracing to the final portion currently without bracing, change Teflon to Rubber bearing and change the cross section

11.1.5.1 Eigenvalue analysis SLS – Associated static pedestrian load case (crowd weight)

Mode	UX	UY	UZ	RX	RY	RZ
EIGENVALUE ANALYSIS						
Mode No	Frequency (rad/sec)	Frequency (cycle/sec)	Period (sec)	Tolerance		

1	18,32	2,92	0,34	0,00				
2	26,27	4,18	0,24	0,00				
3	36,30	5,78	0,17	0,00				
4	37,25	5,93	0,17	0,00				
5	41,52	6,61	0,15	0,00				
6	42,74	6,80	0,15	0,00				
7	50,62	8,06	0,12	0,00				
8	58,08	9,24	0,11	0,00				
9	61,59	9,80	0,10	0,00				
10	62,22	9,90	0,10	0,00				
11	63,80	10,15	0,10	0,00				
12	69,99	11,14	0,09	0,00				
13	79,69	12,68	0,08	0,00				
14	81,73	13,01	0,08	0,00				
15	129,71	20,64	0,05	0,00				
16	147,76	23,52	0,04	0,00				
17	176,45	28,08	0,04	0,00				
18	204,09	32,48	0,03	0,00				
19	242,48	38,59	0,03	0,00				
20	285,60	45,45	0,02	0,00				
21	390,75	62,19	0,02	0,00				

MODAL PARTICIPATION MASSES PRINTOUT

Mode No	TRAN-X		TRAN-Y		TRAN-Z		ROTN-X		ROTN-Y		ROTN-Z	
	MASS(%)	SUM(%)	MASS(%)	SUM(%)	MASS(%)	SUM(%)	MASS(%)	SUM(%)	MASS(%)	SUM(%)	MASS(%)	SUM(%)
1	0,09	0,09	77,69	77,69	0,01	0,01	14,19	14,19	0,00	0,00	5,25	5,25
2	0,10	0,19	0,21	77,90	0,01	0,01	11,19	25,38	0,00	0,00	49,76	55,01
3	7,53	7,73	8,16	86,06	0,58	0,60	5,88	31,27	0,26	0,26	33,35	88,35
4	7,33	15,05	0,44	86,50	32,81	33,40	0,12	31,38	12,66	12,93	1,56	89,91
5	73,48	88,54	0,23	86,72	2,12	35,52	0,06	31,44	0,71	13,64	2,04	91,95
6	1,93	90,47	1,02	87,74	0,02	35,54	9,52	40,96	0,02	13,66	0,38	92,33
7	1,16	91,62	5,88	93,63	0,00	35,54	2,06	43,02	0,00	13,66	0,40	92,74
8	0,00	91,62	0,00	93,63	0,00	35,54	0,00	43,02	0,04	13,70	0,00	92,74
9	0,02	91,65	0,81	94,43	0,00	35,55	2,41	45,43	0,00	13,70	0,00	92,74
10	0,36	92,01	0,00	94,44	5,55	41,09	0,00	45,43	2,75	16,45	0,00	92,74
11	0,04	92,05	0,83	95,27	0,00	41,09	0,12	45,55	0,03	16,48	0,50	93,24
12	0,00	92,05	0,34	95,61	0,00	41,09	0,41	45,97	0,00	16,48	0,34	93,58
13	0,20	92,25	0,00	95,61	1,29	42,38	0,00	45,97	5,10	21,58	0,02	93,60
14	0,00	92,25	0,15	95,76	0,03	42,41	0,06	46,03	0,07	21,65	0,71	94,31
15	0,03	92,28	0,01	95,77	1,67	44,08	0,04	46,07	2,40	24,05	0,01	94,33
16	0,00	92,28	1,36	97,12	0,10	44,18	3,54	49,61	0,16	24,22	0,97	95,29
17	0,01	92,29	0,03	97,15	18,09	62,26	0,18	49,79	17,31	41,52	0,01	95,31
18	3,68	95,97	0,01	97,16	0,19	62,46	0,13	49,92	0,23	41,75	0,03	95,34
19	0,57	96,54	2,06	99,22	0,02	62,48	25,49	75,41	0,18	41,93	1,35	96,69
20	2,60	99,14	0,23	99,45	1,10	63,58	4,53	79,94	4,38	46,31	0,09	96,78
21	0,35	99,49	0,01	99,45	19,95	83,53	0,06	79,99	0,65	46,97	0,00	96,78

Table 11-9 Eigenvalue analysis of Combination of adding bracing to the final portion currently without bracing, change Teflon to Rubber bearing and change the cross section SLS (crowd weight)

Modal identification gives:

- ✓ **Lateral (Y, red):** Mode 1, $f_Y = 2.92Hz$ (TRAN-Y ≈ 78%)
- ✓ **Longitudinal (X, green):** Mode 5, $f_X = 6.61Hz$ (TRAN-X =73%)
- ✓ **Vertical (Z, orange):** Mode 4, $f_Z = 5.93Hz$ (TRAN-Z = 33%)

All three governing frequencies exceed the adopted screening thresholds. Therefore, resonance likelihood under standard pedestrian excitation is low, and time-history comfort checks can be omitted in SLS – Associated static pedestrian load case (crowd weight) under the adopted SÉTRA-based rule.

Risk of resonance:

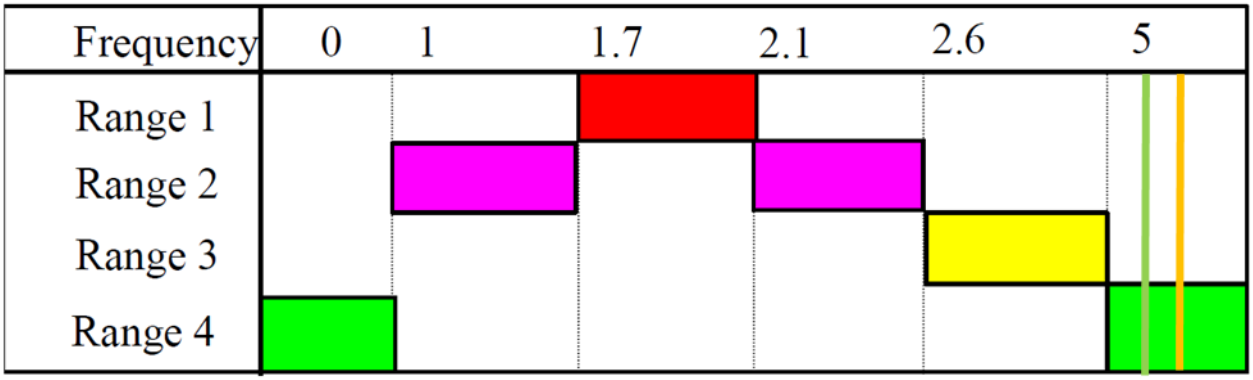

Figure 11-17 Risk of resonance – vertical and longitudinal directions - Combination of adding bracing to the final portion currently without bracing, change Teflon to Rubber bearing and change the cross section SLS (crowd weight)

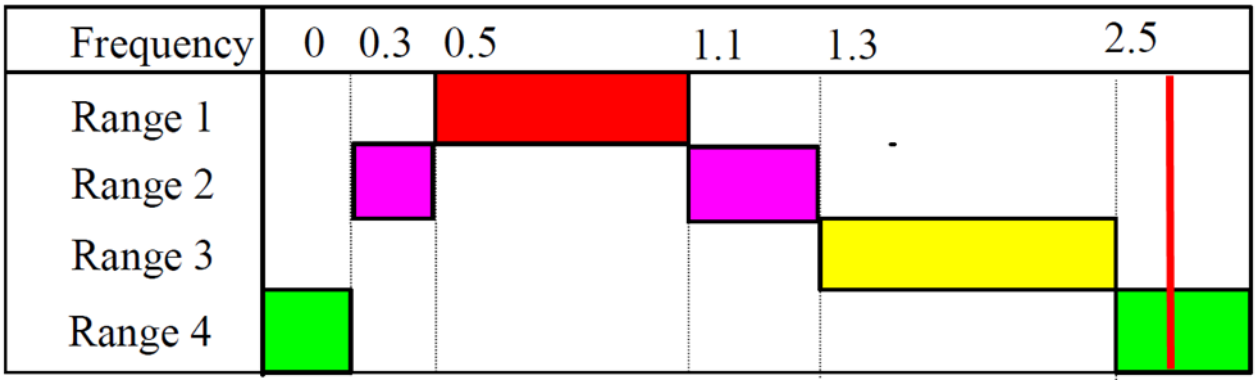

Figure 11-18 Risk of resonance – lateral direction - Combination of adding bracing to the final portion currently without bracing, change Teflon to Rubber bearing and change the cross section SLS (crowd weight)

Result shows that all directions are verified with high differences and performing dynamic analysis are not needed.

11.1.5.2 Eigenvalue analysis SLS-dynamic pedestrian load case (vibration load)

Mode	UX	UY	UZ	RX	RY		RZ	
EIGENVALUE ANALYSIS								
Mode No	Frequency (rad/sec)	Frequency (cycle/sec)	Period (sec)	Tolerance				
1	20,36	3,24	0,31	0,00				
2	29,34	4,67	0,21	0,00				
3	37,48	5,97	0,17	0,00				
4	40,96	6,52	0,15	0,00				
5	43,12	6,86	0,15	0,00				
6	48,69	7,75	0,13	0,00				
7	57,07	9,08	0,11	0,00				
8	57,71	9,18	0,11	0,00				
9	62,29	9,91	0,10	0,00				
10	62,81	10,00	0,10	0,00				
11	67,05	10,67	0,09	0,00				
12	74,97	11,93	0,08	0,00				
13	79,76	12,69	0,08	0,00				
14	98,17	15,62	0,06	0,00				
15	129,72	20,65	0,05	0,00				
16	153,14	24,37	0,04	0,00				
17	177,64	28,27	0,04	0,00				
18	203,28	32,35	0,03	0,00				
19	236,76	37,68	0,03	0,00				
20	296,29	47,16	0,02	0,00				
21	392,28	62,43	0,02	0,00				

MODAL PARTICIPATION MASSES PRINTOUT												
Mode No	TRAN-X		TRAN-Y		TRAN-Z		ROTN-X		ROTN-Y		ROTN-Z	
	MASS(%)	SUM(%)	MASS(%)	SUM(%)	MASS(%)	SUM(%)	MASS(%)	SUM(%)	MASS(%)	SUM(%)	MASS(%)	SUM(%)
1	0,08	0,08	68,20	68,20	0,01	0,01	20,49	20,49	0,00	0,00	1,73	1,73
2	0,01	0,09	4,96	73,16	0,00	0,01	7,10	27,58	0,00	0,00	51,42	53,16
3	1,84	1,93	0,01	73,18	35,59	35,60	0,00	27,58	15,84	15,84	0,01	53,16
4	3,14	5,07	8,32	81,50	0,00	35,60	0,76	28,35	0,00	15,84	29,38	82,54
5	1,89	6,96	4,77	86,26	0,01	35,61	13,07	41,42	0,00	15,84	5,71	88,25
6	80,49	87,45	0,64	86,91	0,03	35,63	0,19	41,61	0,02	15,86	2,00	90,24
7	0,71	88,16	2,61	89,52	0,00	35,64	0,68	42,30	0,00	15,86	0,00	90,24
8	0,00	88,16	0,00	89,52	0,00	35,64	0,02	42,32	0,04	15,90	0,01	90,25
9	0,95	89,11	0,00	89,52	5,44	41,08	0,02	42,34	3,11	19,01	0,01	90,26
10	0,11	89,22	1,08	90,59	0,04	41,12	3,11	45,45	0,05	19,06	0,21	90,47
11	0,23	89,46	2,24	92,84	0,00	41,12	0,39	45,84	0,01	19,07	1,97	92,44
12	0,04	89,50	1,56	94,40	0,00	41,12	0,02	45,86	0,00	19,07	0,03	92,47
13	0,31	89,81	0,01	94,40	1,32	42,44	0,01	45,86	4,95	24,02	0,00	92,47
14	0,00	89,81	0,36	94,76	0,00	42,44	0,11	45,98	0,03	24,04	0,61	93,08

15	0,02	89,84	0,01	94,77	1,67	44,11	0,08	46,06	2,14	26,19	0,05	93,12
16	0,02	89,85	1,28	96,05	0,21	44,32	3,91	49,97	0,46	26,64	1,80	94,92
17	0,00	89,85	0,05	96,10	18,40	62,72	0,24	50,20	16,23	42,87	0,03	94,95
18	4,17	94,02	0,21	96,32	0,00	62,72	1,31	51,52	0,01	42,89	0,19	95,14
19	1,95	95,98	2,45	98,77	0,05	62,77	19,14	70,66	0,29	43,17	0,87	96,01
20	2,97	98,94	0,48	99,25	0,76	63,53	6,49	77,14	3,61	46,79	0,06	96,08
21	0,39	99,33	0,01	99,26	20,09	83,62	0,12	77,27	0,48	47,26	0,00	96,08

Table 11-10 Eigenvalue analysis of Combination of adding bracing to the final portion currently without bracing, change Teflon to Rubber bearing and change the cross section SLS (vibration load)

Modal identification gives:

Lateral (Y, red): Mode 1, $f_Y = 3.24Hz$

Longitudinal (X, green): Mode 6, $f_X = 7.75Hz$

Vertical (Z, orange): Mode 3, $f_Z = 5.97Hz$

In SLS-dynamic pedestrian load case (vibration load), the combined intervention further improves separation from pedestrian excitation. All directions remain safely above screening thresholds; therefore, dynamic acceleration verification can be omitted.

Risk of resonance:

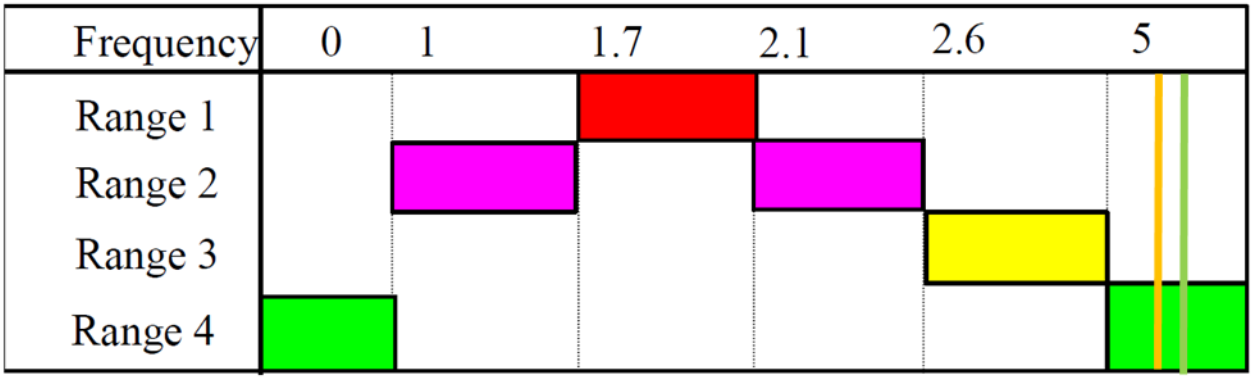

Figure 11-19 Risk of resonance – vertical and longitudinal directions - Combination of adding bracing to the final portion currently without bracing, change Teflon to Rubber bearing and change the cross section SLS (vibration load)

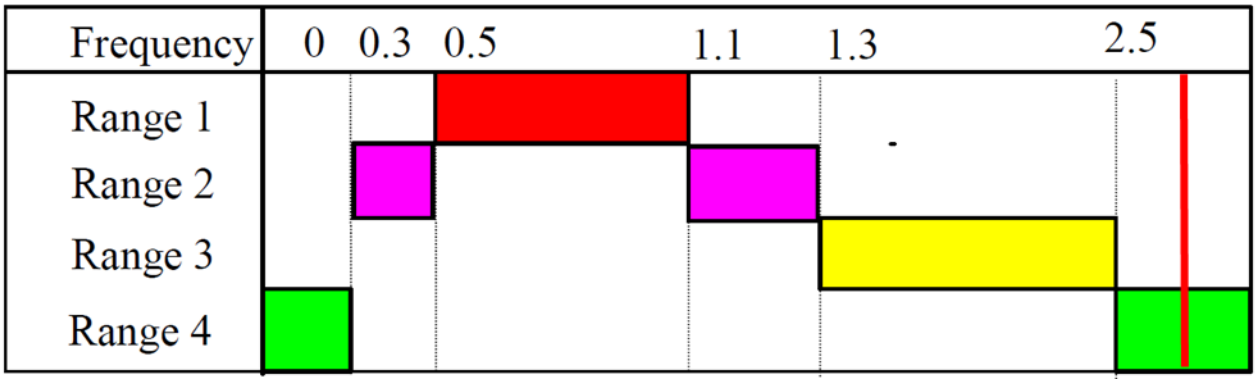

Figure 11-20 Risk of resonance – lateral direction - Combination of adding bracing to the final portion currently without bracing, change Teflon to Rubber bearing and change the cross section SLS (vibration load

Confirm that resonance risk is negligible and dynamic comfort checks are not mandatory under the adopted screening rule.

12 VERIFICATION OF COMFORT LEVEL

12.1 VERIFICATION CRITERIA

Time-history analyses were performed only for those directions where the eigenvalue screening indicates potential resonance risk (based on the SÉTRA thresholds adopted). Accelerations were extracted at deck control points (nodes reported in the plot legends). In all cases, the similarity of responses across points is used to identify whether the vibration is governed by a global mode (similar curves) or by local effects (diverging curves).

Comfort verification is performed against the conservative limit:

$$a_{\text{lim}} = 0.10 \text{ m/s}^2$$

12.2 INCREASING OPENING BETWEEN THE LEGS OF CENTRAL COLUMNS

This intervention increases the lever arm of the central support, boosting lateral and longitudinal stiffness. The lowest frequencies and dynamic-analysis decisions are summarized below.

SLS – Associated static pedestrian load case (crowd weight) modal identification:

- ✓ $f_Y = 2.17Hz \rightarrow$ dynamic check is required (Lateral).
- ✓ $f_X = 6.09Hz \rightarrow$ dynamic check is not required (Longitudinal).
- ✓ $f_Z = 5.25Hz \rightarrow$ dynamic check is not required (vertical).

SLS-dynamic pedestrian load case (vibration load) modal identification:

- ✓ $f_Y = 2.40Hz \rightarrow$ dynamic check is required (Lateral).
- ✓ $f_X = 5.78Hz \rightarrow$ dynamic check is not required (Longitudinal).
- ✓ $f_Z = 6.52Hz \rightarrow$ dynamic check is not required (vertical).

12.2.1 Acceleration verification

12.2.1.1 verification SLS – Associated static pedestrian load case (crowd weight)

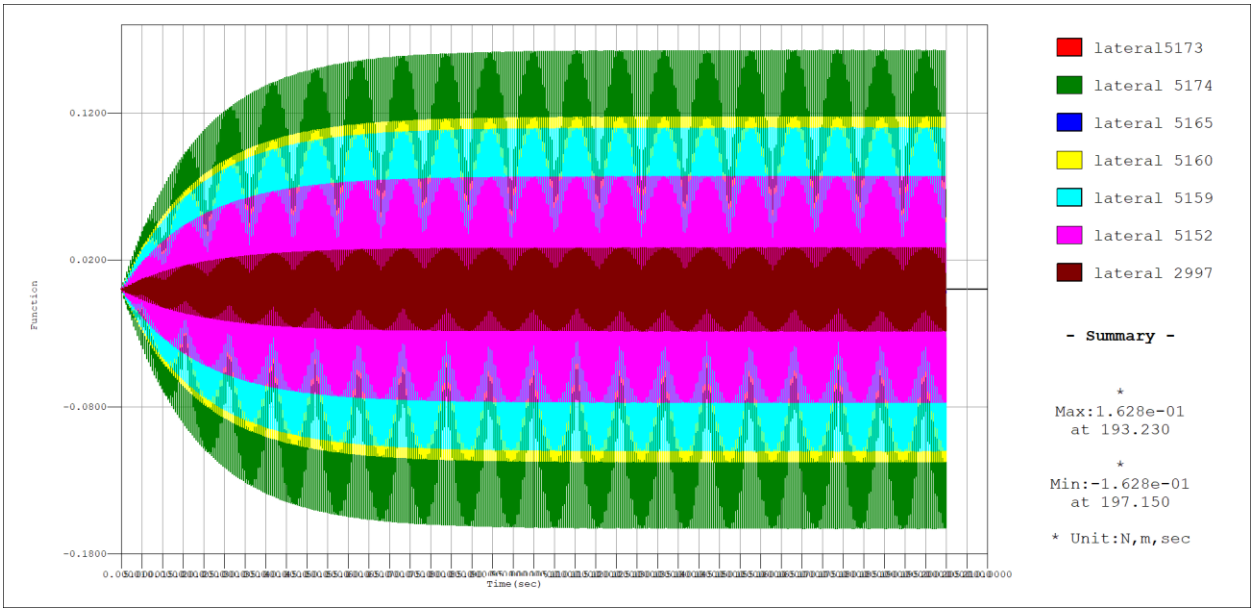

Figure 12-1 Lateral acceleration of points SLS (crowd weight)

Longitudinal (X, green): no check is required.

Lateral (Y, red): The lateral responses are also nearly identical across points. The plot summary gives:

- ✓ $a_{y,\max} = 0.162$ m/s^2

Since $0.162 > 0.10$ m/s^2, according to Figure 6-2, corresponds to Mean comfort level and there is risk of lock-in effect therefore, the lateral comfort criterion is **NOT VERIFIED**.

Vertical (Z, orange): not checked because $f_Z > 5$Hz (screening satisfied).

12.2.1.2 Verification SLS-dynamic pedestrian load case (vibration load)

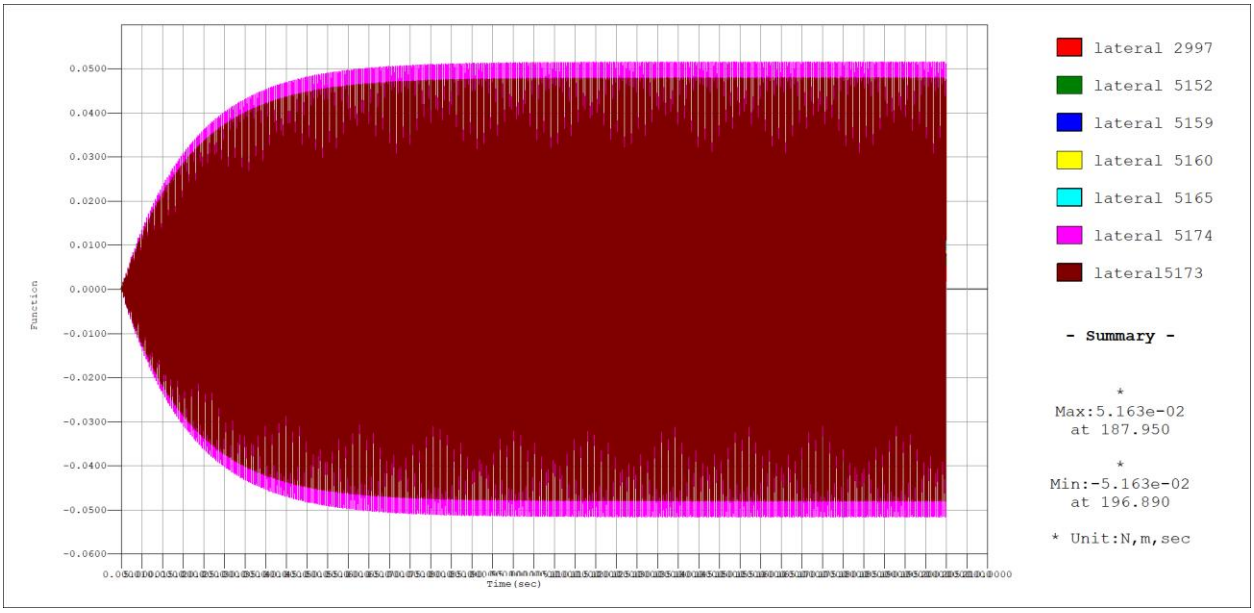

Figure 12-2 Lateral acceleration of points SLS (vibration load)

In SLS-dynamic pedestrian load case (vibration load), the lateral frequency remains below the 2.5 Hz threshold ($f_Y = 2.40$ Hz), therefore a lateral time-history check is required. The response shows resonance-type build-up and a stable plateau, indicating that excitation remains close to a governing lateral mode. The peak value is:

- $a_{y,\max} = 0.051$ m/s^2

Since $0.051 > 0.10$ m/s^2, according to figure 6-2, corresponds to Max comfort level, therefore the lateral comfort criterion is **VERIFIED** in vibration load.

12.3 INCREASING THE CROSS-SECTION OF THE CENTRAL COLUMNS

A larger column section increases bending and torsional stiffness and reduces support flexibility. The principal frequencies are:

SLS – Associated static pedestrian load case (crowd weight):

$f_Y = 2.59$Hz

$f_Z = 6.17$Hz → lateral and vertical checks omitted.

$f_X = 5.63$Hz → verified.

SLS-dynamic pedestrian load case (vibration load):

$f_Y = 2.93$Hz

$f_Z = 5.92$Hz

$f_X = 6.92$Hz

all directions above thresholds; dynamic checks are not required by screening.

12.3.1 Acceleration verification

Checking is not required in three direction all the frequencies are satisfied.

12.4 ADDING BRACING TO THE FINAL PORTION CURRENTLY WITHOUT BRACING

Bracing the previously flexible end bay increases lateral stiffness and reduces local vibration amplification. The approximate fundamental frequencies and their implications are:

SLS – Associated static pedestrian load case (crowd weight) modal identification: $f_Y = 2.71$Hz, $f_Z = 6.03$Hz (safe by screening), but $f_X = 4.67$Hz → **longitudinal check required**.

SLS-dynamic pedestrian load case (vibration load) modal identification:

$f_Y = 3.05$Hz

$f_Z = 6.02$Hz

$f_X = 5.40$Hz → improved.

12.4.1 Acceleration verification

12.4.1.1 verification SLS – Associated static pedestrian load case (crowd weight)

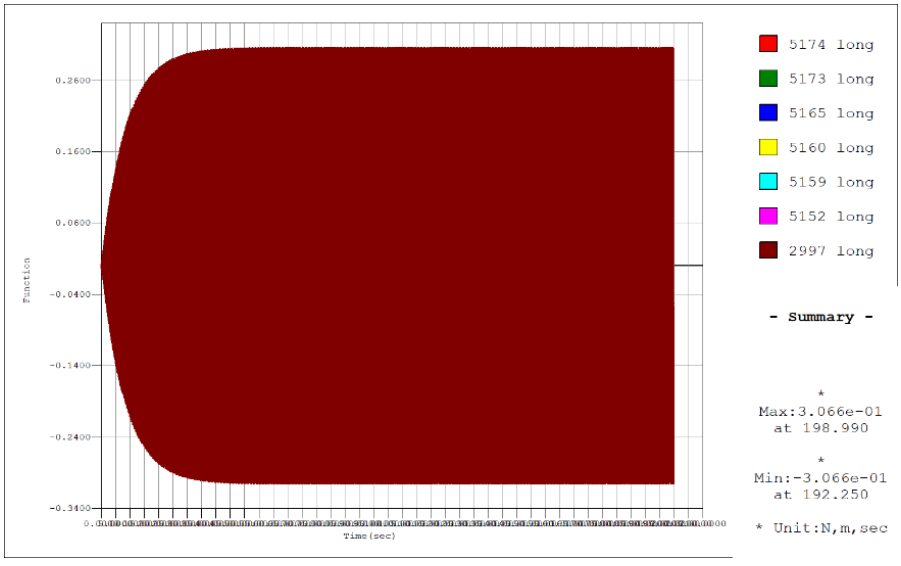

Figure 12-3 Longitudinal acceleration of points SLS (crowd weight)

Because the governing longitudinal mode remains within the critical range ($f_X = 4.67$ Hz), longitudinal time-history verification is required. The extracted acceleration histories at the deck control points are nearly identical, confirming a dominant global longitudinal response. The plot summary provides:

- ✓ $a_{x,\max} = 0.30$ m/s^2

Since $0.30 > 0.10$ m/s^2, according to figure 6-2, corresponds to Mean comfort level and also it is range of risk of Lock-in effect, therefore the longitudinal comfort criterion is **NOT VERIFIED** for intervention in the hand under SLS – Associated static pedestrian load case (crowd weight).

12.4.1.2 Verification SLS-dynamic pedestrian load case (vibration load)

In SLS condition from modal analysis it can be shown that lateral frequency is 3.05Hz, longitudinal frequency 5.40Hz and vertical frequency 6.02Hz in this case no check is required because all the frequencies are above the threshold are in comfort level.

12.5 REPLACING TEFLON BEARINGS WITH RUBBER BEARINGS

SLS – Associated static pedestrian load case (crowd weight) modal identification:

- ✓ $f_Y = 2.27$Hz → **lateral check required**.
- ✓ $f_Z = 6.02$Hz → **no vertical check**.
- ✓ $f_X = 5.33$Hz → **no longitudinal check**

SLS-dynamic pedestrian load case (vibration load) modal identification:

- ✓ $f_Y = 2.51$Hz (marginal)
- ✓ $f_X = 5.19$Hz
- ✓ $f_Z = 6.05$Hz.

Because lateral is close to the threshold and damping modelling can influence peaks, the configuration is assessed conservatively.

12.5.1 Acceleration verification

12.5.1.1 verification SLS – Associated static pedestrian load case (crowd weight)

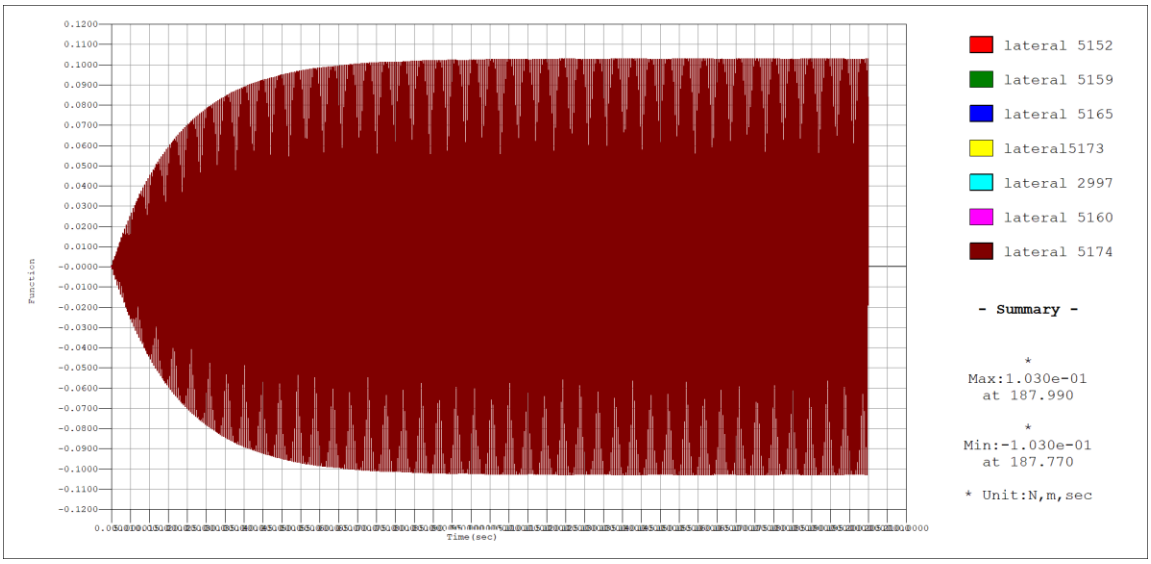

Figure 12-4 Lateral acceleration of points SLS (crowd weight)

In the graph it can be shown that, maximum lateral frequency reaches 0.103m/s^2 which is close to the value of verification but still not verified because in exact value it is greater than 0.1m/s^2 and acceleration enters to the range of lock-in effect.

12.5.1.2 Verification SLS-dynamic pedestrian load case (vibration load)

In the SLS check modal analysis shows in three directions, all the frequencies are above the threshold.

12.6 COMBINATION OF ADDING BRACING TO THE FINAL PORTION CURRENTLY WITHOUT BRACING, CHANGE TEFLON TO RUBBER BEARING AND CHANGE THE CROSS SECTION

12.6.1 verification SLS – Associated static pedestrian load case (crowd weight)

From the combined model eigenvalue results (ULS), the governing frequencies are:

- ✓ **Lateral (Y, red):** $f_Y = 2.92$Hz
- ✓ **Longitudinal (X, green):** $f_X = 6.61$Hz
- ✓ **Vertical (Z, orange):** $f_Z = 5.93$Hz

All are above the adopted screening thresholds; therefore, dynamic comfort time-history verification is **not required** by the SÉTRA-based rule in SLS – Associated static pedestrian load case (crowd weight).

12.6.2 verification SLS – Associated static pedestrian load case (crowd weight)

For SLS, the governing frequencies are:

- ✓ **Lateral (Y, red):** $f_Y = 3.24$Hz
- ✓ **Longitudinal (X, green):** $f_X = 7.75$Hz
- ✓ **Vertical (Z, orange):** $f_Z = 5.97$Hz

All are comfortably above the adopted screening thresholds; therefore, dynamic acceleration verification can be **omitted in all directions**.

The combined intervention improves dynamic behavior through **three mechanisms acting together**:

- ✓ The **CHS 273×16 mm** central columns significantly increase global stiffness and shift the longitudinal and lateral modes to higher frequencies.
- ✓ The **added bracing** reduces the flexibility of the previously unbraced end segment and improves the global distribution of stiffness.
- ✓ The **rubber bearings** introduce additional damping and modify boundary conditions, reducing resonance amplification.
  As a result, the governing modal frequencies move above the adopted SÉTRA thresholds in both ULS and SLS, reducing the resonance risk and limiting the need for time-history comfort checks.

12.7 SUMMARY OF DYNAMIC ANALYSIS REQUIREMENTS

Using the adopted SÉTRA-based screening, lateral and vertical time-history checks are required only when $f_Y \leq 2.5$Hz or $f_Z \leq 5$Hz. Among the single interventions, increasing the central column cross-section provides the most effective global improvement, shifting all governing frequencies above thresholds and verifying accelerations in the critical direction. Bracing alone improves lateral behaviour but does not sufficiently mitigate longitudinal response. Rubber bearings alone increase damping but do not resolve low-frequency sensitivity in the lateral direction. The combined intervention provides the most robust solution, ensuring screening compliance in all directions for both load cases.

13 CONCLUSION OF PROPOSED INTERVENTIONS

The vibration comfort verification of the reference footbridge identified a clear resonance-driven serviceability problem. Modal and time-history analyses showed that the bridge response under pedestrian excitation is governed primarily by **horizontal modes**, with the **longitudinal direction (X, green)** being the most critical. Peak accelerations in the reference configuration reached values far above the adopted comfort limit of **0.10 m/s²**, confirming that mitigation measures are required to ensure acceptable user comfort.

Four interventions were assessed individually and then in combination. The interventions were designed either to increase stiffness (shifting modal frequencies upward) or to increase damping (reducing resonance amplification):

1. **Increase opening between the legs of central columns** improved stiffness at midspan and shifted modal frequencies upward; however, the lateral frequency remained below the SÉTRA threshold and time-history checks confirmed excessive accelerations ($a_{y,\max} = 0.162$m/s² in associated static pedestrian load case, and $a_{y,\max} = 0.051$m/s² in SLS-dynamic pedestrian load case). Therefore, comfort requirements were not satisfied.

2. **Increasing the cross-section of the central columns (CHS 273×16)** produced the most significant improvement as a single measure. Eigenvalue results showed that governing frequencies in all directions exceeds screening thresholds and governs comfort limit in all directions.

3. **Adding bracing to the final portion currently without bracing** increased lateral stiffness and improved stiffness distribution, but longitudinal behavior remained critical. Time-history verification still produced excessive longitudinal accelerations ($a_{x,\max} = 0.30$ m/s² in SLS-associated static pedestrian load case and SLS-dynamic pedestrian load case verified). Hence, bracing alone is insufficient.

4. **Replacing Teflon bearings with rubber bearings** increased damping and modified boundary behavior, but the lateral frequency remained near/below the threshold and longitudinal classified in comfort level because of stiffness that rubber bearings have in longitudinal direction ($a_{y,\max} = 0.103$m/s² in SLS-associated static pedestrian load case and in SLS-dynamic pedestrian load case verified). Therefore, damping alone cannot overcome the resonance problem.

Because single measures (except column cross-section enlargement) did not ensure robust compliance, a **combined** intervention was assessed (CHS 273×16 + end bracing + rubber bearings). The combined solution produced governing frequencies of $f_Y = 2.92$Hz, $f_X = 6.61$Hz, $f_Z = 5.93$Hz in ULS and $f_Y = 3.24$Hz, $f_X = 7.75$Hz, $f_Z = 5.97$Hz in SLS, all above the adopted SÉTRA screening thresholds. Consequently, resonance risk is significantly reduced, and dynamic comfort checks can be omitted under the adopted rule.

In conclusion, the study confirms that vibration mitigation in slender pedestrian bridges generally requires either a strong stiffness intervention at the governing support region or a combined strategy. The most effective single retrofit is the **increase of the central column cross-section**, which directly addresses the principal weakness and verifies comfort. For maximum robustness against modelling uncertainty and load

variability, the recommended retrofit is the **combined solution**, which improves stiffness distribution and damping simultaneously and ensures screening compliance in all directions for both load cases.